

# Onset Voltage of Corona on Coated Conductors

by

Yahya Abdul-Rahman Saleh Abu-Shal

A Thesis Presented to the

FACULTY OF THE COLLEGE OF GRADUATE STUDIES

KING FAHD UNIVERSITY OF PETROLEUM & MINERALS

DHAHRAN, SAUDI ARABIA

In Partial Fulfillment of the  
Requirements for the Degree of

**MASTER OF SCIENCE**

In

**ELECTRICAL ENGINEERING**

December, 1994

## **INFORMATION TO USERS**

**This manuscript has been reproduced from the microfilm master. UMI films the text directly from the original or copy submitted. Thus, some thesis and dissertation copies are in typewriter face, while others may be from any type of computer printer.**

**The quality of this reproduction is dependent upon the quality of the copy submitted. Broken or indistinct print, colored or poor quality illustrations and photographs, print bleedthrough, substandard margins, and improper alignment can adversely affect reproduction.**

**In the unlikely event that the author did not send UMI a complete manuscript and there are missing pages, these will be noted. Also, if unauthorized copyright material had to be removed, a note will indicate the deletion.**

**Oversize materials (e.g., maps, drawings, charts) are reproduced by sectioning the original, beginning at the upper left-hand corner and continuing from left to right in equal sections with small overlaps. Each original is also photographed in one exposure and is included in reduced form at the back of the book.**

**Photographs included in the original manuscript have been reproduced xerographically in this copy. Higher quality 6" x 9" black and white photographic prints are available for any photographs or illustrations appearing in this copy for an additional charge. Contact UMI directly to order.**

# **UMI**

A Bell & Howell Information Company  
300 North Zeeb Road, Ann Arbor, MI 48106-1346 USA  
313/761-4700 800/521-0600



**ONSET VOLTAGE OF CORONA ON  
COATED CONDUCTORS**

**BY**

**YAHYA ABDUL-RAHMAN SALEH ABU-SHAL**

**A Thesis Presented to the  
FACULTY OF THE COLLEGE OF GRADUATE STUDIES  
KING FAHD UNIVERSITY OF PETROLEUM & MINERALS  
DHAHRAN, SAUDI ARABIA**

**In Partial Fulfillment of the  
Requirements for the Degree of**

**MASTER OF SCIENCE  
In  
ELECTRICAL ENGINEERING**

**DECEMBER, 1994**

**UMI Number: 1360833**

---

**UMI Microform Edition 1360833**  
**Copyright 1995, by UMI Company. All rights reserved.**

**This microform edition is protected against unauthorized  
copying under Title 17, United States Code.**

---

**UMI**  
**300 North Zeeb Road**  
**Ann Arbor, MI 48103**

KING FAHD UNIVERSITY OF PETROLEUM AND MINERALS  
DHAHRAN 31261, SAUDI ARABIA

COLLEGE OF GRADUATE STUDIES

This thesis, written by Yahya Abdul-Rahman Saleh Abu-Shal under the direction of his Thesis Advisor and approved by his Thesis Committee, has been presented to and accepted by the Dean of the College of Graduate Studies, in partial fulfillment of the requirements for the degree of MASTER OF SCIENCE IN ELECTRICAL ENGINEERING.

Thesis Committee



Dr. M. ABDEL-SALAM  
Thesis Advisor

  
Dr. F. ZEDAN  
Member  
Dr. A. AL-SHEHRI  
Member  
Dr. Y. ABDEL-MAGID  
Member  
Department Chairman  
Dean, College of Graduate Studies

20-12-141

Date



## شكرو عرفان

إلى والدي الذي علمني أن محبة العلم تين يُدان به ، وبه يكسب الأ نسان الطاعه في حياته  
وجميل الاحدوئه بعد وفاته ، وإلى والدتي التي شملتني بوثير حنانها في الصغر ودفء عطفها في  
الكبر فكنت بذلك مهياً لخدمة ديني ووطني و نفسي وأهلي ، وإلى زوجتي التي وفرت لي  
الظروف المناسبه للأستذكار وإلى ولدي عبد الرحمن قره عيني ومهجة فؤادي ، وإلى جميع  
الأخوة والزملاء الذين ساندوني قولاً وفعلأ جعلنا الله وإياهم ممن لا تغيب أمثالهم إذا غابت  
أعيانهم .

## **ACKNOWLEDGMENT**

**Acknowledgment is due to King Fahd University of Petroleum and Minerals for support of this research.**

**I wish to express my appreciation to Professor Mazen Abdel-Salam who served as my major advisor. I also wish to thank the other members of my Thesis Committee Dr. Fareed Zedan, Dr.Abdallah Al-Shehri and Dr.Youssef Abdel-Magid**

**Finally, I would like to acknowledge the support provided by Saudi Consolidated Electrical Company in the Eastern Province to accomplish this research.**



# TABLE OF CONTENTS

	<b>Page</b>
LIST OF TABLES	ix
LIST OF FIGURES	x
ABSTRACT (ARABIC)	xv
ABSTRACT (ENGLISH)	xvi
CH. 1 INTRODUCTION	1
1.1 Problem Statement	1
1.2 Thesis Objective	2
1.3 Thesis Description	4
CH. 2 LITERATURE REVIEW	6
2.1 Introduction	6
2.2 Electric Field Calculation	6
2.2.1 Finite - Difference Technique	7
2.2.2 Finite - Element Technique	9
2.2.3 Charge - Simulation Technique	12
2.3 Onset Voltage Calculation	13
2.3.1 Positive Onset Voltage	14
2.3.2 Negative Onset Voltage	15

<b>CH. 3 ELECTRIC FIELD CALCULATION</b>	<b>Page</b>
	17
3.1 Introduction	17
3.2 Charge Simulation Technique	18
3.2.1 Field Calculation in Single Dielectric Medium	18
3.2.1.1 Boundary Conditions	20
3.2.1.2 Electric Field	21
3.2.2 Field Calculation in Two - Dielectric Medium	22
3.2.2.1 Boundary Conditions	24
3.2.2.2 Electric Field	27
3.3 Application to Coated Transmission Lines	27
3.3.1 Location of Simulation Charges	29
3.3.2 Location of Contour Points	30
3.3.3 Coefficient Matrix Formulation	31
3.3.4 Accuracy Measurement	36
3.4 Programming	37
3.5 Numerical Data	39
3.6 Accuracy of the Calculated Potential and Field Values	40
 <b>CH. 4 CORONA ONSET VOLTAGE CRITERIA</b>	 45
4.1 Introduction	45
4.2 Positive Corona	45
4.2.1 Criterion of Onset Voltage	45
4.2.2 Mathematical Formulation of Onset Criterion	51
4.2.3 Programming of Onset Criterion	58
4.2.3.1 Ionization-Zone Boundary Computation	62

	<b>Page</b>
4.2.3.2 Primary Avalanche Growth	64
4.2.3.3 Calculation of Photoelectrons in the sub-volume	67
4.2.3.4 The Growth of Successor Avalanches	70
4.3 Negative Corona	73
4.3.1 Criterion of Onset Voltage	73
4.3.2 Mathematical Formulation of the Onset Criterion	74
4.3.3 Programming of Onset Criterion	77
4.4 Numerical Data	81
4.4.1 Ionization ( $\alpha$ ) and Attachment ( $\eta$ ) Coefficients	81
4.4.2 Photoionization Product $f_1 f_2$	82
4.4.3 Absorption Coefficient ( $\mu$ )	82
4.4.4 Primary Avalanche Radius	83
4.4.5 Geometry Factor ( $g(y)$ )	84
4.5 Accuracy of the Calculated Onset Voltages	85
 CH. 5 RESULTS AND DISCUSSION	 90
5.1 Introduction	90
5.2 Effect of Line Parameters on the Onset Voltage	91
5.2.1 Effect of Conductor Radius	91
5.2.2 Effect of Conductor Height	98
5.3 Effect of Dielectric Permittivity on Onset Voltage	101
5.4 Effect of Conductor Radius on Ionization - Zone Thickness	101
5.5 Effect of Line Parameters on the Primary Avalanche Size	106

	<b>Page</b>
5.5.1 Effect of Conductor Radius	107
5.5.2 Effect of Conductor Height	110
5.6 Effect of Dielectric Permittivity on Primary Avalanche Size	113
5.7 Comparison Between Coated and Bare Conductors of the Same Outer radius	113
5.7.1 Effect of Conductor Radius	116
5.7.2 Effect of Conductor Height	116
5.7.3 Effect of Dielectric Permittivity	121
<b>CH. 6 CONCLUSIONS AND SUGGESTIONS FOR FUTURE WORK</b>	<b>126</b>
6.1 Conclusions	127
6.2 Suggestions for Future Work	129
<b>APPENDIX-A FOUR COMPUTER PROGRAMS FOR CALCULATING POSITIVE AND NEGATIVE ONSET VOLTAGE</b>	<b>130</b>
<b>APPENDIX-B SAMPLES OF THE PROGRAM OUTPUT</b>	<b>177</b>
<b>NOMENCLATURE</b>	<b>189</b>
<b>REFERENCES</b>	<b>197</b>

## **LIST OF TABLES**

<b>Table</b>	<b>Page</b>
3.1 Calculated relative permeability of the dielectric	41
3.2 Potential at the interface between air and coating-layer	41

# LIST OF FIGURES

Figure	Page
1.1 Water Droplets on Conductor	3
2.1 Grid for the finite - element technique and arrangement of the element	10
3.1 Arrangement of simulation charges and contour point: (a) hemispherically capped rod, (b) sphere with cylindrical shank	19
3.2 Discrete simulation charges at an electrode and a dielectric boundary.	23
3.3 Location of charges and boundary points for coated conductor.	28
3.4 Flow chart for calculating electric field by using charge simulation technique	38
3.5 The potential distribution along gap axis for coated conductor, $R_2=0.5$ cm, $R_1=0.1$ cm and $H=50$ cm	43
3.6 Electric field distribution along gap axis for bare and coated conductor, $R_2=0.5$ cm, $R_1=0.1$ cm and $H=50$ cm.	44
4.1 Ionization zone around coated conductor	47
4.2 The growth of primary avalanche and the emission of photons	48
4.3 The growth of successor avalanche	50
4.4 Photoelectrons created in sub-volume	55
4.5 The main flow chart for positive corona criteria	59

<b>Figure</b>	<b>Page</b>
4.6 One quarter of the ionization zone around coated conductor	60
4.7 The flow chart for determining the ionization zone boundary	61
4.8 Computation of ionization zone boundary	63
4.9 The flow chart for primary avalanche growth	65
4.10 Division of the Ionization-Zone into Sub- Volumes	68
4.11 The flow Chart for the Creation of Photoelectrons in a Sub-Volume	69
4.12 The Flow Chart of Successor Avalanche Growth	71
4.13 Development of the primary avalanche in negative corona discharge	75
4.14 The Flow chart for negative corona onset condition	79
4.15 Test set-up and clearances for corona onset measurement on bare conductors [21]	87
4.16 Measured and calculated positive onset voltages versus conductor radius	88
4.17 Measured and calculated negative onset voltages versus conductor radius	89
5.1 Effect of coating-layer thickness on positive onset voltage ( $V_{0+}$ ) for different values of R1	92
5.2 Effect of coating-layer thickness on negative onset voltage ( $V_{0-}$ ) for different values of R1	93
5.3 Electric field distribution across ionization zone for bare conductor stressed by voltage $V_{0+} = 271.18$ and $588.5$ kV	94

<b>Figure</b>	<b>Page</b>
5.4 Electric field distribution across ionization zone for coated conductor stressed by voltage $V_0 = 372.85$ and $669.6$ kV	95
5.5 Electric field distribution across ionization zone for bare conductor stressed by voltage $V_0 = 243.5$ and $525$ kV	96
5.6 Electric field distribution across ionization zone for coted conductor stressed by voltage $V_0 = 334.1$ and $596.6$ kV	97
5.7 Effect of coating-layer thickness on the positive onset voltage for different conductor heights .	99
5.8 Effect of coating-layer thickness on the negative onset voltage for different conductor heights .	100
5.9 Effect of coating layer thickness on the positive onset voltage for different permittivities of the coating layer	102
5.10 Effect of coating layer thickness on the negative onset voltage for different permittivities of the coating layer	103
5.11 Effect of conductor radius on the ionization - zone thickness for bare conductor stressed by the onset voltage ( $V_{0+} / V_{0-}$ )	104
5.12 Effect of conductor radius on the ionization - zone thickness for coated conductor stressed by the onset voltage ( $V_{0+} / V_{0-}$ )	105
5.13 Primary avalanche size at the positive onset voltage versus the thickness of coating layer for different values values of R1	108



<b>Figure</b>	<b>Page</b>
5.14 Primary avalanche size at the negative onset voltage versus the thickness of coating layer for different values of R1	109
5.15 Primary valanche size at the positive onset voltage versus the thickness of coating layer for different values conductor heights in the range 10-20	111
5.16 Primary valanche size at the negative onset voltage versus the thickness of coating layer for difierent values conductor heights in the range 10-20	112
5.17 Primary valanche size at the positive onset voltage versus the thickness of coating layer for different relative permittivitie in the range 2.3-6.0	114
5.18 Primary valanche size at the negative onset voltage versus the thickness of coating layer for different relative permittivitie in the range 2.3-6.0	115
5.19 Positive onset voltage for coated and bare conductors of the same outer radius with R1 =22 mm	117
5.20 Positive onset voltage for coated and bare conductors of the same outer radius with R1 =15.16 mm	118
5.21 Negative onset voltage for coated and bare conductors of the same outer radius with R1 =22 mm	119
5.22 Negative onset voltage for coated and bare conductors of the same outer radius with R1 =15.16 mm	120

<b>Figure</b>		<b>Page</b>
5.23	Positive onset voltage for coated and bare conductors of the same outer radius at heights (12.5 m and 20 m)	122
5.24	Negative onset voltage for coated and bare conductors of the same outer radius at heights (12.5 m and 20 m)	123
5.25	Positive onset voltage for coated and bare conductors of the same outer radius at relative permittivities (2.3 and 6 )	124
5.26	Negative onset voltage for coated and bare conductors of the same outer radius at relative permittivities (2.3 and 6 )	125

## ملامة الرسالة

اسم الطالب الكامل : يحيى عبدالرحمن صالح ابوشال  
عنوان الدراسة : ظاهرة التفريغ الهالي للموصلات المطلية  
التخصص : هندسة كهربائية  
تاريخ الشهادة : ١٤١٥/٧ (١٩٩٤/١٢)

أحدثت الحاجة الحالية والمتوقعة مستقبلاً - الى نقل الطاقة الكهربائية على خطوط الضغط العالي ذات التيار المتردد تنامياً جلياً في الأهتمام بدراسة المشاكل المرتبطة بظاهرة التفريغ الهالي التي تحصل على هذه الخطوط ، واهم هذه المشاكل زيادة الطاقه المفقودة والزين العالي المسموع بالإضافة الى التشويش على أجهزة الراديو و التلفزيون، وتزداد هذه المشاكل في حالة تساقط الأمطار إلى درجة الحد من التفكير في مسألة التوسع في تصميم خطوط نقل طاقة ذات جهد عالي جداً. لقد كان استخدام موصلات مطلية بطبقة من مادة عازلة هو الحل المقترح في هذه الرسالة لتقليل ظاهرة التفريغ الهالي و الحد من مشاكلها ، هذا وقد تمت في هذه الرسالة أول دراسة نظرية لحساب كلاً من جهد بدء التفريغ الهالي الموجب وكذلك السالب التي تبدأ ببلوغه هذه الظاهرة للموصلات المطلية وذلك بمحاكاة هذا النظام باستخدام الحاسب الآلي .

كذلك تمت دراسة عدة عوامل أخرى كتأثير نصف قطر الموصل وارتفاعه بالإضافة الى نوعية المادة التي يطلى بها الموصل على سماكة المنطقة التي يتم فيها تكاثر الألكترونات والجهد الذي تحدث عنده ظاهرة التفريغ الهالي وكذلك تمت المقارنة بين الموصل المطلي وغير المطلي عندما يكون لهما نفس نصف القطر الخارجي في ظل تأثير تغير العوامل المشار اليها آنفاً. للاستدلال على اهمية طلاء موصلات الجهد العالي

درجة الماجستير في العلوم  
جامعة الملك فهد للبترول والمعادن  
الظهران، المملكة العربية السعودية  
(١٩٩٤/١٢) ١٤١٥/٧

# **THESIS ABSTRACT**

**Student name:** Yahya Abdul-Rahman Abu-Shal  
**Title of study:** Onset Voltage of Corona on Coated Conductors.  
**Major field:** Electrical Engineering  
**Date of degree:** December 1994

Increased prospects of transmitting electric power by high voltage AC have created a growing interest in the study of the problems associated with corona on AC transmission lines. These problems are power loss, audible noise and radio interference. In rainfall weather, these problems increase to such an extent that they represent serious limitation to the use of extra high voltage. Using coated conductors is a solution proposed to reduce these problems. In this thesis, a theoretical study using computer simulation is presented to calculate, for the first time, both the positive and the negative corona onset voltages for coated conductor.

In addition, the effect of different parameters such as the conductor radius, height and the coating layer permittivity on the ionization zone thickness, the growth of primary avalanche and the onset voltage is presented. A comparison between the onset voltage for coated and bare conductors of the same outer radius is made to appreciate the effect of coating on improving the corona performance of high voltage conductors.

**MASTER OF SCIENCE DEGREE  
KING FAHD UNIVERSITY OF PETROLEUM AND MINERALS  
Dhahran, Saudi Arabia  
December 1994**

# **CHAPTER 1**

## **INTRODUCTION**

AC and DC extra - high voltage overhead transmission lines have been used in transmitting large amounts of electric power over long distances . AC lines are more economical than DC lines for transmission distances less than 800 km [1], and so AC lines are more widely used than DC lines . Consequently, the various problems associated with AC transmission lines are being studied extensively . One of these problems is the phenomenon of corona , which is defined as the partial breakdown that develop in the highly-stressed zone around the conductor.

### **1.1 Problem Statement**

Corona has been a main concern for power transmission engineers because of its associated power loss in the lines, audible noise and radio &TV interference [2,3]. In wet weather , the audible noise increases to such an extent that it represents one of the most serious limitation to the use of extra high voltages. A systematic study [4] has shown that corona discharges from water droplets on the under side of the conductor, Fig.(1.1), produce a random noise having frequency components as high as

the ultrasonic frequency , with substantial peaks in the audible range of humans [5].

A proposed solution to keep the noise level permissible in the audible range is to eliminate the effects of the water droplets in some way . A coating material on a solid bare conductor may lead to an acceptable solution . Tests have shown that a conductor having a thick insulation layer is less noisy than the bare conductor [5] . Also, this coating material may increase the corona onset voltage [6] which is defined as the minimum voltage for a sustained (self-maintained) discharge . Consequently, this solution will encourage the transmission lines engineers to construct extra high voltage transmission lines.

## **1.2 Thesis Objective**

Based on the proposed solution , the objective of this thesis is to investigate the effect of surface coating on the onset voltage of corona from transmission - line conductors. This calls at first for accurate calculation of the electric field in the vicinity of a coated conductor and its correlation to the field values near bare conductor of the same radius. The method of field calculation is based on the charge simulation technique which is different from previous methods [7,8] . Secondly , the calculated electric field will be utilized in the calculation of positive and negative corona onset voltages for both coated and bare conductors .



*Fig.(1.1) Water Droplets on Conductor*

### **1.3 Thesis Description**

This thesis consists of six chapters and two appendices. In chapter two , a literature survey on both the electric field calculation and the corona onset voltage criteria are presented. Three numerical techniques for calculating electric field are reported. However , the charge simulation technique is [9] selected because it offers several advantages when compared with the other techniques. Several publications on the criteria of positive and negative onset voltages of corona in different gap arrangements and gas conditions are reviewed .

In the third chapter, electric field calculation by using charge simulation technique is discussed. This chapter explains at first detailed electric field calculation in one and two dielectric media surrounding HV-stressed conductors. Then, the method of field calculation is extended to coated transmission-line conductors . This is followed by a description of the computer program written to calculate the field values around the coated conductor . Finally, the continuity of potential and the discontinuity of the electric field at the surface of the coating layer are investigated to check the accuracy of the simulation .

Chapter four presents the onset criteria of corona which is the second objective of this thesis . Both positive and negative onset criteria are studied in detail in this chapter . Along with the criteria of onset , the pertinent mathematical formulation and computer programming are explained . The computed onset voltages of corona on bare conductors are



compared with those measured experimentally for positive and negative coronas .

Chapter five reports the results obtained throughout the thesis work. Firstly, the effects of conductor radius and height on the positive and negative onset voltages are presented . Secondly, the effect of dielectric permittivity of the coating layer on the positive and negative onset voltages is explained. Thirdly, the effect of the thickness of the coating layer on the positive and negative onset voltages is discussed. Finally, a comparison between coated and bare conductors of the same outer radius is reported for different values of conductor radius, conductor height and dielectric permittivity of the coating layer.

Conclusions and suggestions for future work pertinent to the present study are reported in chapter six . Four FORTRAN programs developed for the thesis work concerning the calculation of the electric field and corona onset voltage are given in Appendix-A . Appendix-B contains several examples of the computer output results for several case studies.

## **CHAPTER 2**

### **LITERATURE REVIEW**

#### **2.1 Introduction**

The objective of this chapter is to survey the work published in the literature on the different techniques adopted for calculating high-voltage electric fields and the onset criteria of both positive and negative coronas . Therefore, this chapter is divided into two main sections. The first section is devoted to electric field calculation with different numerical techniques; namely, finite-differences, finite-elements and charge simulation techniques . The advantages and drawbacks of each technique are presented . The second section of this chapter reviews the onset criteria of both positive and negative coronas in different gap arrangements .

#### **2.2 ELECTRIC FIELD CALCULATION**

In the design of high -voltage transmission lines, the knowledge of accurate electric field at the conductor surface as well as in the interelectrode space is essential to calculate corona onset voltage, corona

power loss, and radio interference [10] . At voltages below the onset value, the electric field is a space-charge-free one and the evaluation of field requires the solution of Laplace's equation , equation (2.1), with boundary conditions satisfied .

$$\nabla^2 \Phi = 0 \quad (2.1)$$

where  $\Phi$  is the electrical potential . This can be done either by analytical or numerical methods .

Analytical field calculations can be done only for simple geometries such as concentric spheres, coaxial cylinders, separated equal spheres and equal parallel cylinders [9]. However, in more complex electrode geometries such as coated conductor-to-plane gaps, the analytical calculation of electric field is extremely difficult . For such geometries, the electric field may be calculated by numerical techniques .

Three main numerical techniques have been reported in the literature, namely, the Finite-Difference Technique (FDT), the Finite-Element Technique (FET) and the Charge-Simulation Technique (CST) [9,11] .

### **2.2.1 Finite-Difference Technique**

The basis of this technique is the replacement of a continuous domain representing the entire space surrounding the stressed

electrodes with a rectangular or polar grid of discrete "nodes" at which the value of unknown potential is to be computed . Thus, we replace the derivatives describing Laplace's equation with "divided- difference" approximations obtained as a functions of the nodal values [8,9]. The difference equation at each node (m,n) contains the potentials at the four surrounding nodes:

$$K_1 V_{m-1,n} + K_2 V_{m,n-1} + K_3 V_{m+1,n} + K_4 V_{m,n+1} - K_0 V_{m,n} = 0 \quad (2.2)$$

where  $K_0$  to  $K_4$  are constants determined by the grid sizes, the permittivities , and the boundary conditions. The basic equation of the FDT to be solved is [12] :

$$[G][\Phi] = [B] \quad (2.3)$$

where:

[G] is a square  $N_f \times N_f$  matrix,  $N_f$  is the number of unknown node potential  $[\Phi]$

[B] is  $N_f \times 1$  column matrix whose elements include known potentials of the bounding electrodes

The electric field is obtained by numerical differentiation of the obtained potential .

### 2.2.2 Finite - Element Technique

According to this technique, the space in which the electric field is to be calculated is divided up into triangular elements as shown in Fig.(2.1). All the elements have the same depth in the Z direction .

Solution of the electric field problems by the finite-element technique is based on a fact , known from variational calculus , that Laplace's equation is satisfied when the total energy functional is minimal . If the permittivity of the medium is  $\epsilon$  , the electrostatic energy functional  $F$  for a flat two - dimensional field is :

$$F = \iint_A \frac{1}{2} \epsilon (\text{grad } \Phi)^2 dA \quad (2.4)$$

where  $A$  represents the area scanned by the triangular element.

The potentials  $\Phi$  at the different nodes are unknown variables and for minimum energy functionals , for all the potentials at the nodes :

$$\frac{\partial F}{\partial \Phi} = 0 \quad (2.5)$$

The minimization of the energy functional for the specific element is expressed as:

$$\frac{\partial F}{\partial [\Phi]} = [S][\Phi] \quad (2.6)$$

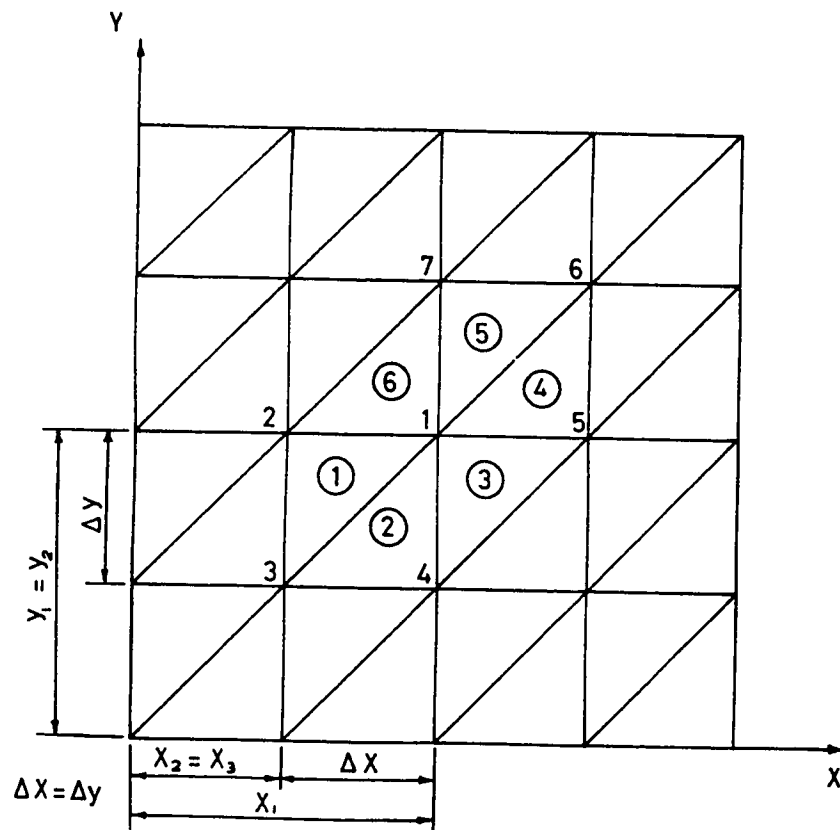


*Fig.(2.1) Grid for the finite - element technique and arrangement of the element*

where:

$[S]$  is the stiffness matrix of the element under consideration.

$[\Phi]$  is the column vector of potential values at element vertices.

Any composite triangular-element assembly may be built up one triangle at a time. It is therefore sufficient to consider how continuity is enforced when one triangular element is added to an already existing assembly. For minimum energy functional, and with properly arranged nodes, equations (2.4) and (2.6) yield :

$$\begin{bmatrix} [S]_f & [S]_b \end{bmatrix} \begin{bmatrix} [\Phi]_f \\ [\Phi]_b \end{bmatrix} \quad (2.7)$$

where:

$[\Phi]_b$  are the bound (known) potential of the nodes lying on the electrode surfaces.

$[\Phi]_f$  are the free (unknown) potentials of the other nodes.

This equation can be rearranged so that the potential at every point in the space between the electrodes could be evaluated in terms of the electrode voltages. Thus:

$$[\Phi]_f = -[S]_f^{-1} [S]_b [\Phi]_b = [T]^{-1} [\Phi]_b \quad (2.8)$$

The solution of Laplace equation takes the form of set of nodal potential values as obtained from equation (2.8).[9,11,13]

Similar to the finite-difference technique, the electric field is obtained by numerical integration of the obtained potential .

### **2.2.3 Charge - Simulation Technique**

A third numerical technique widely and successfully used today to calculate electric fields is known as the Charge Simulation Technique (CST) [11] .

In this technique, the potential of fictitious point, ring and line charges are taken as particular solutions of Laplace's equation . These charges are placed outside the space in which the field is to be computed . The type of these charges is selected according to the geometry of the electrodes to be simulated . The magnitudes of these charges have to be calculated so that their integrated effect satisfies the boundary conditions exactly at a selected number of points on the boundary. As the potential due to these charges satisfy Laplace's equation inside the space under consideration, the solution is unique inside that space.[14,15,16]

The Charge simulation technique has several advantages compared with finite-element and finite-difference techniques. The CST can easily simulate the curved boundaries , however , FET and



FDT can not exactly simulate there boundaries[17]. The FDT and FET are useful only in bounded regions but CST is useful for both bounded and unbounded regions [17]. The attractiveness of CST emanates from its simplicity in representing the equipotential surfaces of the electrodes [15]. The CST is relatively simple to program in comparison with the FET and FDT[12]. The CST is appealing because it is not necessary to compute the potential at points where it is not desired [12]. Another attractive quality is that the analysis of problems, which are not bounded, does not require additional programming effort or additional unknown quantities as in the case of FDT and FET[12]. CST can be applied for two and three dimensional geometries. Also, CST can be used in one and two dielectric materials. The CST uses the potential and field function which are directly based on Coulomb's law and, therefore, automatically fulfill Laplace's equation without any principal error [17]. The field strength computed by the CST is thus very accurate [17].

The above advantages of the charge simulation technique in comparison with the other techniques dictate its selection for calculating the electric field in coated conductor-to-plane gaps.

### **2.3 Onset Voltage Calculation**

The calculation of positive and negative corona onset voltages for coated conductors has not been published in the literature. Also,

measurements of positive and negative onset voltages for coated conductor-plane gaps at different thicknesses have not yet been reported .

However, most previous calculations and measurements of positive and negative onset voltages were for bare conductor - plane and rod-plane configurations as will be presented in the following sub-sections .

### **2.3.1 Positive Onset Voltage**

The criterion of positive corona onset is based on the condition of self-sustained discharge [18]. The criteria was applied for bare conductor-plane and rod-plane gaps . There are many approximations in deriving the equation of positive corona onset voltage[18] . This is because the ionization zone can always be divided into sub-volumes depending on the shape of the ionization zone . Among these approximations is the assumption that one-half of the emitted photons from the primary avalanche will be lost to the anode side which is not true.

In 1976, Abdel-salam ,et al. [19] published a paper on the analysis of discharge development of a positive rod-plane gap in air . In this paper, an improved method is suggested for calculating and correlating the burst-pulse and onset-streamer coronas of positive rod-plane gap in air. It has been found for the first time that the photoelectron distribution within the ionization zone, which depends upon the gap geometry, plays an important role in deciding the discharge

development from burst corona to either onset-streamer or positive glow .

In 1969, Comsa and Vuhuu [20] measured positive ,negative, and ac corona characteristics in wire-plane configurations for wire diameters ranging from 0.175 - 4.6 mm and for gap distances up to 20 cm. The results show that the gap length like the wire diameter plays an important role in the form of corona discharge.

In 1971 , Mosca , Ostano and Rumi [21] measured positive and negative onset voltages of both smooth and stranded conductors. All the measurements carried-out at a height of 12.5m at different conductor diameters.

### **2.3.2 Negative Onset Voltage**

In the literature, the criterion of negative corona onset has received the attention of several investigators over the years . In 1973, Abdel-Salam , et al.[22]described a method for calculating the negative corona onset voltage for any nonuniform field gap with known field distribution without need of experiments. This method is based on a criterion for the recurrence of negative corona pulses.

In 1980, Abou-Seada and Ali [23] published a calculation of the negative corona thresholds of compressed SF6 in space charge

modified nonuniform fields. A mathematical model equivalent to the different possible primary and secondary ionization mechanisms that lead to stable negative corona pulse formation in SF<sub>6</sub> is presented and used to calculate the negative corona threshold of compressed SF<sub>6</sub> in different gap geometries yielding applied electric field distributions of varying degrees of divergence .

Recently , Abdel-Salam and Wiitanen [24] presented theoretical method for calculating the onset voltage of corona in duct-type precipitators that is independent of the arrangement of discharge wires relative to the collecting plates. This method is based on a criterion for self - recurring single electron avalanche in a known field distribution in the ionization zone surrounding the discharge wire . The results computed by this method are in reasonable agreement with those measured experimentally.

As shown from section 2.3 that the positive and negative onset criteria for coated conductors at different coating thickness and permittivity have not yet been studied . This thesis is aimed to formulate mathematically the positive and negative onset criteria for coated conductors to calculate the onset voltages. The calculated positive and negative onset voltages at zero thickness of the coated layer will be compared with those for bare conductors [21].

## **CHAPTER 3**

# **ELECTRIC FIELD CALCULATION**

### **3.1 Introduction**

In the design of high-voltage transmission lines , the knowledge of the exact electric field in the near vicinity of stressed conductors (coated or bare) is a pre-requisite for determining the corona onset voltage .

This chapter presents the calculation method for the electric field in the vicinity of stressed conductors using charge simulation technique . At first, the application of charge simulation technique to both single and two dielectric media is explained . Then, the method is applied to coated transmission lines which are an application of two dielectric media . After that, the computer program written to calculate the electric field around coated transmission lines is demonstrated. Finally, pertinent numerical data and check results to validate the calculation method are given .

## **3.2 Charge Simulation Technique**

The charge simulation technique can be employed successfully for the computation of the electric field between electrodes in a medium composed of one or two dielectrics .

### **3.2.1 Field Calculation in a Single Dielectric Medium**

The distributed charges on the surface of the electrode which bounds the medium are replaced by a set of fictitious discrete charges arranged inside the electrode , that is , outside the medium in which the field is to be computed [12,14,16]. The number of charges and their coordinates are arbitrary . However, the larger the number of charges, the higher is the possible accuracy of computation. In order to determine the magnitudes of these simulation charges, contour points on the surface of the electrode , equal in number to the simulation charges ,are chosen and it is required to satisfy pertinent boundary condition at any of these points [9,11,13].

The charges simulating a given electrode could be chosen as point charges , ring charges, or as finite, semi-infinite, or infinite line charges[9,15]. This choice should suit the shape of the electrode being simulated. Figure (3.1) shows different choices of the simulation charges.

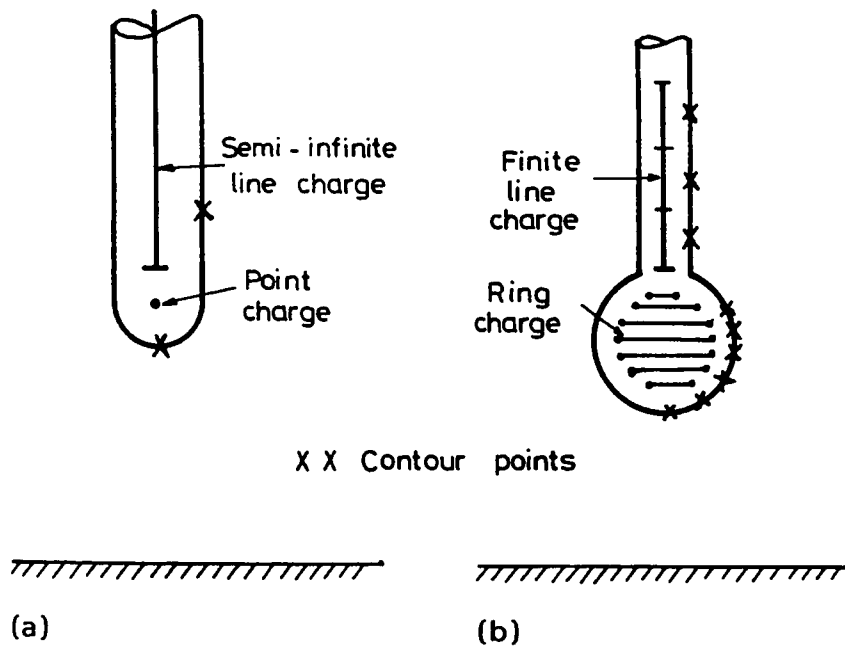


**Fig.(3.1) Arrangement of simulation charges and contour point:**  
**(a) hemispherically capped rod, (b) sphere with cylindrical shank**

for a hemispherically capped rod electrode and a sphere with cylindrical shank.

### 3.2.1.1 Boundary Conditions

The boundary condition at the  $i$  th contour point on the electrodes' surface is that the calculated potential  $\Phi_i$  due to the simulation charges is equal to the applied electrode voltage  $V_i$  at the  $i$  th contour point [9,13,14] .

$$\Phi_i = \sum_{j=1}^{j=n} p_{i,j} q_j = V_i \quad (3.1)$$

$$p_{i,j} = \frac{1}{2 * \pi * \epsilon_0} * \text{Ln} \left[ \frac{1}{\text{distance between } i\text{th point and } j\text{th charge}} \right] \quad (3.2)$$

Where

$q_j$  is the  $j$  th simulation charge

$p_{i,j}$  is the potential coefficient calculated at the  $i$  th point  
due to the  $j$  th simulation charge

$n$  is the number of simulation charges

$\epsilon_0$  is the permittivity of air

If the electrodes are at a finite height from the ground plane ,  
assumed horizontally flat , then , images of the simulation charges



are considered to simulate the effect of the ground plane. In this case, the potential coefficient  $P_{i,j}$  is expressed as:

$$P_{i,j} = \frac{1}{2\pi\epsilon_0} \text{Ln} \left[ \frac{\text{distance between } i\text{th point and image of the } j\text{th charge}}{\text{distance between } i\text{th point and the } j\text{th charge}} \right] \quad (3.3)$$

Satisfaction of the boundary condition using equation.(3.1) applied at all the contour points formulates a set of simultaneous equations whose solution determines the unknown simulation charges [9,11,13,14];

$$[p] [q] = [v] \quad (3.4)$$

Where:

$[P]$  is a square  $n \times n$  potential coefficient matrix

$[q]$  is  $(n \times 1)$  column matrix whose elements are the unknown simulation charges

$[v]$  is  $(n \times 1)$  column matrix whose elements are the potential values of the contour points

### 3.2.1.2 Electric Field

Once the unknown simulation charges are determined, the electric field  $\vec{E}$  at any point in the medium surrounding the

electrodes or on the surface of the electrodes themselves is expressed as [9,11]:

$$\bar{\mathbf{E}} = \mathbf{E}_x \bar{\mathbf{U}}_x + \mathbf{E}_y \bar{\mathbf{U}}_y = \sum_{j=1}^{i=n} \mathbf{f}_{i,j} \mathbf{q}_j \quad (3.5)$$

where:

$\mathbf{f}_{i,j}$  is the field coefficient calculated at the  $i$ th point due to  $j$ th charge

$\bar{\mathbf{U}}_x$  &  $\bar{\mathbf{U}}_y$  are unit vectors along the X and Y directions

$\mathbf{E}_x$  &  $\mathbf{E}_y$  are the components of  $\bar{\mathbf{E}}$  along the X and Y directions

The potential and field coefficients for the different simulation charges are reported in [13].

For sufficient accuracy, effort should be devoted to choose the proper number and location of simulation charges. The calculated potential can not be easily equal to the applied voltage  $V$  at every point on the electrode surface under the effect of the simulation charges.

### 3.2.2 Field Calculation in a Two - Dielectric Medium

In a two dielectric medium, the simulation charges are located as shown in Fig.(3.2) where there is a boundary electrode and two dielectrics **I** and **II**.

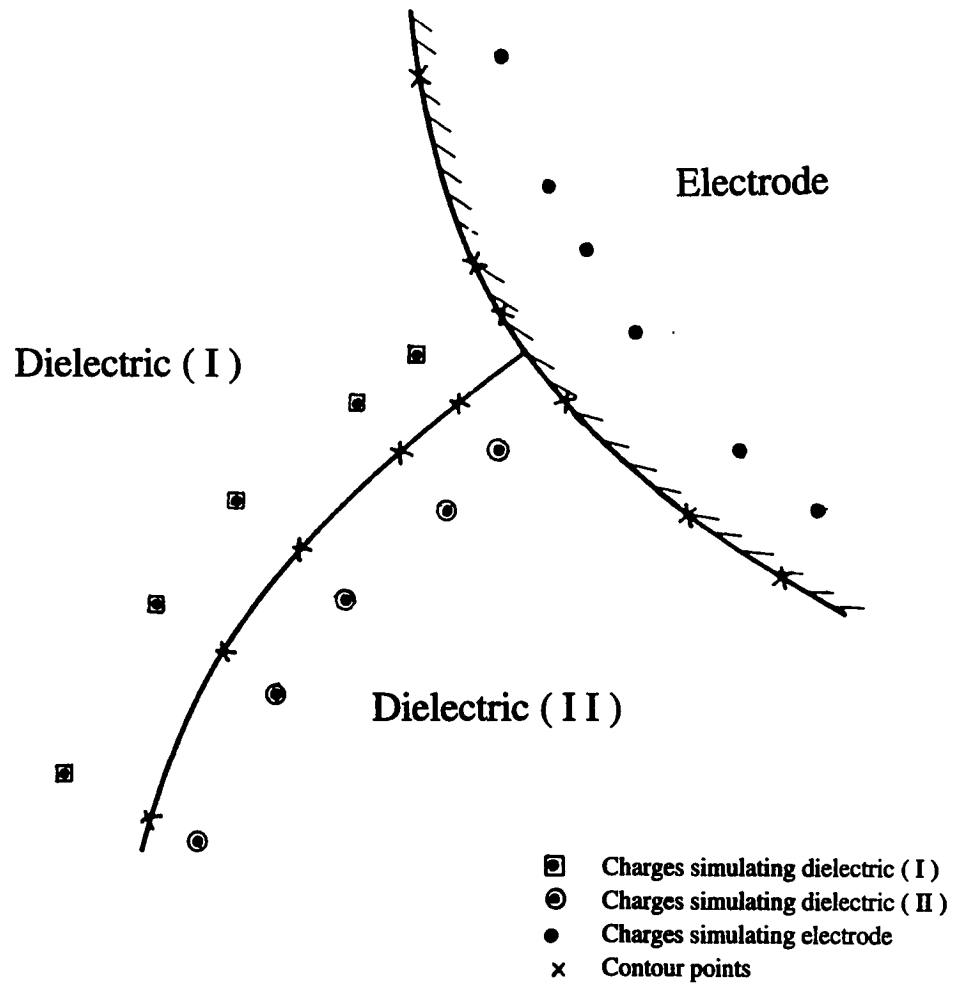


*Fig.(3.2) Discrete simulation charges at an electrode and a dielectric boundary.*

The distributed charge on the electrode surface is replaced by fictitious charges arranged inside the electrode as described in 3.2.1. In each dielectric, dipoles are aligned by the electric field - due to the voltage applied to the electrode and compensate each other through the volume of the dielectric, leaving net charges at the interface. These charges are simulated by two fictitious charges one in dielectric I and the other in dielectric II. The number of simulation charges in dielectric I is the same as that in dielectric II.[9,11,14]

In order to determine the magnitudes of simulation charges in dielectrics I and II, contour points are chosen:

- 1)-On the electrode surface with number equal to that of the charges inside the electrode
- 2)-On the interface between dielectrics with number equal to that of the simulation charges either in dielectric I or II, are chosen.

It is required to satisfy pertinent boundary conditions at any of these points.

### **3.2.2.1 Boundary Conditions**

The following boundary conditions should be applied to calculate the field in a two-dielectric medium :

1)-The potential  $\Phi_I$  calculated at any point on the electrode / dielectric-I boundary is the algebraic sum of the potentials at this point produced by the simulation charges belonging to the electrode and dielectric-II . Similarly, the potential  $\Phi_{II}$  at any point on the electrode / dielectric-II boundary is the algebraic sum of the potentials at this point produced by the simulation charges belonging to the electrode and dielectric-I. Of course, these potentials  $\Phi_I$  and  $\Phi_{II}$  must be equal to the voltage  $V$  applied to the electrode ;[9,11]

$$\begin{aligned}\Phi_I &= V \\ \Phi_{II} &= V\end{aligned}\tag{3.6}$$

Instead of one boundary condition at each point on the electrode surface, two boundary conditions are satisfied at each contour point on the interface between dielectrics I and II .

2)-The potential  $\Phi_I$  at any point along the dielectric interface is the algebraic sum of potentials at this point due to the simulation charges belonging to the electrode and dielectric-II, if the point is seen from dielectric-I side . If the point is seen from dielectric-II side , the potential  $\Phi_{II}$  is the algebraic sum of the potentials due to the simulation charges belonging to the electrode and dielectric-I [9,11,14]. Of course, the potentials  $\Phi_I$  and  $\Phi_{II}$  are equal ;

$$\Phi_I - \Phi_{II} = 0 \quad (3.7)$$

3)-The electric field  $E_{nI}$  normal to the interface between dielectrics at any point along this interface is the vector sum of the normal components at this point due to the simulation charges belonging to the electrode and dielectric-II, if the point is seen from the dielectric-I side. If the point is seen from dielectric-II side, the normal electric field  $E_{nII}$  is the vector sum of the normal field components due to the simulation charges belonging to the electrode and dielectric-I. The normal field  $E_{nI}$  and  $E_{nII}$  are related to each other through the permittivities  $\epsilon_I$  and  $\epsilon_{II}$  of dielectrics I and II respectively, to satisfy the continuity of the electric flux normal to the dielectrics interface ;[9,11,14]

$$\epsilon_I E_{nI} - \epsilon_{II} E_{nII} = 0 \quad (3.8)$$

Satisfaction of the boundary conditions (using equations 3.6 - 3.8), applied at the respective boundary point, formulates a set of simultaneous equations expressed as ;

$$\begin{bmatrix} \frac{P}{f} \end{bmatrix} \begin{bmatrix} \mathbf{q} \end{bmatrix} = \begin{bmatrix} \frac{V}{0} \end{bmatrix} \quad (3.9)$$

where:

$P$  is the potential coefficient

$f$  is the field coefficient

Solution of the set (3.9) determines the unknown simulation charges .

### 3.2.2.2 Electric Field

Once the unknown simulation charges are determined , the electric field  $\bar{E}$  at any point in the dielectrics I and II or at the dielectrics interface can be calculated.

## 3.3 Application to Coated Transmission Lines

The charge simulation technique is applied for field calculation around a coated transmission line which is located at height  $H$  above the ground plane . The model of a coated conductor , Fig. (3.3) , is represented in one half only because of the symmetry about Y-axis. The fictitious simulation infinite line charges is divided into 3 equal sets, one for simulating the conductor and two sets for the two dielectrics (coating layer and surrounding air ) . The following subsections describe the detailed location of the three sets of fictitious charges, the location of the contour points and the formulation of coefficient matrix whose solution determines the unknown charges .

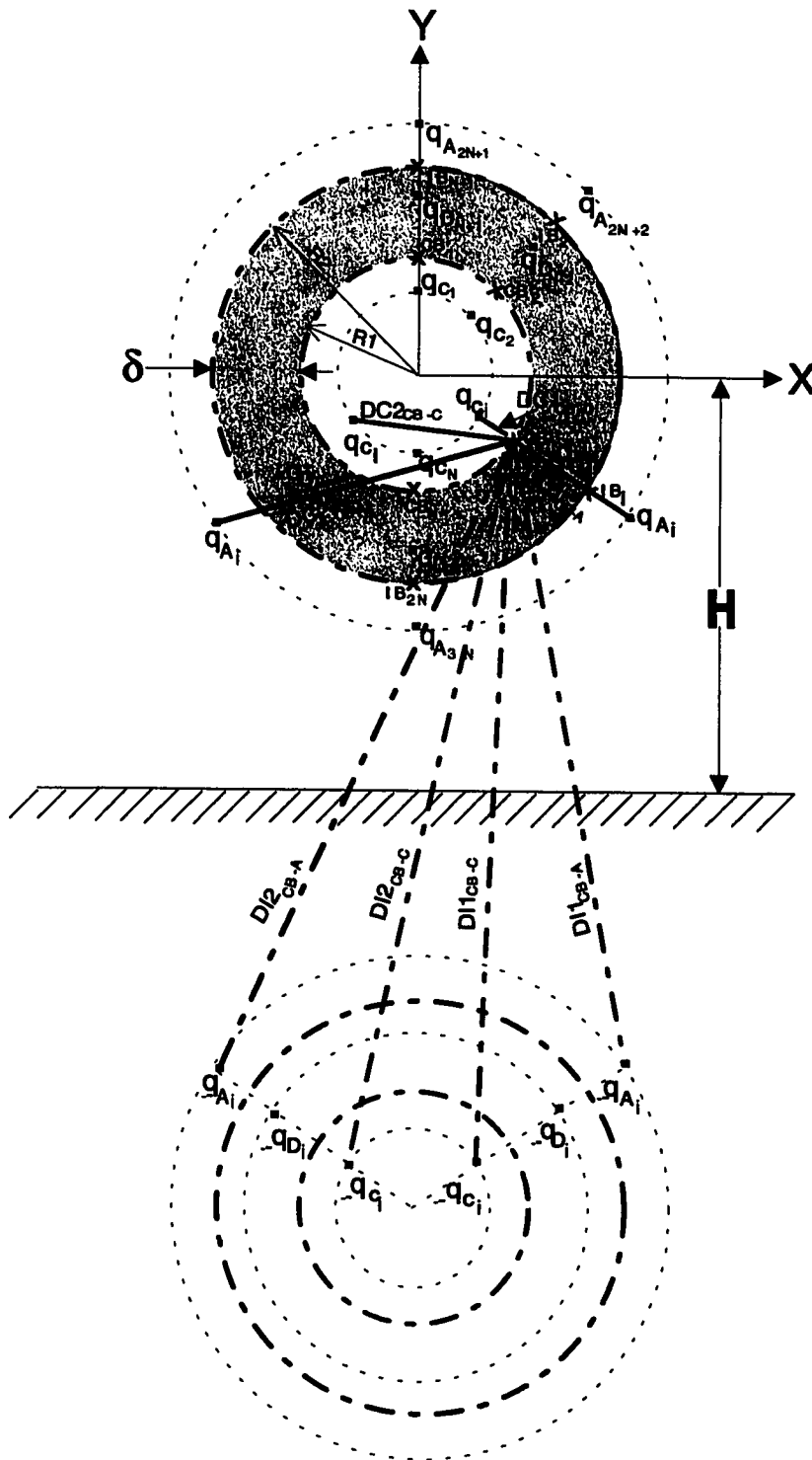


*Fig.(3.3) Location of charges and boundary points for coated conductor*



### 3.3.1 Location of Simulation Charges:

As shown from Fig. (3.3) ,  $3 * N$  unknown fictitious simulation charges are located in the right side of the Y-axis as follows :

- Locate simulated charges  $q_{c_i}$  where  $i = 1, 2, \dots, N$  inside the conductor at coordinates expressed as :

$$\begin{aligned} X(i) &= F1 * R1 * \sin(\theta) \\ Y(i) &= F1 * R1 * \cos(\theta) \end{aligned} \quad (3.10)$$

where :

**F1** is a fraction to locate the charges inside the conductor .

**R1** is the conductor radius

**$\theta$**  is the angle at which the charges are located

- Locate simulated charges  $q_{d_i}$  where  $i = N+1, N+2, \dots, 2*N$  inside the dielectric layer at coordinates expressed as :

$$\begin{aligned} X(i) &= F2 * R2 * \sin(\theta) \\ Y(i) &= F2 * R2 * \cos(\theta) \end{aligned} \quad (3.11)$$

where :

**F2** is a fraction to locate the charges inside the dielectric .

**R2** is the conductor radius after being coated (equal to  $R1 + \delta$ )

**$\delta$**  is the thickness of the coating layer

- Locate simulated charges  $q_{a_i}$  where  $i = 2*N+1, 2*N+2, \dots, 3*N$  in the air at coordinates expressed as :

$$\begin{aligned} X(i) &= F3 * R2 * \sin(\theta) \\ Y(i) &= F3 * R2 * \cos(\theta) \end{aligned} \quad (3.12)$$

where **F3** is a fraction exceeding unity to locate the charges in the air.

### 3.3.2 Location of Contour Points

Corresponding to each simulated charge in the conductor, a contour point is chosen on the conductor surface as shown in Fig.(3.3). Also, corresponding to each simulation charge in the dielectric coating layer or in the surrounding air, a contour point is chosen on the interface between the dielectric and air. The coordinates of these boundary points are as follows :

- The coordinates of contour points ( $CB_i$  where  $i=1,2,\dots,N$ ) on the conductor surface are:

$$\begin{aligned} X(i) &= R1 * \sin(\theta) \\ Y(i) &= R1 * \cos(\theta) \end{aligned} \quad (3.13)$$

- The coordinates of contour points ( $IB_i$  where  $i=N+1, N+1, \dots, 2N$  & for  $i=2N+1, 2N+2, \dots, 3N$ ) at the interface between the air and the dielectric layer are:

$$\begin{aligned} X(i) &= R2 * \sin(\theta) \\ Y(i) &= R2 * \cos(\theta) \end{aligned} \quad (3.14)$$

### 3.3.3 Coefficient Matrix Formulation

To find the solution of  $3*N$  unknown fictitious simulation charges, a coefficient matrix should be formulated. The formulation of the coefficient matrix elements will be according to the following boundary conditions which have been mentioned briefly in the previous section :

- 1)-The potential at a contour point ( $CB_i$ ) on the conductor / dielectric interface must be equal to the applied voltage ( $V_{ap}$ ) :

$$\sum_{j=1}^N P_{CB-C_{i,j}} q_{C_j} + \sum_{j=2N+1}^{3N} P_{CB-A_{i,j}} q_{A_j} = V_{ap} \quad (3.15)$$

The potential coefficients ( $P_{CB-C}$  &  $P_{CB-A}$ ) calculated at the  $i$ th contour point on the surface of the conductor ( $CB_N$ ) due to the  $j$ th simulation charges  $q_{C_j}$  &  $q_{A_j}$  are given as:

$$P_{CB-C_{i,j}} = \frac{1}{2 * \pi * \epsilon_0} \text{Ln} \left( \frac{DI1_{CB-C_{i,j}} * DI2_{CB-C_{i,j}}}{DC1_{CB-C_{i,j}} * DC2_{CB-C_{i,j}}} \right) \quad (3.16)$$

$$P_{CB-A_{i,j}} = \frac{1}{2 * \pi * \epsilon_0} \text{Ln} \left( \frac{DI1_{CB-A_{i,j}} * DI2_{CB-A_{i,j}}}{DC1_{CB-A_{i,j}} * DC2_{CB-A_{i,j}}} \right)$$

where :

$DC1_{CB-C}$  &  $DC2_{CB-C}$  are the distances between the  $i$ th contour point on the conductor surface and the

$j$  th charges which are located to the right and left sides of the Y-axis inside the conductor, Fig.(3.3) .

$DI1_{CB-C}$  &  $DI2_{CB-C}$  are the distances between the  $i$  th contour point on the conductor surface and the two images of the  $j$  th charges (located in the conductor) , w.r.t. the ground plane, Fig.(3.3).

$DC1_{CB-A}$  &  $DC2_{CB-A}$  are the distances between the  $i$  th contour point on the conductor surface and the  $j$  th charges which are located to the right and left side of Y-axis in the air as shown in section (3.3.1), Fig.(3.3).

$DI1_{CB-A}$  &  $DI2_{CB-A}$  are the distances between the  $i$  th contour point on the conductor surface and the two images of the  $j$  th charges (located in the air) , w.r.t. the ground plane, Fig.(3.3).

2)-The potential at each of the contour points ( $IB_i$ ) on the interface between the coating-layer and the air is the same from either side : that is,

$$\sum_{j=N+1}^{2N} P_{IB-D \ i,j} q_{D_j} - \sum_{j=2N+1}^{3N} P_{IB-A \ i,j} q_{A_j} = 0 \quad (3.17)$$

The potential coefficients ( $P_{IB-D}$  &  $P_{IB-A}$ ) calculated at the  $i$  th contour point on the interface between air and dielectric ( $IB_i$ ) due to the  $j$ th simulation charges  $q_{D_j}$  &  $q_{A_j}$  in air and dielectric respectively, are expressed as :

$$P_{IB-D \ i,j} = \frac{1}{2 * \pi * \epsilon_0} \text{Ln} \left( \frac{DI1_{IB-D \ i,j} * DI2_{IB-D \ i,j}}{DC1_{IB-D \ i,j} * DC2_{IB-D \ i,j}} \right) \quad (3.18)$$

$$P_{IB-A \ i,j} = \frac{1}{2 * \pi * \epsilon_0} \text{Ln} \left( \frac{DI1_{IB-A \ i,j} * DI2_{IB-A \ i,j}}{DC1_{IB-A \ i,j} * DC2_{IB-A \ i,j}} \right)$$

where :

$DC1_{IB-D}$  &  $DC2_{IB-D}$  are the distances between the  $i$  th contour point on interface between air and dielectric and the  $j$ th charges which are located to the right and left side of Y-axis inside the dielectric .

$DI1_{IB-D}$  &  $DI2_{IB-D}$  are the distances between the  $i$  th contour point on interface between air and dielectric and the two images of the  $j$ th charges (located in the dielectric) , w.r.t. the ground plane.

$DC1_{IB-A}$  &  $DC2_{IB-A}$  are the distances between the  $i$  th contour point on interface between air and dielectric and the  $j$  th charges which are located to the right and left side of Y-axis in the air.

$DI1_{IB-A}$  &  $DI2_{IB-A}$  are the distances between the  $i$  th contour point on interface between air and dielectric and the two images of the  $j$  th charges (located in the air) , w.r.t. the ground plane.

3)-The electric flux at the interface between the coating-layer and the air is continuous. This continuity is expressed as:

$$\epsilon_r \epsilon_0 \left( \sum_{j=1}^N f'_{IB-C_{i,j}} q_{C_j} + \sum_{j=2N+1}^{3N} f'_{IB-A_{i,j}} q_{A_j} \right) - \epsilon_0 \left( \sum_{j=1}^N f'_{IB-C_{i,j}} q_{C_j} + \sum_{j=N+1}^{2N} f'_{IB-D_{i,j}} q_{D_j} \right) = 0 \quad (3.19)$$

Equation (3.19) can be rewritten as:

$$(\epsilon_r - 1) \sum_{j=1}^N f'_{IB-C_{i,j}} q_{C_j} - \sum_{j=N+1}^{2N} f'_{IB-D_{i,j}} q_{D_j} + \epsilon_r \sum_{j=2N+1}^{3N} f'_{IB-A_{i,j}} q_{A_j} \} = 0 \quad (3.20)$$

where:

$\epsilon_r$  is the relative permittivity of the coating layer  
 $f'_{IB-C}$  is the electric field coefficient calculated at the  $i$  th contour point on the interface between air and dielectric due to the

$j$  th simulation charges in the conductor and their images w.r.t. the ground plane.

$f'_{IB-D}$  is the electric field coefficient calculated at the  $i$  th contour point on the interface between air and dielectric due to the  $j$  th simulation charges in the dielectric layer and their images w.r.t. the ground plane.

$f'_{IB-A}$  is the electric field coefficient calculated at the  $i$  th contour point on the interface between air and dielectric due to the  $j$  th simulation charges in the air and their images w.r.t. the ground plane.

Thus,  $3*N$  linear equations are formulated as shown in equation (3.21) for the calculation of the same number of unknown fictitious simulation charges.

$$\begin{array}{c}
 \begin{array}{ccc}
 1 & N & 2N & 3N \\
 \begin{array}{c} N \\ 2N \\ 3N \end{array} &
 \begin{array}{|c|c|c|}
 \hline
 P_{CB-C} & 0 & P_{CB-C} \\
 \hline
 0 & P_{IB-D} & -P_{IB-A} \\
 \hline
 (\epsilon_r - 1)f'_{IB-C} & -f'_{IB-D} & \epsilon_r f'_{IB-A} \\
 \hline
 \end{array}
 \end{array}
 \begin{array}{c}
 \begin{array}{|c|}
 \hline
 q_{C_1} \\
 \hline
 q_{C_N} \\
 \hline
 q_{D_{N+1}} \\
 \hline
 q_{D_{2N}} \\
 \hline
 q_{A_{2N+1}} \\
 \hline
 q_{A_{3N}} \\
 \hline
 \end{array}
 =
 \begin{array}{|c|}
 \hline
 V \\
 \hline
 0 \\
 \hline
 0 \\
 \hline
 \end{array}
 \end{array}
 \quad (3.21)
 \end{array}$$

After formulating the coefficient matrix (equation (3.21)), the method of Gauss elimination is used to solve for the  $3*N$  unknown charges.

### 3.3.4 Accuracy Measurement

After solving equation (3.21) for the  $3*N$  unknown charges, it is necessary to check whether the set of calculated charges satisfy the boundary conditions with acceptable accuracy. Therefore, equations (3.15) & (3.17) must be additionally used to compute the potentials at a number of check points located on the conductor and on the interface between the air and the coating-layer. The location of the check points is different from that of the contour points. Usually, check points are located midway between contour points. If the difference between the calculated potentials at the check points selected on conductor surface and the applied voltage  $V_{ap}$  is not acceptable then more charges should be added. If the calculated potential  $\Phi_{air}$  at the check points selected on the surface of the coating layer when seen from the air side differs from the corresponding potential  $\Phi_{dielec}$  when the check points are seen from the coating-layer side, then more charges have to be adopted. The accuracy is improved by increasing the number of simulated charges, but on the expense of computational time.

Also, the ratio between electric field at the air side over the electric field at the coating-layer side ( $E_{air} / E_{dielec}$ ) at the interface



between the coating-layer and surrounding air is considered another check of the accuracy of the simulation. This ratio should be equal to the relative permeability of coating-layer.

### **3.4 Programming**

In order to calculate the electric field around a coated transmission line by using the charge simulation technique, a computer program is written for this purpose which follows the flow chart of Fig.(3.4).

The block diagram shows that the calculation of electric field using charge simulation technique goes through several steps . These steps can be explained as follows :

- Simulated fictitious charges are located in the conductor , coating-layer and in the air as described in section 3. 3.1 .
- Contour points equal in number to the simulated charges are located at the conductor surface and on the interface between the air and the coating-layer as described in section 3.3.2 .
- Coefficient matrix is formulated at the boundary points . It contains  $3*N$  linear equations and  $3*N$  unknown charges
- A subroutine based on Gauss elimination is used to calculate the inverse of the coefficient matrix and to solve for the  $3*N$  unknown charges.

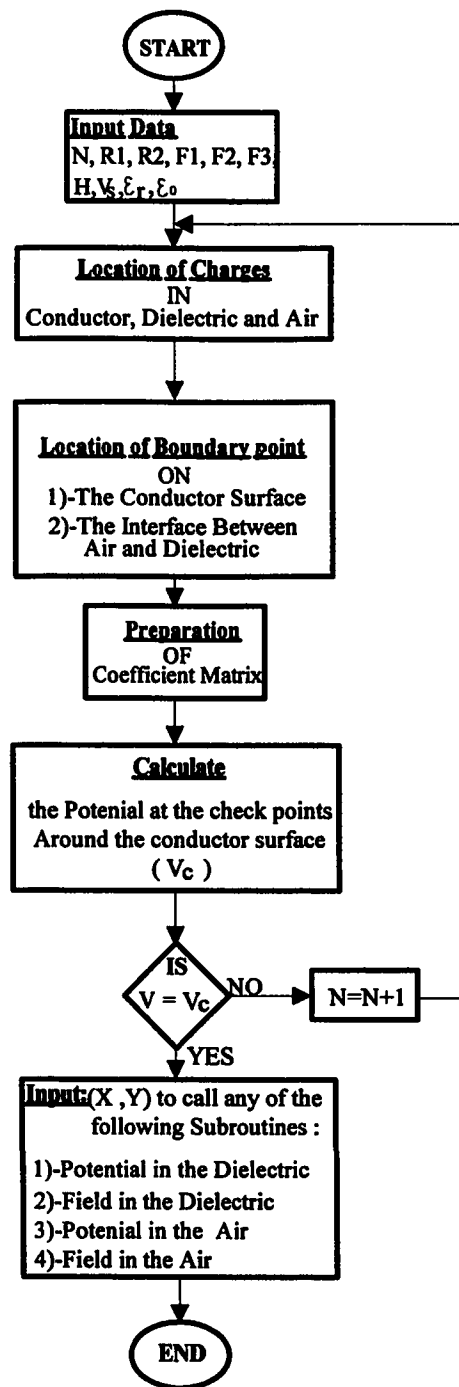


*Fig.(3.4)Flow chart To calculate Electric Field  
by using charge simulation Technique*

- Locate number of check points on the conductor and on the interface between the air and the coating-layer.
- The known charges are used to calculate the potential at the check points on the conductor. The difference between these potential and the applied potential is a measure of the accuracy. More charges are needed for better accuracy.
- The difference between  $\Phi_{\text{air}}$  and  $\Phi_{\text{dielec}}$  at the check points on the interface between the air and the coating-layer is another measure of the accuracy of simulation.
- Check that the ratio between  $E_{\text{air}} / E_{\text{dielec}}$  at the check points on the interface between the air and the coating-layer is equal to the relative permeability of the coating-layer. For better accuracy, more charges are required.
- Separate subroutines are prepared to calculate the electric field and the potential in the air and the coating-layer.

### 3.5 Numerical Data

The proposed method has been applied to a coated conductor which is located at height  $H$  above the ground plane. This conductor has the following particulars :

- The radius of the conductor ( $R_1$ ) = 0.001 m
- The radius of the conductor after being coated ( $R_2$ ) = 0.005 m where the coating-layer assumes larger values . This is aimed to check the correctness of the field calculation .
- The distance between the ground plane and the center of the conductor ( $H$ ) = 0.5 m
- The fraction  $F_1$  defining the location of the simulation charges inside the conductor = 0.2
- The fraction  $F_2$  defining the location of the simulation charges inside the dielectric layer = 0.5
- The fraction  $F_3$  defining the location of the simulation charges in the air = 1.2

The above choice for the values of  $F_1$ ,  $F_2$  and  $F_3$  resulted in acceptable accuracy of the simulation.

Several numbers of the simulation charges were attempted . It has been found that a satisfactory accuracy of the simulation is achieved when the number of simulation charges  $N$  is 50 .

### **3.6 Accuracy of the Calculated Potential and Field Values**

Based on the numerical data mentioned in the previous section , it has been found that the error in the potential at the conductor surface did not exceed 0.0000001 % .

Also, Table (3.1) shows that the error in the ratio  $E_{\text{air}} / E_{\text{dielec}}$  on the interface between the coated-layer and the air did not exceed 0.00271%.

Angle (degree)	$E_{\text{air}} / E_{\text{dielec}}$	Error %
0	4.1999998	0.0000047
30	4.1999717	0.000674
60	4.1999150	0.00202
90	4.1998862	0.00271
120	4.1999146	0.00203
150	4.1999714	0.0006809
180	4.1999997	0.0000095

*Table(3.1) Error in the calculated ratio  $E_{\text{air}} / E_{\text{dielec}}$*

Angle (degree)	$V_{\text{air}}$ (V)	$V_{\text{dielec}}$ (V)
0	0.932869369248	0.932286936926
30	0.932827347570	0.932827347578
60	0.932712107529	0.932712107537
90	0.932553962374	0.932553962408
120	0.932394973259	0.932394973267
150	0.932278045131	0.932227804514
180	0.932235131556	0.932235131590

*Potential at the interface between air and coating-layer*

Table (3.2)

Moreover, Table (3.2) indicates that the potential calculated at air side and that at the coating-layer side at the check points on the interface between the coating-layer and the air are almost the same .

Figure (3.5) shows the per-unit potential distribution along the gap axis starting from the conductor surface. It is quite clear that the potential decreases continuously along the gap axis without showing discontinuity at the interface between the dielectric and surrounding air .

Finally, Figure (3.6) shows the field distribution along the gap axis starting from the conductor surface. It is quite clear that the field shows a discontinuity at the interface where the ratio  $E_{\text{air}} / E_{\text{dielec.}}$  equals the relative permittivity of the dielectric as shown in table-1 (with an error not exceeding .002%).

For comparison purposes, the Figure (3.6) shows also that the field distribution for a bare conductor of the same radius as the coated one . It appears that the coated layer suppresses the field in the vicinity of the conductor surface in comparison with the bare conductor. This reflects itself on increasing the corona onset voltage at the surface of coated conductors . The area under the curves describing the field distribution for bare and coated conductors, Fig. (3.6), is equal to the applied voltage .

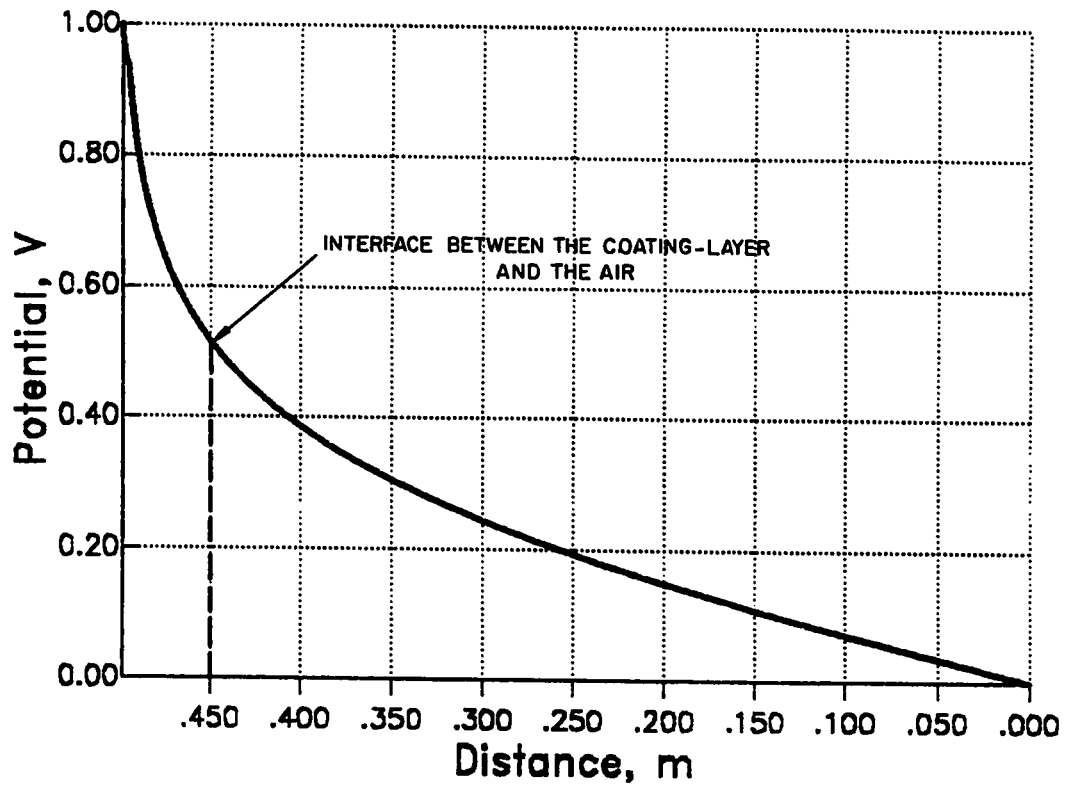


Fig.(3.5) The potential distribution along gap axis for coated conductor,  
 $R_2=0.5$  cm,  $R_1=0.1$  cm and  $H=50$  cm

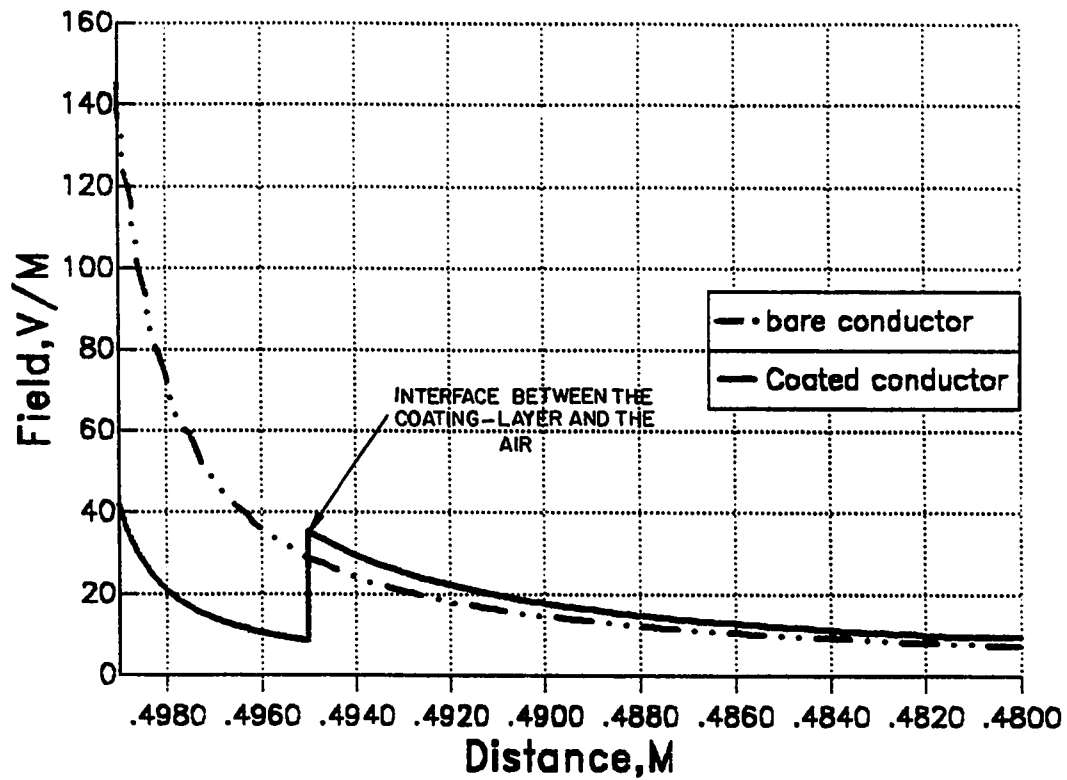


Fig.(3.6) Electric field distribution along gap axis for bare and coated conductor,  $R_2=0.5$  cm,  $R_1=0.1$  cm and  $H=50$  cm.



## **CHAPTER 4**

### **CORONA ONSET VOLTAGE CRITERIA**

#### **4.1 Introduction**

This chapter presents the corona onset criteria for both positive and negative coronas. Firstly, the onset criteria will be briefly described. Secondly, the criteria will be formulated mathematically. Thirdly, the computer programs written for calculating the onset voltage will be explained in detail. Finally, some numerical data and results for checking the accuracy of the calculation will be reported.

#### **4.2 Positive Corona**

The positive onset voltage criterion for a coated transmission line located at a height  $H$  above the ground is explained in this section .

##### **4.2.1 Criterion of Onset Voltage**

When a high voltage,  $V_{ap}$ , is applied to a coated conductor located at a height  $H$  above the ground plane, a small volume of space, called

the ionization-zone, exists around the conductor if the voltage is sufficiently high . The ionization-zone around the conductor is defined as the space where the field-strength is so high that the coefficient of ionization by electron collision,  $\alpha$ , is greater than the electron attachment coefficient,  $\eta$ , i.e.  $\alpha \geq \eta$ (Fig.(4.1)).[2]

If a free electron originates in the ionization-zone from cosmic-rays or from any other source of radiation , an electron avalanche will be created by a process called ionization by electron impact. This electron avalanche is called Primary Avalanche (or the first generation of avalanches). As the primary avalanche builds up, an increasing number of electrons crowd at its progressing tip while positive ions form a growing cloud in its wake. The electrons at the tip of the primary avalanche accelerate under the resultant of both the applied field and the field produced by the positive space charge at the wake.[18,19]

While the primary avalanche builds up, excitation of air atoms has been taking place at the same time ionizations have been occurring. Excited states have lifetimes that can be as short as  $10E-13$  second . Thus, before the primary avalanche has reached its full size, photons will be emitted from these excited states as they return to the ground state (see Fig.(4.2))[18,25]. The ratio between the number of excitation events and the number of ionization events is  $f_2$ .

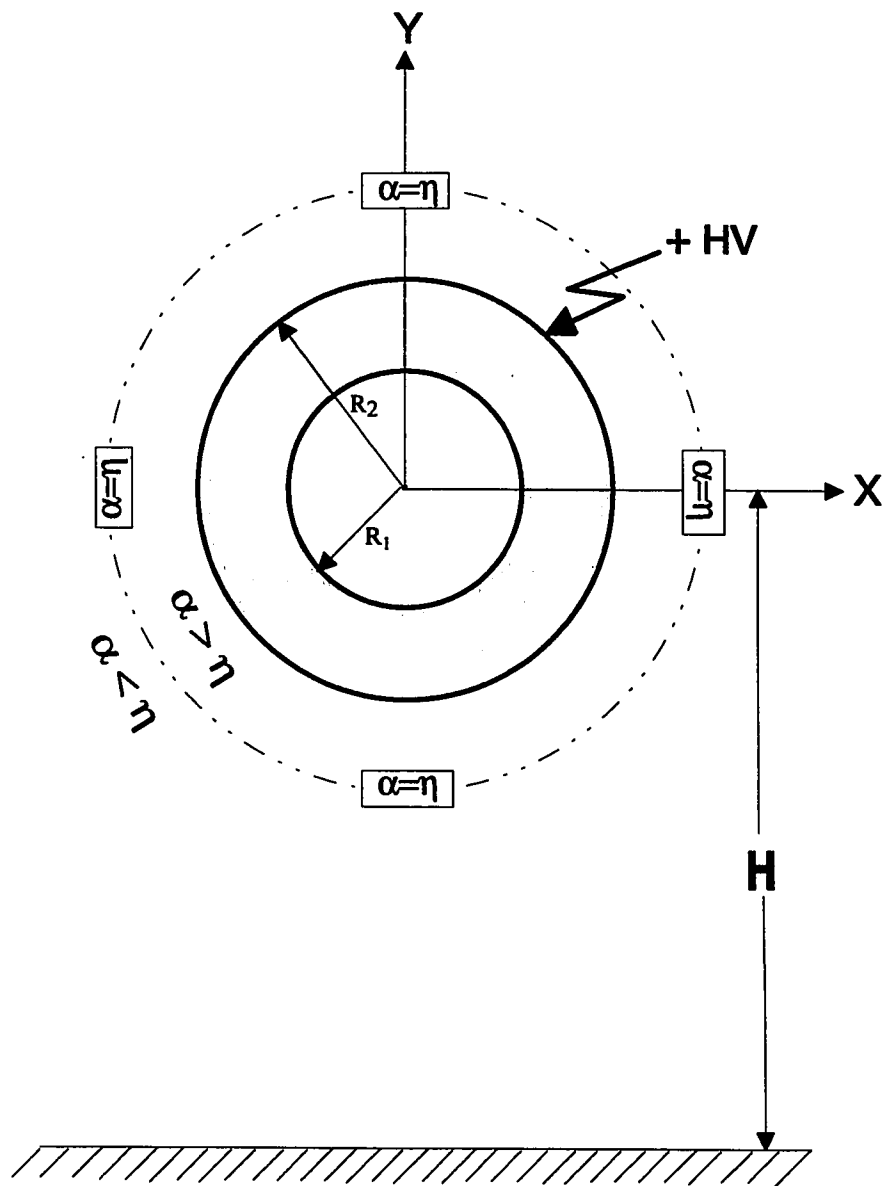


*Fig.(4.1) Ionization zone around a coated conductor*

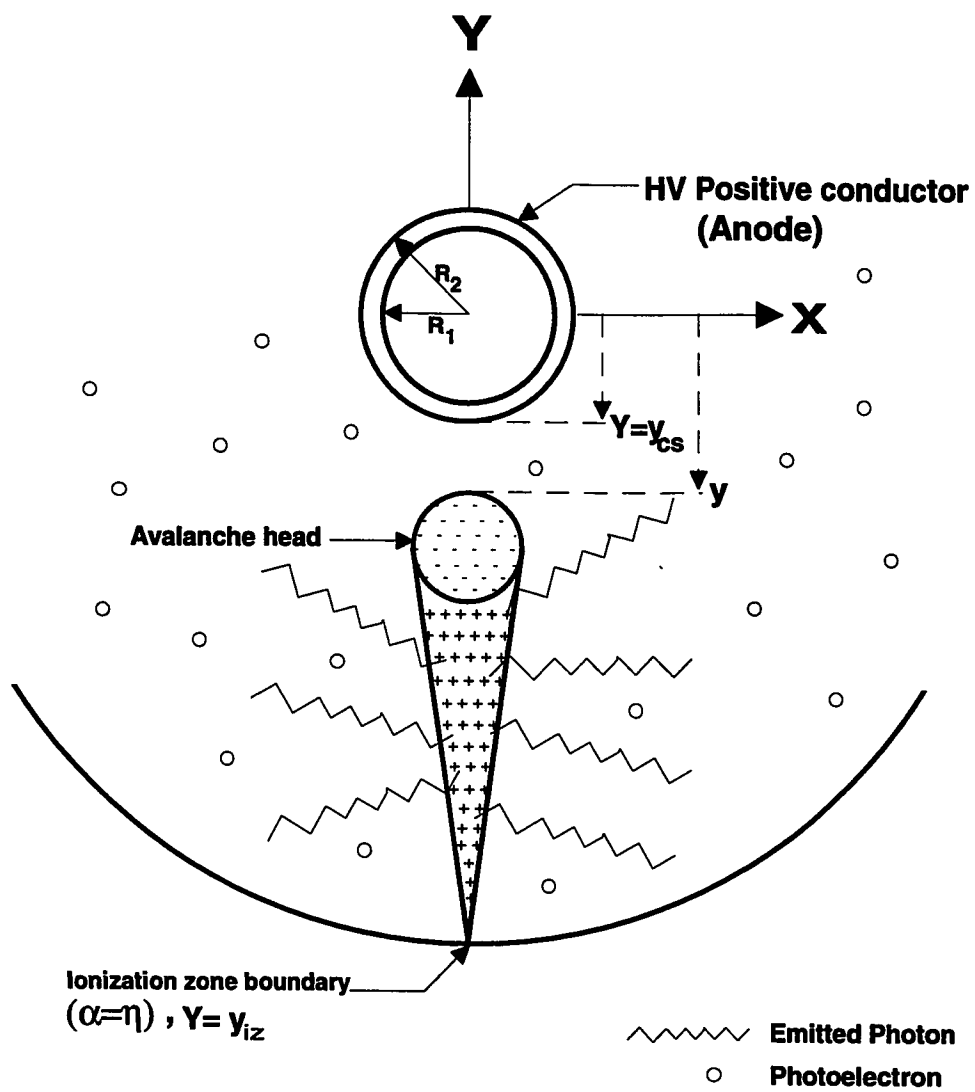


*Fig.(4.2) The growth of Primary avalanche and the emission of photons*

As shown from Fig.(4.2), photons will be emitted in all directions and will be absorbed at various distances from their origin, depending on the absorption coefficient,  $\mu$ , of the air which is a function of the electric field.

Many processes can take place when a photon is absorbed and many processes combined may lead to photoionization of the air inside the ionization zone with a probability factor  $f_1$ [18,19] .

Now, new photoelectrons are available in the air to start successor avalanches (of the second generation) at various distances from the primary avalanche (see Fig.(4.3))that is still advancing toward the conductor. Most of these successor avalanches get started at the instant of termination of the primary avalanche.

It should be recalled that each successor avalanche of the second generation during its growth is subjected to three components of electric field. These components are the field applied due to  $V_{ap}$  the voltage applied to the conductor , the field produced by the positive ions in the wake of the primary avalanche and the field due to positive ions in the wake of successor avalanche . The successor avalanches grow towards the positive space-charge left by the primary avalanche, Fig.(4.3) .

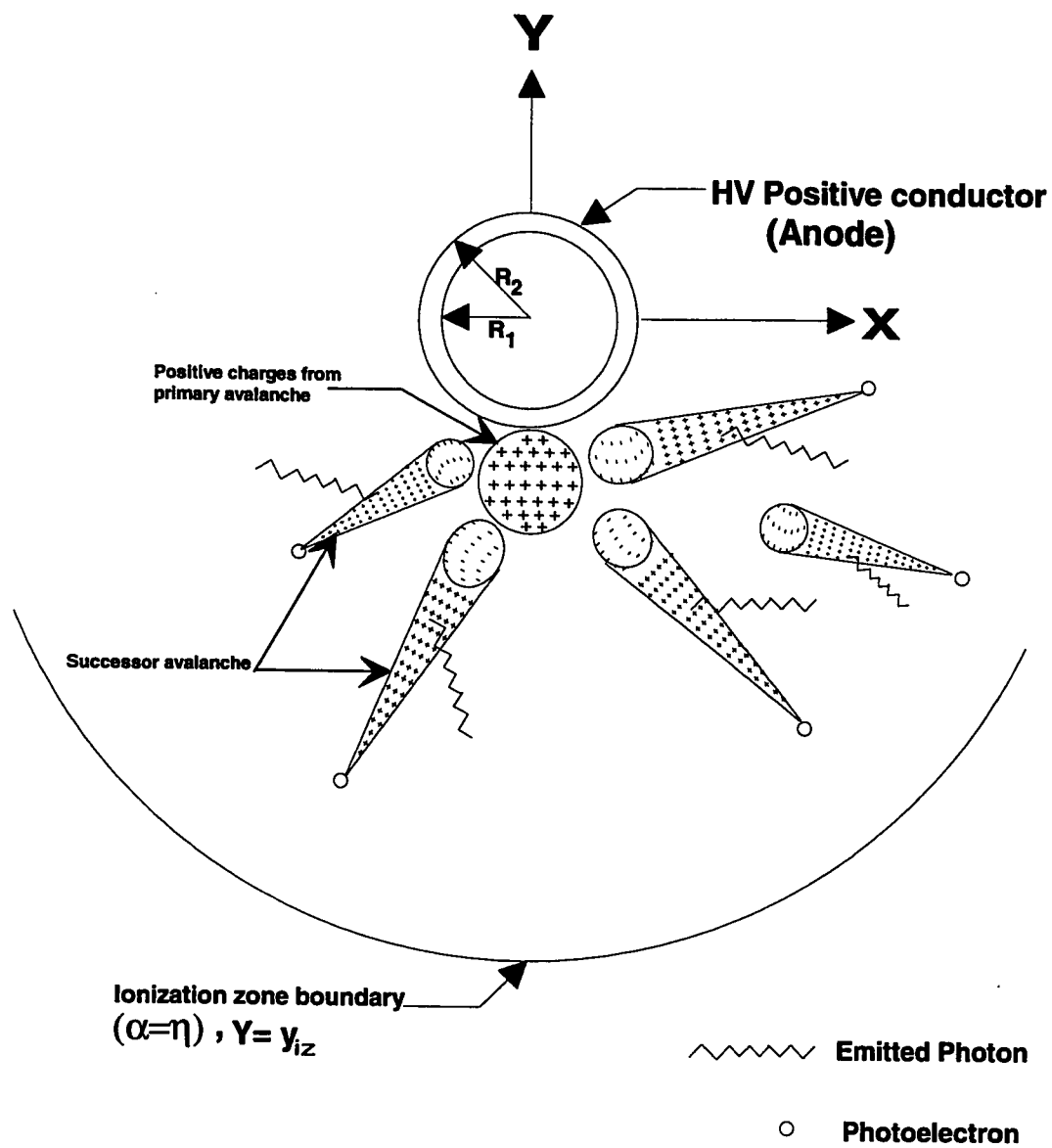


Fig.(4.3) The growth of successor avalanche

Likewise, in the growth of the primary avalanche, all successor avalanches of the second generation will emit photons as they are being formed. These photons create new photoelectrons which will start a third-generation of avalanches and so on. [18]

With the accumulation of the positive ions created by the successor avalanches, an onset-streamer develops.

As a result, the criterion for a self-propagating onset-streamer is that all the successor avalanches of the second generation produce a positive space charge at least equal to the positive space charge of the primary avalanche [18,25,27].

#### **4.2.2 Mathematical Formulation of the Onset Criterion**

The mathematical expression of the onset criterion for positive corona is formulated based on the physical phenomenon described in the previous section.

One electron is assumed to start from rest at the ionization boundary, where  $\alpha > \eta$ . The number of electrons at the tip of the primary avalanche, during its growth along the Y-axis, is expressed as [18,19,25]:

$$N_{pe}(y) = e^{\int_{y_{iz}}^y (\alpha(y) - \eta(y)) dy} \quad (4.1)$$

where:

$y$  is the y-coordinate of the tip of the primary avalanche.

$y_{iz}$  is the y-coordinate where the primary avalanche starts

The coefficients  $\alpha$  and  $\eta$  at any point throughout the length of the primary avalanche are calculated. As the coefficients  $\alpha$  and  $\eta$  depend on the electric field,  $E(y)$  at the head of the avalanche is given by (4.2).

$$\bar{E}(y) = E_{ap.}(y)\bar{u}_{-y} + E_{p.sc}(y)\bar{u}_y \quad (4.2)$$

$$E_{p.sc}(y) = 1.6 * 10^{-19} * \frac{e^{\sum_{l=y_{iz}}^y (\alpha(l) - \eta(l)) * \Delta X} - 1}{4 * \pi * \epsilon_0 * D_{psc}^2(y)} \quad (4.3)$$

where:

$E_{ap.}$  is the electric field due to the voltage applied to the conductor

$E_{p.sc}$  is the electric field due to the positive space charge left in the wake of the primary avalanche

$\Delta X$  is a constant increment distance

$D_{psc}$  is the distance between the positive space charge left in the wake of the primary avalanche and the point at which the field is to be calculated

$\bar{u}_{-y}$  is the unit vector in the negative Y-direction



It has been realized that the positive space charge in the wake of primary avalanche is assumed lumped as a point charge located at a distance  $1/\alpha$  from the head of the primary avalanche [28].

Since the primary avalanche during its growth emits photons, the number of emitted photons are given as :

$$N_{ph}(y) = N_{pe}(y) * f_2 \quad (4.4)$$

where :

$f_2$  is the ratio between the number of excitation events and the number of ionization events.

As shown in Fig.(4.4), the number of photoelectrons  $(\Delta N_{ph})_j$  created in the  $j$ th sub-volume at a distant  $\rho$  from the center of the primary avalanche is expressed as :

$$(\Delta N_{ph})_j = \frac{\Delta Y_j * \Delta Z_j}{4 * \pi * \rho_j^2} * f_1 * f_2 * N_{pe}(y)_j * \mu_j * e^{-\mu_j \rho_j} * \Delta \rho_j \quad (4.5)$$

where :

$f_1$  is the probability of photoionization  
 $\mu$  is the photon absorption coefficient ( $m^{-1}$ )  
 $\rho_j$  is the distance between the tip of the primary avalanche and the  $j$ th sub volume

All the photoelectrons created in each sub-volume inside the ionization zone will start successor avalanches of the second generation. Each successor avalanche will produce a number of electrons. The number of electrons at the tip of the successor avalanche starting from the  $j$  th sub-volume are given as :

$$N_{s,e_j}(L) = e \int_{L_{st,j}}^L (\alpha(L) - \eta(L)) dL \quad (4.6)$$

where :

$L_{st,j}$  defines the starting point of the  $j$  th successor avalanche

It should be noted that the electric field where the successor avalanche accelerates is the resultant of three components, equation (4.7), namely, the applied electric field, the electric field produced by the positive space charges left by the primary avalanche which is located at the conductor surface and the electric field due to the positive space charges of the successor avalanche itself [18]. Therefore,  $\alpha(L)$ , and  $\eta(L)$  are determined according to the resultant field  $E(L)$

$$\bar{E}(L) = \bar{E}_{ap}(L) + \bar{E}_{p.sc}(L) + \bar{E}_{s.sc}(L) \quad (4.7)$$

$$\bar{E}_{p.sc_j}(L) = 1.6 * 10^{-19} * \frac{(N_e(y_{cs}) - 1.0)}{4.0 * \pi * \epsilon_0 * D_{s-psc_j}^2(L)} \quad (4.8)$$

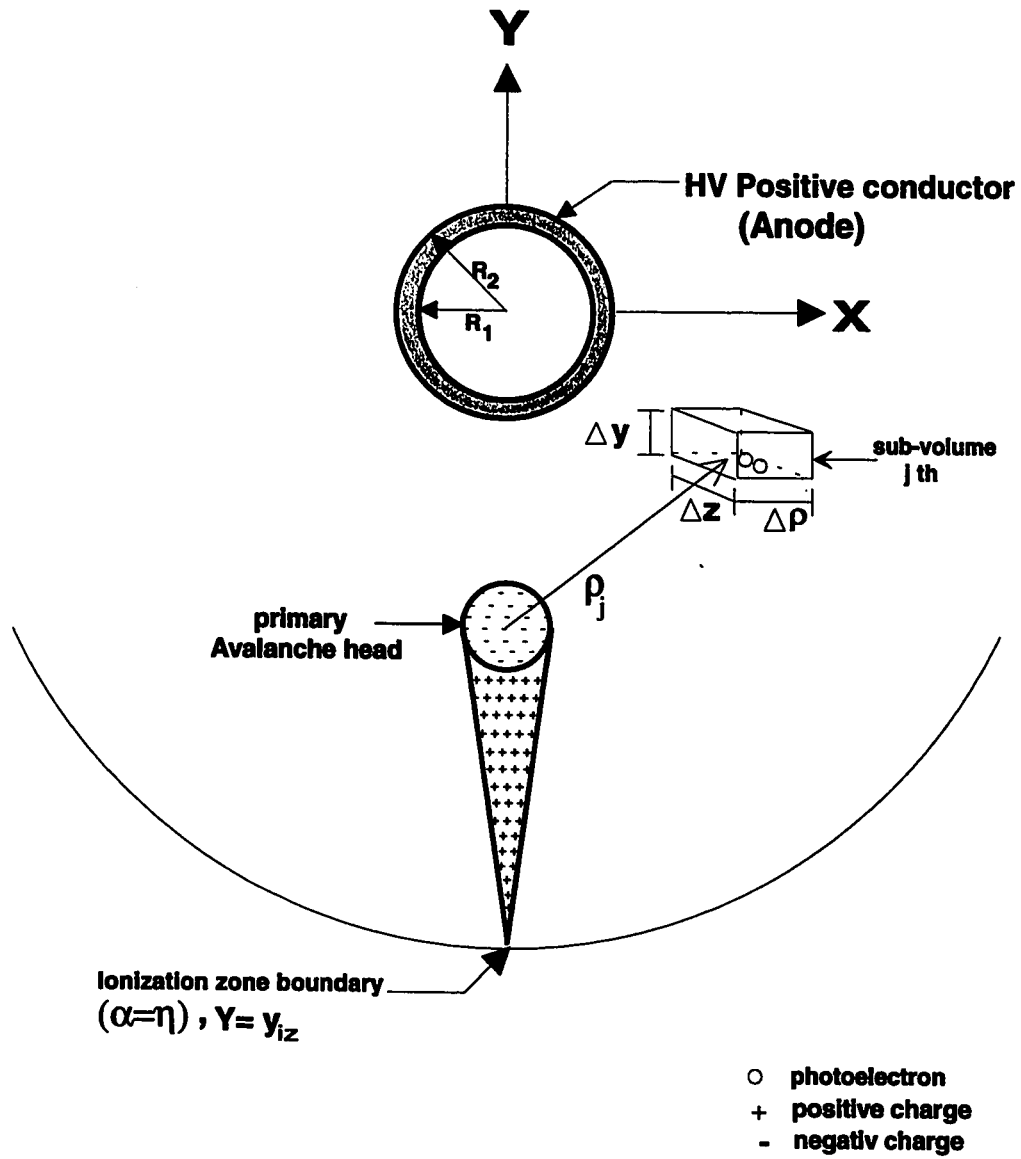


*Fig.(4.4) photoelectrons created in sub-volume*

$$\bar{E}_{s.sc_j}(L) = 1.6 * 10^{-19} * \frac{e^{\sum_{l=L_{st,j}}^L [\alpha_j(l) - \eta_j(l)]} - 1.0}{4.0 * \pi * \epsilon_0 * D_{s.sc_j}^2(L)} \quad (4.9)$$

Where :

$\bar{E}_{p.sc_j}$  is the electric field due to the positive space charges left by the primary avalanche .

$N_{pe}(y_{cs})$  is the total number of electrons produced by the primary avalanche.

$D_{s-p.sc_j}$  is the distance between the location of the positive space charges left by of the primary avalanche and the point at which the field is to be calculated.

$\bar{E}_{s.sc_j}$  is the electric field due to the positive space charges at the wake of the successor avalanche for the jth sub-volume.

$D_{s.sc_j}$  is the distance between the location of the positive space charges left in the wake of the successor avalanche and the point at which the field is to be calculated .

Equation (4.10) shows that the number of positive ions produced by the jth sub-volume  $(\Delta N_{secondary})_j$  is equal to the product of the number of photoelectrons in that sub-volume (equation (4.5)) and the number of positive ions produced by each photoelectron (equation (4.6))[18].

$$(\Delta N_{\text{secondary}})_j = \frac{\Delta Y_j \Delta Z_j}{4\pi\rho_j^2} f_1 f_2 N_{pe}(y_{cs})_j \mu_j e^{-\mu_j \rho_j} \Delta\rho_j e^{\int_{L_{st,j}}^{L_{f,j}} (\alpha(L) - \eta(L)) dL} \quad (4.10)$$

where:

$L_{f,j}$  defines the end points of the successor avalanche starting from the  $j$  th sub-volume.

As a result of the growth of all successor avalanches, the total number of positive space charges produced by the second generation is given as[18,29]:

$$N_{\text{secondary}} = \sum_{j=1}^M \frac{\Delta Y_j \Delta Z_j}{4\pi\rho_j^2} f_1 f_2 N_{pe}(y_{cs})_j \mu_j e^{-\mu_j \rho_j} \Delta\rho_j e^{\int_{L_{st,j}}^{L_{f,j}} (\alpha(L) - \eta(L)) dL} \quad (4.11)$$

Where :

$N_{\text{secondary}}$  is the total number of positive ions produced by all successor avalanches.

$M$  is the total number of sub-volumes in the ionization zone.

The onset criterion for a self-maintained ionization process is that  $N_{\text{secondary}}$ , the total number of positive ions produced by all successor avalanches (equation(4.12)), is equal to  $N_{pe}(y_{cs})$  the total number of positive ions left by the primary avalanche [18,19,25,29]. Thus, the mathematical expression for the of onset voltage criterion is given as:

$$\sum_{j=1}^M \frac{\Delta Y_j \Delta Z_j}{4\pi\rho_j^2} f_1 f_2 \mu_j e^{-\mu_j \rho_j} \Delta\rho_j e^{\int_{L_{st,j}}^{L_{tj}} (\alpha(L) - \eta(L)) dL} = 1.0 \quad (4.12)$$

The onset voltage  $V_{0+}$  does not appear explicitly in equation(4.12). However, the critical value of the applied voltage  $V_{ap}$  which satisfies the equality (4.12) is the onset value .

### 4.2.3 Programming of Onset Criterion

A computer program has been built to calculate the onset voltage for positive corona which satisfies the equality (4.12) . The flow chart of this computer program which is supported by three subroutines is shown in Fig.(4.5).

The computer program and all subroutines are written in double precision Fortran language. The details of the field calculation have been previously explained in Chapter 3.

Since there is a symmetry around both the Y and the Z-axes , the computation is limited to one quarter of the ionization zone around the coated conductor (see Fig.(4.6)) .

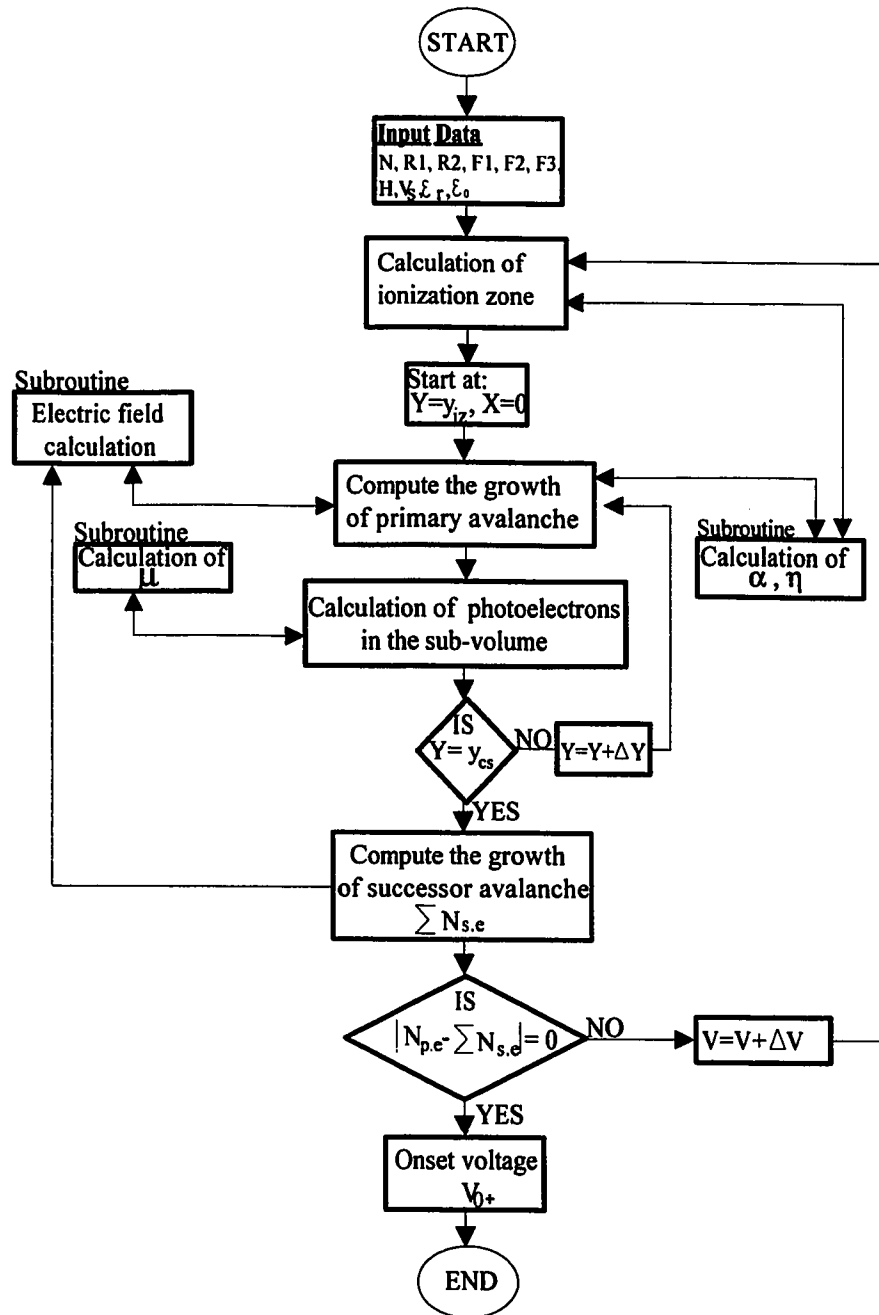
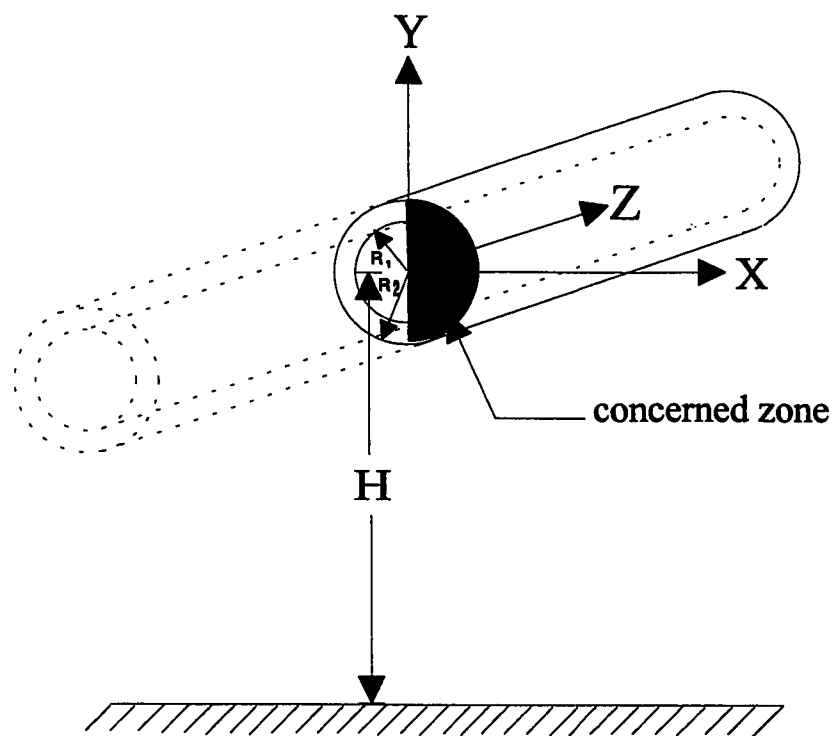
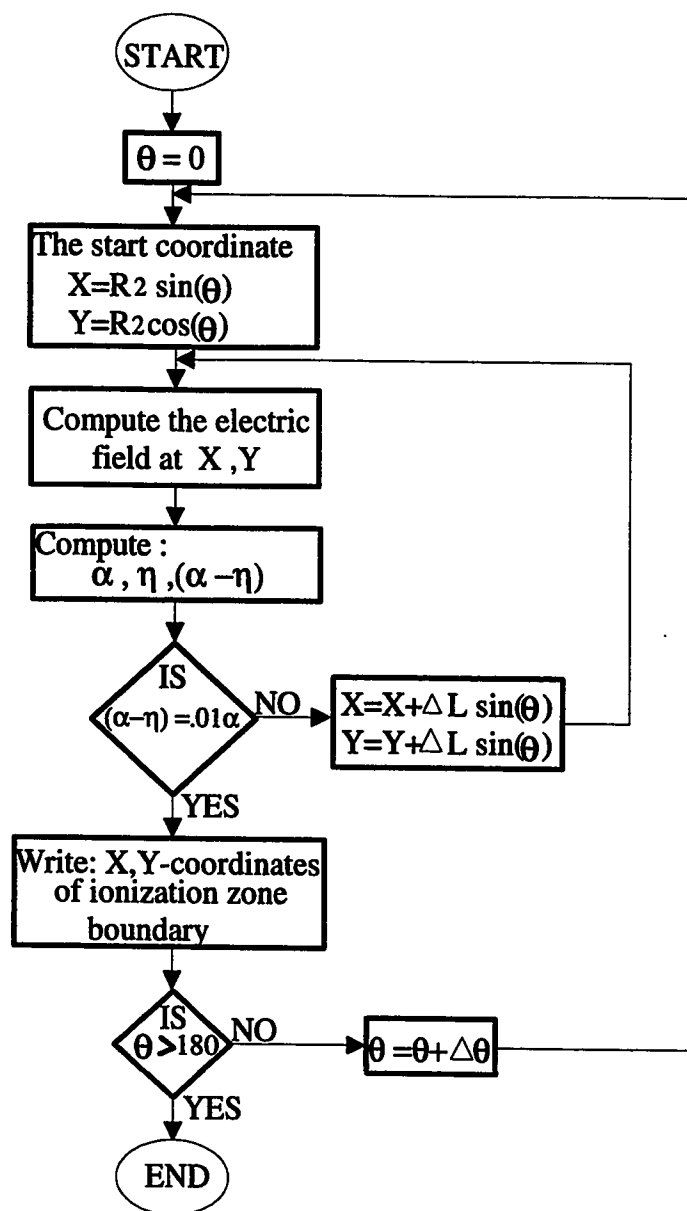


Fig.(4.5) The main flow chart



*Fig.(4.6) One quarter of the ionization zone around coated conductor*





*Fig. (4.7) The flow chart for determining the ionization zone boundary*

### 4.2.3.1 Ionization-Zone Boundary Computation

The flow chart of Fig.(4.7) describes the steps required to determine the coordinates of the ionization-zone boundary:

- Start from the conductor surface at point P, Fig.(4.8), of coordinates expressed by:

$$\begin{aligned} X &= R2 * \sin(\theta) \\ Y &= R2 * \cos(\theta) \end{aligned} \tag{4.13}$$

where:

$\theta$  is the angle measured from the vertical axis as shown in Fig.(4.8)

- Compute the electric field at the point P.
- Compute the corresponding values of the ionization coefficient  $\alpha$  and the attachment coefficient  $\eta$ .
- If the absolute value of the difference between  $\alpha$  and  $\eta$  is less than  $(.01 * \alpha)$ , then  $\alpha$  becomes equal  $\eta$  within  $\pm 1\%$  and the point P is located at the ionization-zone boundary along the radial  $\theta$ -direction. Otherwise, X and Y coordinates are to be increased by  $\Delta L$ . Thus, the new coordinates for the point P are expressed as:

$$\begin{aligned} X &= X + \Delta L * \sin(\theta) \\ Y &= Y + \Delta L * \cos(\theta) \end{aligned} \tag{4.14}$$

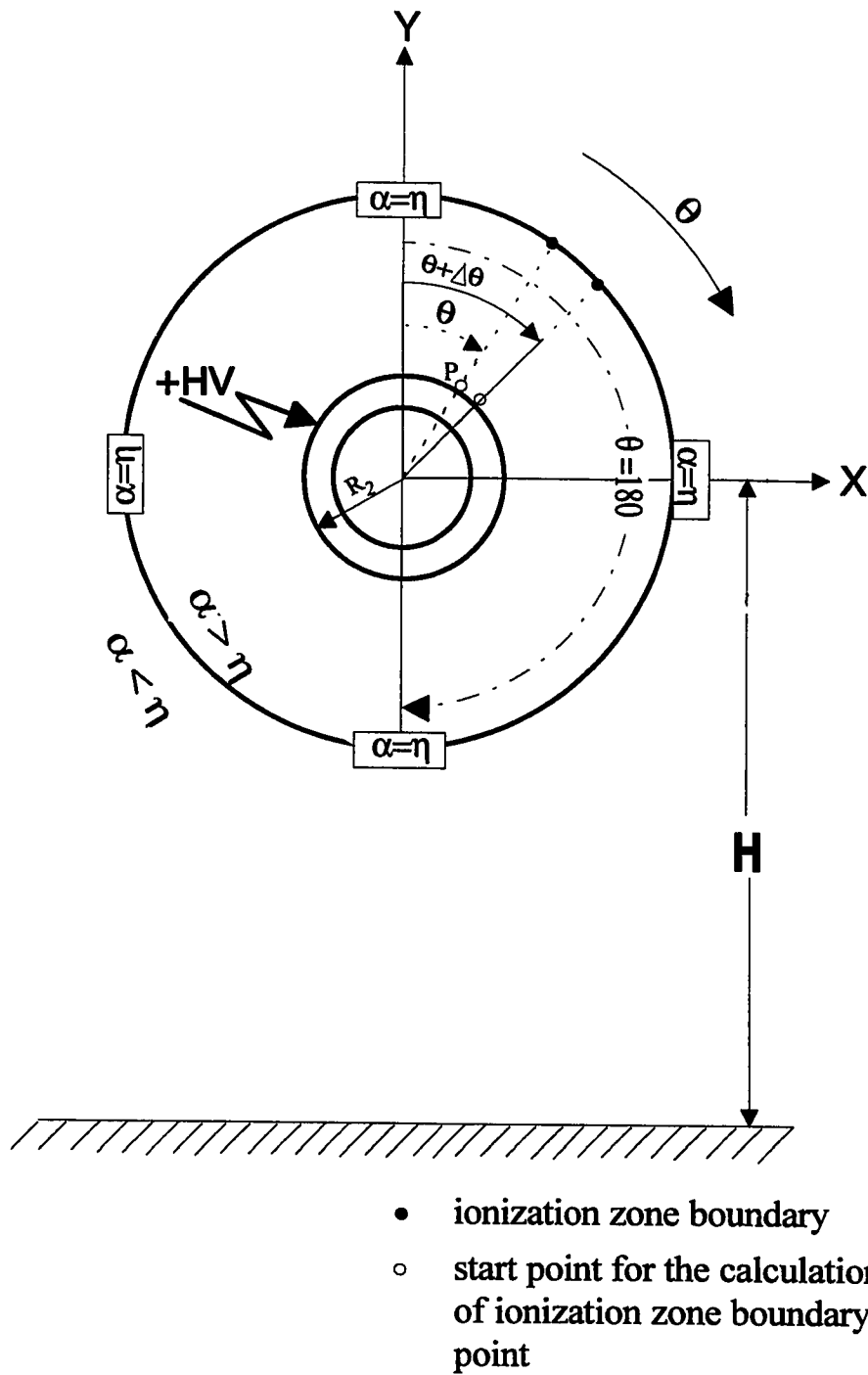


*Fig.(4.8) Computation of ionization zone boundary*

- Repeat all the above steps for other values of  $\theta$  in the range 0-180°, where there is a symmetry about the Y-axis .

#### **4.2.3.2 Primary Avalanche Growth**

Figure (4.9) shows the detailed flow chart for the primary avalanche growth. This flow chart is described through the following steps:

- A free electron is assumed to start from rest at the ionization zone boundary coordinate ( $Y=Y_{iz}, X=0$ ) where  $\alpha=\eta$  at  $\theta=180^\circ$ .
- The applied electric field is computed at any instant during the growth of the primary avalanche.
- Electric field due to the positive charge in the primary avalanche's wake is calculated at any instant during the avalanche growth except at the ionization-zone boundary where no space charge because the positive point has not been yet created .
- The total electric field which is the resultant of the applied field and the field produced by the positive charge in the primary avalanche's wake is computed .

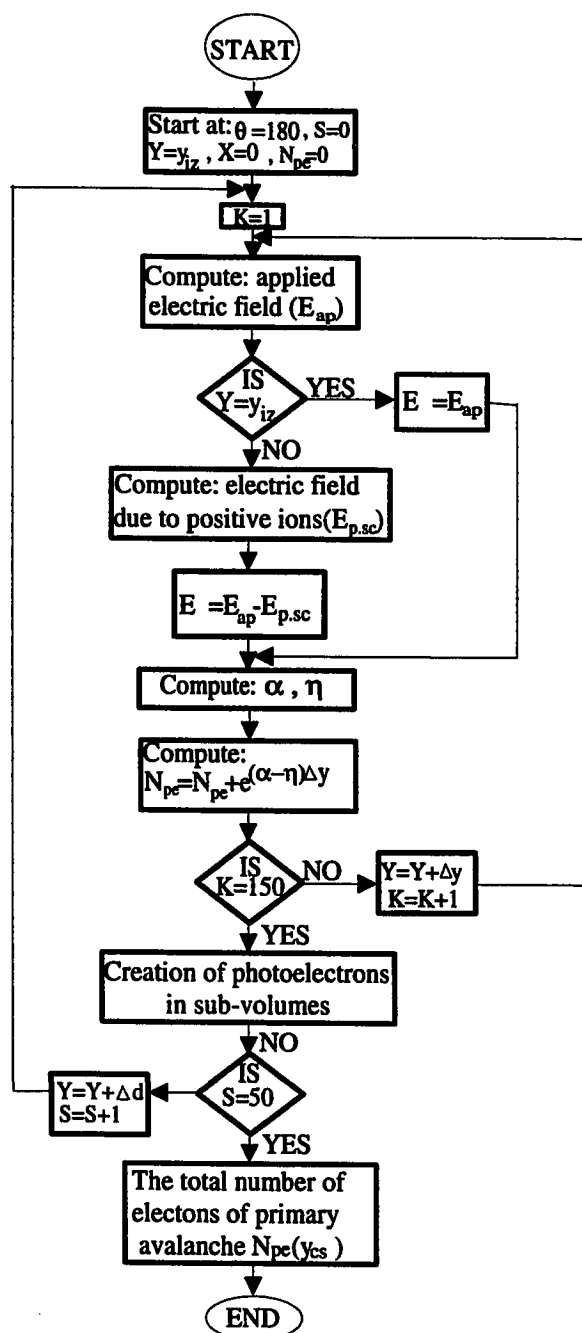


Fig.(4.9)The flow chart for primary avalanche

- All field dependent parameters (  $\alpha$  and  $\eta$  ) are calculated as a function of the total field .
- Use equation (4.1) to calculate number of electrons created in the head of the primary avalanche after a distance  $\Delta y$  .
- The above steps should be repeated during the growth of the primary avalanche taken into account that number of electrons at a particular  $\Delta y$  should always be added to the previous number of electrons.
- As mentioned in Section (4.2.1), the primary avalanche during its growth emits photons. The growth of the primary avalanche is divided into 150 steps and the emission of photons is determined every these steps . Thus, photon emission is computed 50 times along the avalanche growth .
- The above steps should be repeated until the primary avalanche reach the surface of the coated conductor.
- The total number of electrons produced during the growth of the primary avalanche is equal to the summation of the electrons produced in the above steps .

#### 4.2.3.3 Calculation of Photoelectrons in the Sub-Volume

This section describes the process of dividing the ionization zone into sub-volumes (Fig.(4.10) ) and the calculation of photoelectrons generated in each sub-volume.

As shown in Fig.(4.10), the division of ionization zone begins by dividing it into levels along the y-axis direction. These levels are determined at each boundary point on the ionization-zone as described in Section (4.2.3.1). Then, each level is divided into equal number of segments in the X-axis direction. Finally, each slab is divided into five equal sub-volumes along the z-axis direction, Fig.(4.10) .

The flow chart of Fig.(4.11) describes how photoelectrons are created in each sub-volume. The steps are as follows:

- Compute number of sub-volumes in each level. Then, find the location of each sub-volume in each level.
- Calculate the applied electric field ( $E_{ap}$ ) at each sub-volume. Then, use this field to compute the absorption coefficient  $\mu$ .
- Use equation (4.5) to find number of photoelectrons created in the  $j$  th sub-volume at a distance  $\rho_j$  from the center of the primary avalanche while growing.

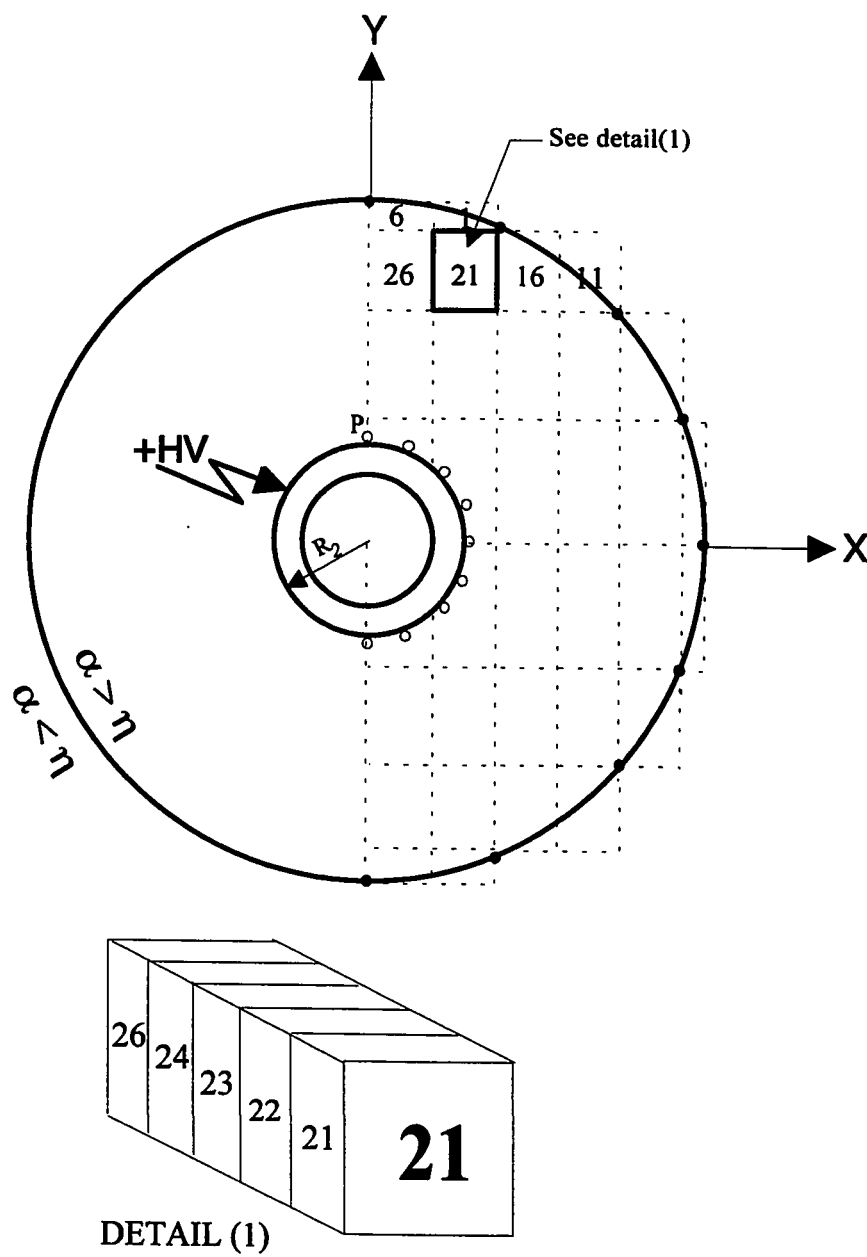


*Fig.(4.10) Division of the ionization zone into sub-volumes.*



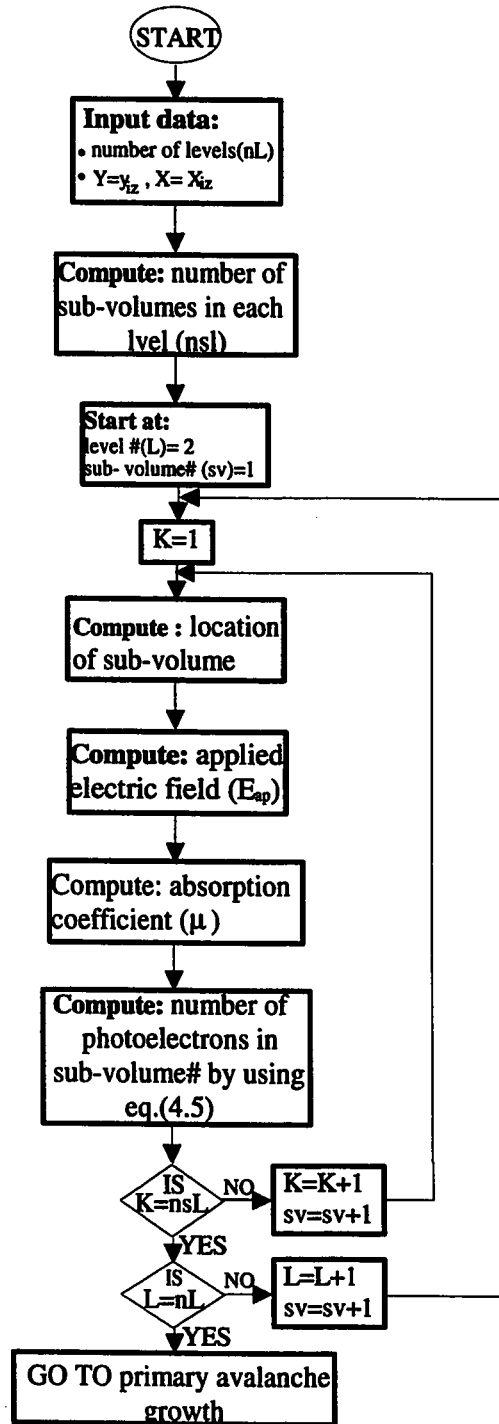


*Fig.(4.11) The flow chart for the creation of photoelectrons in a sub-volume*

- Repeat the above steps for all sub-volumes starting from level number 2 up to the last level.
- Repeat the above process 50 times, each time the photoemission from the primary avalanche is calculated.

#### 4.2.3.4 The Growth of Successor Avalanches

This section explains how all the photoelectrons created in each sub-volume will be accelerated in the prevailing field to produce successor avalanches. The procedure is outlined in Fig. (4.12) as follows:

- The growth of any successor avalanche starts by locating the X, Y and Z coordinates of each sub-volume.
- Calculate the applied electric field ( $E_{ap}$ ) and electric field due to the total positive space charge left by the primary avalanche ( $E_{p.sc}$ ) at any point along the path of the successor avalanche .
- For a point other than the starting one, the electric field due to the positive point space charges ( $E_{s.sc}$ ) accumulated in the wake of the successor avalanche is to be calculated .

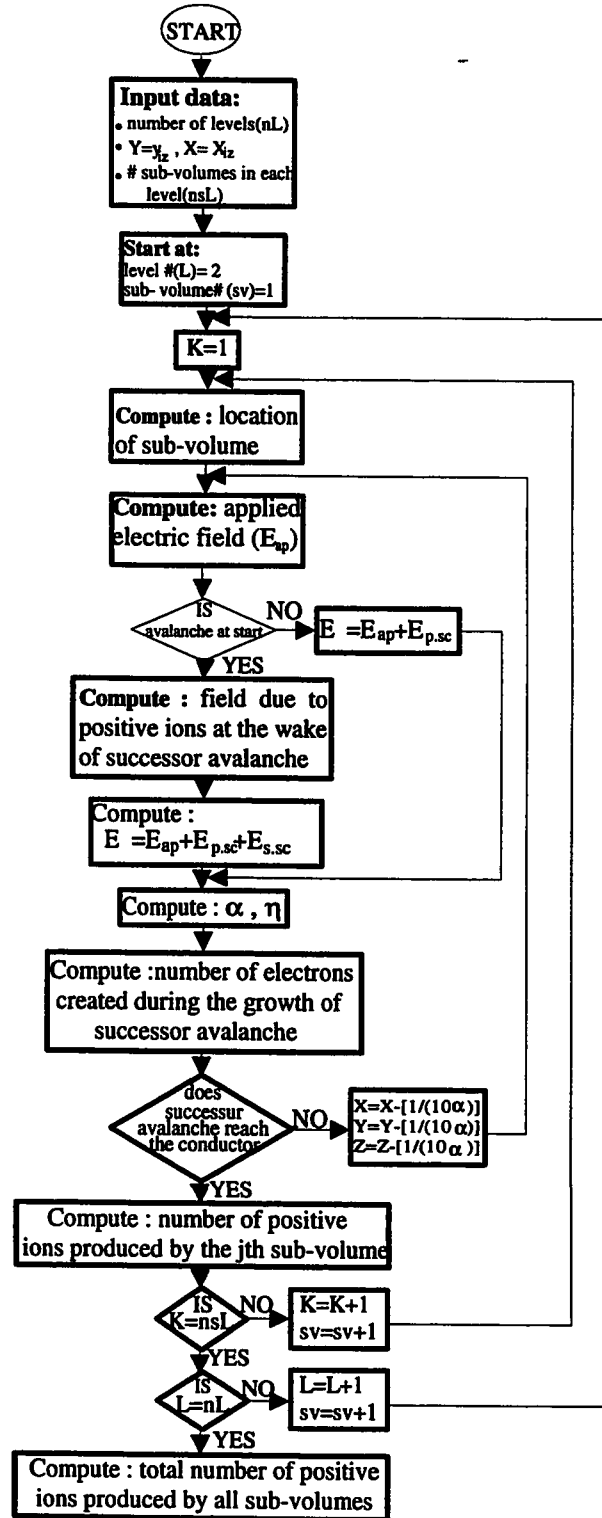


Fig.(4.12) The flow chart of successor avalanches growth

- The resultant of the three electric-field components are used to calculate the ionization coefficient  $\alpha$ , attachment coefficient  $\eta$  and the difference  $(\alpha-\eta)$ .
- Compute number of electrons created at the head of each successor avalanche .
- If the successor avalanche does not reach the conductor or the positive space charge left by the primary avalanche , the above steps are repeated for the next step of avalanche growth ; where the coordinates are:

$$\begin{aligned}
 X &= X - \left(\frac{1}{10 * \alpha}\right) * \frac{(E_{x_{ap}} + E_{x_{p.sc}} + E_{x_{s.sc}})}{E} \\
 Y &= Y - \left(\frac{1}{10 * \alpha}\right) * \frac{(E_{y_{ap}} + E_{y_{p.sc}} + E_{y_{s.sc}})}{E} \\
 Z &= Z - \left(\frac{1}{10 * \alpha}\right) * \frac{(E_{y_{p.sc}} + E_{y_{s.sc}})}{E}
 \end{aligned} \tag{4.15}$$

where the step length along the resultant field (E) is equal to  $(1/10 \alpha)$  . Therefor, the increment  $\Delta x$  along the X-direction is equal  $\left(\frac{1}{10 * \alpha}\right) * \frac{(E_{x_{ap}} + E_{x_{p.sc}} + E_{x_{s.sc}})}{E}$  . The increments  $\Delta y$  and  $\Delta z$  are expressed in the same way as  $\Delta x$  .

- Repeat the previous steps until the successor avalanche reaches the conductor or the positive space charge left by the primary avalanche .

- The total number of positive ions created by each sub-volume is equal to the number of ions produced by one photoelectron times the number of photoelectrons in the sub-volume as expressed by equation (4.10).
- The sum of all the positive ions produced by all the successor avalanches of all sub-volumes times 4 represents the number of positive ions produced by the second generation of avalanches in conformity with Fig.(4.6) .
- The voltage at which the number of positive ions of the primary avalanche equals that produced by the second generation is the onset voltage.

### **4.3 Negative Corona**

This section presents the onset criterion of negative corona . At first, the criterion of onset is described. Then, a mathematical formulation for the criterion is explained . Finally, a description of the computer program written for the calculation of the onset voltage is outlined .

#### **4.3.1 Criterion of Onset Voltage**

When the electric field strength in the vicinity of the stressed conductor reaches the threshold value for ionization of air molecules by

electron collision, a primary avalanche starts to develop along the direction away from the conductor ,as shown in Fig.(4.13). With the growth of the avalanche, more electrons are developed at its head , more photons are emitted in all directions ,and more positive ions are left in the avalanche wake. The growth of the primary avalanche is terminated at the ionization zone boundary ( $\alpha=\eta$ ) where the electrons get attached to the air molecules and form negative ions [24,30].

The mechanism of successor (secondary) avalanche in negative corona is different from the positive corona. In negative corona the successor avalanches are initiated from the cathode surface .

For the successor avalanche to be started , the emitted photons from the primary avalanche reaching the cathode should act for the emission of new electrons to insure self-sustained discharge.

#### 4.3.2 Mathematical Formulation of the Onset Criterion

The number of electrons  $N_e(y)$  at a distance  $y$  from the starting point of the avalanche is given as [12,23,24].

$$N_e(y) = e^{R_2 \int_0^y (\alpha - \eta) dy} \quad (4.16)$$

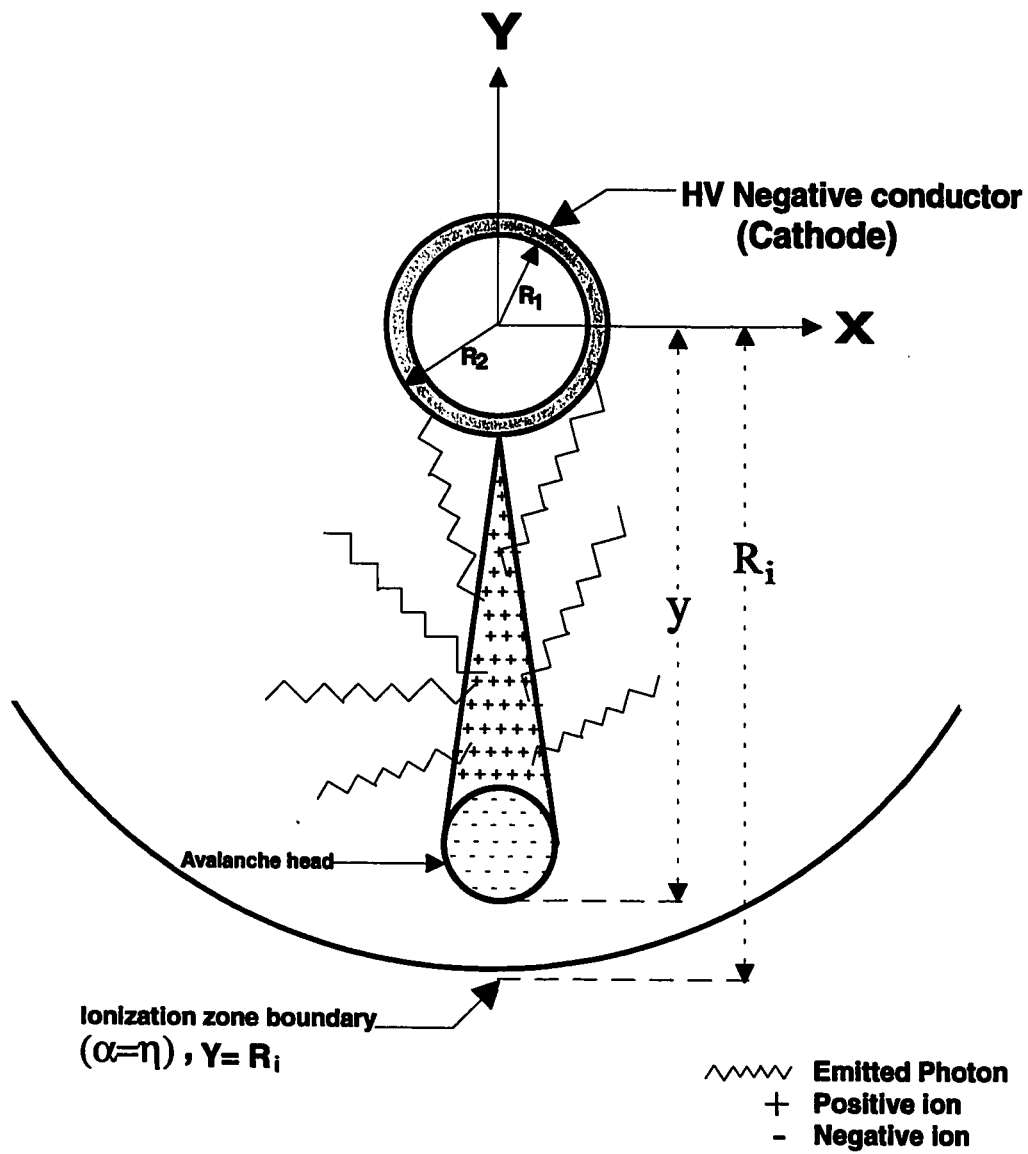


*Fig.(4.13) Development of the Primary avalanche in negative corona discharge*

The ionization  $\alpha$  and the attachment  $\eta$  coefficients depend on the total electric field  $E$ . The total electric field is the resultant of the positive space charge field at the wake of the primary avalanche and the applied field due to the applied voltage. The positive space charge field of the avalanche is the same as if all its positive ions were concentrated at a distance  $1/\alpha$  from the avalanche tip[24].

The number of photons produced over the step  $\Delta y$  of the primary avalanche's progress is :

$$\Delta n(y) = \vartheta(y) * \Delta y * N_e(y) \quad (4.17)$$

where  $\vartheta(y)$  is the rate of production of photons. It was found [22,24] to be proportional to  $\alpha(y)$

$$\vartheta(y) = f * \alpha(y) \quad (4.18)$$

where:

$f$  is a constant of proportionality .

Only some of the photons produced reach the cathode , i.e.

$$\Delta n_f = f * \alpha(y) * \Delta y * N_e(y) * g(y) * e^{-\eta y} \quad (4.19)$$

where:

$g(y)$  is a geometry factor that accounts for the loss of photons to the space surrounding the stressed conductor .



The primary avalanche will continue to grow until it reaches the ionization-zone boundary  $y=R_i$  (Fig.(4.13)), where  $\alpha=\eta$ . Thus, the number of electrons photoemitted from the conductor is [22,24]:

$$N_{e\text{ph}} = \gamma_{\text{ph}} \int_{R_2}^{R_i} \alpha(y) * N_e(y) * g(y) * e^{-\mu y} * dy \quad (4.20)$$

where:

$\gamma_{\text{ph}}$  is Townsend's second coefficient due to the action of photons which is equal to  $3*10E-3$  for both bare and coated surface[31].

The condition for a new (successor) avalanche to develop and, hence, the condition for a self-sustained discharge is :

$$N_{e\text{ph}} \geq 1.0 \quad (4.21)$$

The onset voltage does not appear explicitly in equation(4.21). However, the applied voltage affects the values of  $\alpha(y)$  and  $\eta(y)$  and, hence,  $N_e(y)$ . The onset voltage  $V_{O-}$  is the critical value that fulfills the equality (4.21) .

### 4.3.3 Programming of Onset Criterion

A computer program has been written to calculate the onset criteria for negative corona as described in section (4.3.1).The flow

chart in Fig.(4.14) shows the steps required to determine the onset voltage for negative corona. These steps are as follows :

- Read the input data such as  $R_1$ ,  $R_2$ ,  $H$ ,  $\epsilon_r$  and the starting applied voltage .
- Compute the ionization zone boundary coordinate ( $Y_{IZ}$ ,  $X_{IZ}$ ) at  $\theta = 180$  .
- Start from the coated conductor surface at point P that has a coordinate ( $Y=R_2, X=0$ ) .
- Calculate the electric field due to the applied voltage at the point P.
- Electric field due to the positive space charges left in the primary avalanche wake is calculated at any point P during the growth of the primary avalanche except at the point P that has a coordinate ( $Y=R_2, X=0$ ) where the field assume zero value because the positive space charges have not yet been created .
- The total electric field which is the resultant of the applied field and the field produced by the positive space charge in the primary avalanche wake is computed .
- All field dependent parameters ( $\alpha$ ,  $\eta$ ,  $\mu$ , and  $g(y)$ ) are calculated as a function of the total field .

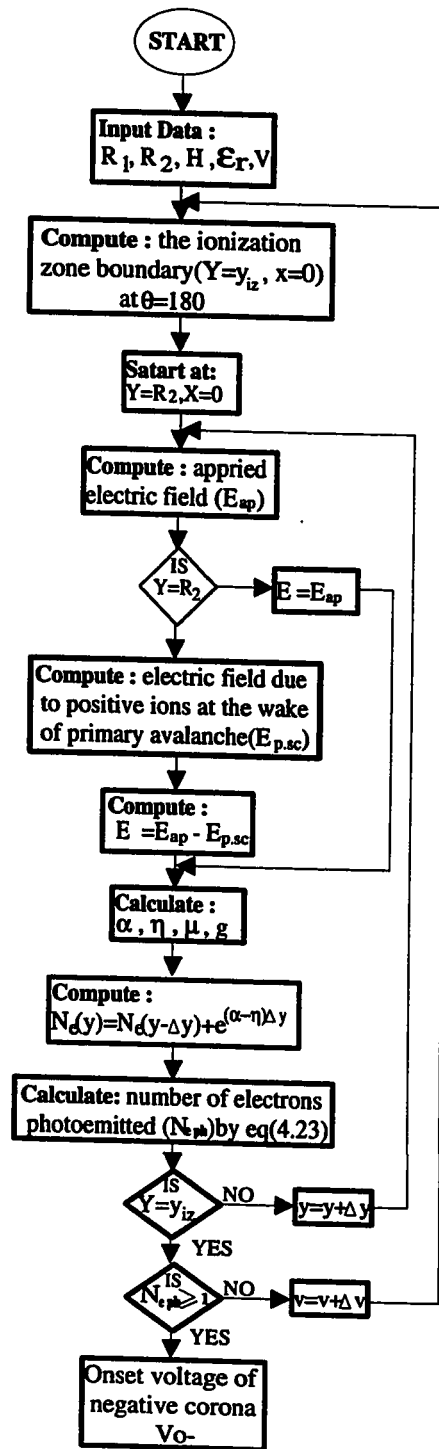


Fig.(4.14) The flow chart for negative corona onset condition

- Use equation (4.22) to calculate number of electrons created in the head of the primary avalanche after a distance  $\Delta y$ .

$$N_e(y) = N_e(y - \Delta y) + e^{(\alpha - \eta) \Delta y} \quad (4.22)$$

where  $N_e(y - \Delta y)$  at the starting point is equal to zero.

- Use equation (4.23) to calculate number of electrons photoemitted from the surface of coated conductor after a distance  $\Delta y$ .

$$N_{eph}(y) = N_{eph}(y - \Delta y) + (\gamma_{ph} \cdot \alpha(y) \cdot N_e(y) \cdot g(y) \cdot e^{-\mu y}) \Delta y \quad (4.23)$$

where  $N_{eph}(y - \Delta y)$  at the starting point is equal to zero.

- The above steps are repeated if the primary avalanche does not reach the ionization zone boundary coordinate ( $y = Y_{IZ}$ ,  $x = 0$ ). The new point P coordinate is ( $y = y + \Delta y$ ,  $x = 0$ ).
- The above steps should be repeated at a voltage equal to  $V = V + \Delta V$  if number of electrons photoemitted from the surface of coated conductor does not equal to 1.
- The voltage at which number of electrons photoemitted from the surface of coated conductor is equal to 1 is the onset voltage of negative corona.

## 4.4 Numerical Data

The following numerical data is used in the calculation of the positive and the negative onset voltages as described in section 4.2 and 4.3.

### 4.4.1 Ionization ( $\alpha$ ) and Attachment ( $\eta$ ) Coefficients

The coefficient of ionization by electron collision ( $\alpha$ ) and the electron attachment coefficient ( $\eta$ ) are used in calculating both the positive and the negative onset voltages. The numerical values of  $\alpha$  and  $\eta$  in air as determined from the experimental data are expressed as [27]:

- Attachment Coefficient ( $\eta$ ):

$$\frac{\eta}{P_r} = 0.01298 - 0.541 \times 10^{-3} \left( \frac{E}{P_r} \right) + 0.87 \times 10^{-5} \left( \frac{E}{P_r} \right)^2 \quad \left( \frac{\text{number}}{\text{cm. torr}} \right) \quad (4.23)$$

- Ionization Coefficient ( $\alpha$ ):

$$1)\text{- IF } 25 \leq \frac{E}{P_r} \leq 60 \quad \left( \frac{\text{V}}{\text{cm. torr}} \right):$$

$$\frac{\alpha}{P_r} = 4.7786 e^{-221 P_r / E} \quad \left( \frac{\text{number}}{\text{cm. torr}} \right) \quad (4.24)$$

$$2)\text{- IF } 60 \leq \frac{E}{P_r} \leq 240 \quad \left( \frac{\text{V}}{\text{cm. torr}} \right):$$

$$\frac{\alpha}{P_r} = 9.682 e^{-264.2 P_r / E} \quad \left( \frac{\text{number}}{\text{cm. torr}} \right) \quad (4.25)$$

where:

$P_r$  is the atmospheric pressure ( 760 torr )

#### 4.4.2 Photoionization Product $f_1.f_2$

The photoionization product  $f_1.f_2$  is used in calculating the number of photoelectrons created in the sub-volume , equation(4.7)for positive corona. This product  $f_1.f_2$  was measured and expressed as [32]:

$$f_1.f_2 = 246 e^{-696.92 \rho} + 283 e^{-3002 \rho} + 528 e^{-30590 \rho} \quad (4.25)$$

where:

$\rho$  is the distance between the tip of the primary avalanche and the sub volume

#### 4.4.3 Absorption Coefficient ( $\mu$ )

The absorption coefficient ( $\mu$ ) is used in the calculation of the positive and the negative onset voltages . The absorption coefficient was measured and expressed as [32] :

1)- If  $26.6 \leq E \leq 190$  (kv/cm) then :

$$\mu = 100 e^{(-31.568 + 6.785 \ln(E))} \quad (\text{m}^{-1}) \quad (4.26)$$

2)- If  $E > 190$  (kv/cm) then :

$$\mu = 100 e^{(-11.743 + 2.78 \ln(E))} \quad (\text{m}^{-1}) \quad (4.27)$$

#### 4.4.4 Primary Avalanche Radius

To calculate  $D_{s-p.sc}$  which appeared in equation(4.8), the radius of the primary avalanche space charge located on the surface of the conductor is to be calculated. This radius is expressed as [19,32]:

$$R_{p.sc} = \sqrt{6D_e \tau} \quad (4.28)$$

where :

$D_e$  is the electron diffusion coefficient

$\tau$  is the avalanche transit time

The diffusion coefficient  $D_e$  ( $\text{m}^2/\text{s}$ ) is expressed as [32]:

$$D_e = k_e (k/e) (T_e/T_g) T_g \quad (\text{m}^2 / \text{s}) \quad (4.29)$$

where:

$k_e$  is the electron mobility ( $\text{m}^2/\text{sV}$ )

$k$  is Boltzmann's constant ( $=1.37 \times 10^{-23} \text{ W s/K}$ )

$T_e$  is the electron temperature in K

$T_g$  is the gas temperature (=298 K at N.T.P)

$e$  is the electron charge(=1.6x 10<sup>-19</sup> C)

The temperature ratio  $T_e / T_g$  was measured and expressed as:

$$T_e / T_g = 12267 + 316 \ln(E) \quad \text{for } E < 0.532 \quad (\text{kV/cm}) \quad (4.30)$$

$$T_e / T_g = 20632 + 1429 \ln(E) \quad \text{for } E \geq 0.532 \quad (\text{kV/cm}) \quad (4.31)$$

The electron mobility  $k_e$  (m<sup>2</sup>/sV) is the electron velocity ( $V_e$ ) divided by the actuating field  $E$  (V/m). The electron velocity  $V_e$  (m/s) was expressed as [32]:

$$V_e = 1217 \times 10^4 E^{0.715} \quad \text{for } E \leq 76 \quad (\text{kV/cm}) \quad (4.32)$$

$$V_e = 1837 \times 10^4 E^{0.62} \quad \text{for } E > 76 \quad (\text{kV/cm}) \quad (4.33)$$

#### 4.4.5 Geometry Factor ( $g(y)$ )

The geometry factor ( $g(y)$ ) is used in the calculation of the negative onset voltage. The geometry factor has two components one is the radial and the other is the axial. The purpose of this geometry factor is to account for photon absorption within the ionization zone around the conductor. It can be expressed as: [22,24]

$$g(y) = g_{\text{rad}}(y) g_{\text{axl}}(y) \quad (4.34)$$



$$g_{\text{rad}}(y) = \frac{1}{\pi e^{-\mu(y-R_2)} \int_0^{\sin^{-1} \frac{R_2}{y}} e^{-\mu(y^2 + R_2^2 - 2yR_2 \cos \phi)} d\phi} \quad (4.35)$$

$$g_{\text{axl}}(y) = \frac{1}{\pi e^{-\mu(y-R_2)} \int_0^{\pi/2} e^{-\mu \frac{y-R_2}{\cos \phi}} d\phi} \quad (4.36)$$

#### 4.5 Accuracy of the Calculated Onset Voltages

This section presents calculated values of the positive and the negative onset voltages for smooth bare conductors. The calculated values are compared with those measured experimentally[21].

The measurements were carried-out [21] on single smooth aluminum conductors having diameters of 15, 30, 60, 80 and 130 mm. The length of each conductor was about 8 meters. During the tests the conductors were placed between the top electrode of the HVDC generator and HV electrode of the voltage divider at a height of 12.5 meter above earth.(Fig.(4.15))

Figure(4.16) shows the calculated and the measured positive onset voltages for bare conductors. The measured values are represented by the shaded area, however, the calculated one's are indicated in Fig.(4.16) by small circles. It is obvious that most of the calculated values lies within the shaded area.

Figure(4.17) shows the calculated and the measured negative onset voltages for bare conductors . The measured values are represented by the shaded area., however , the calculated one's are indicated in Fig.(4.17) by small circles . It is quite clear that most of the calculated values agreed satisfactorily with those measured experimentally .

Therefore, the positive and the negative onset criteria predict satisfactory onset voltages Figs.(4.16) and (4.17) for bare conductors . They are applied for calculating the onset voltages of corona on coated conductors . The results obtained are discussed in the next chapter .

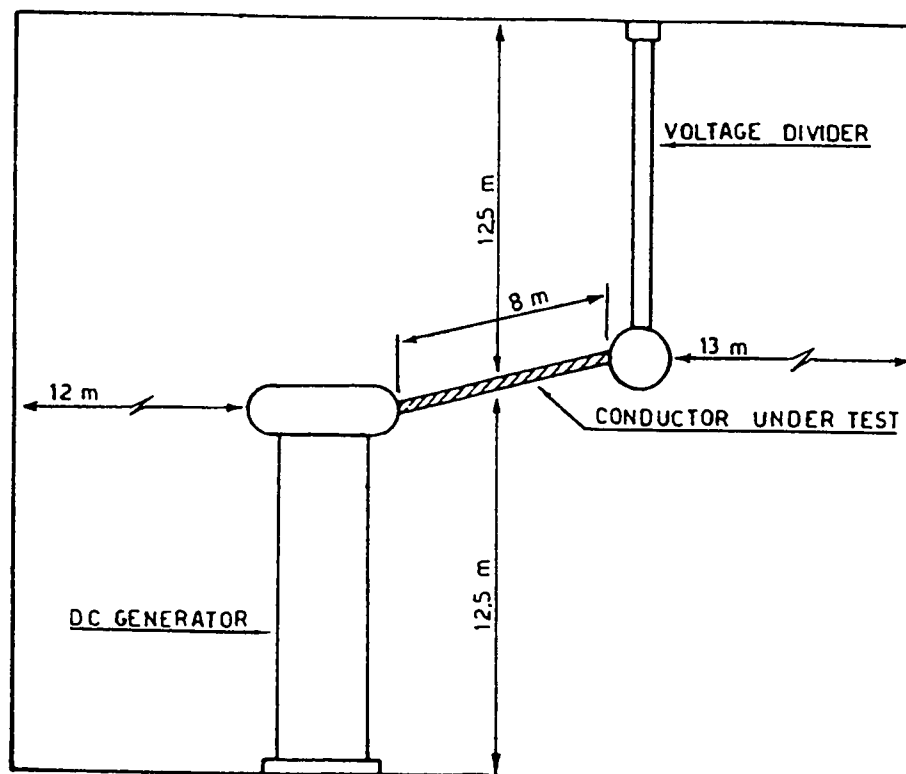


*Fig.(4.15) Test set-up and clearances for corona onset measurement on bare conductors [21]*

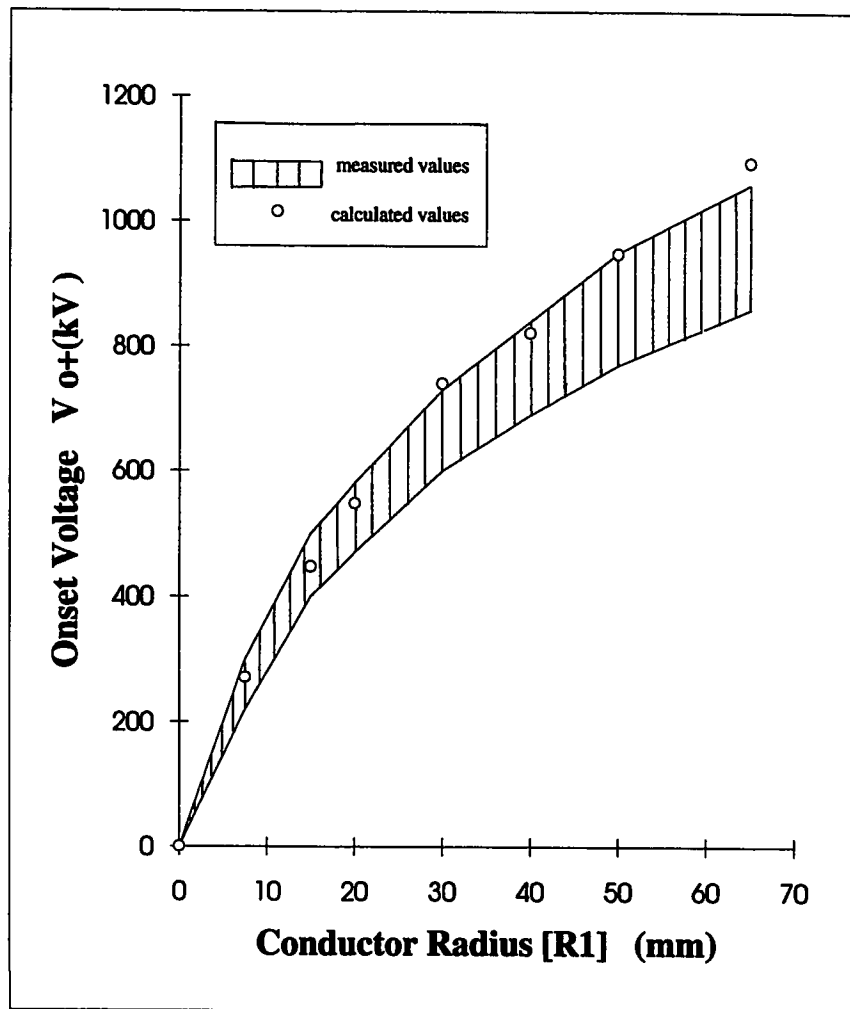


*Fig.(4.16) Measured and calculated positive onset voltages versus conductor radius*

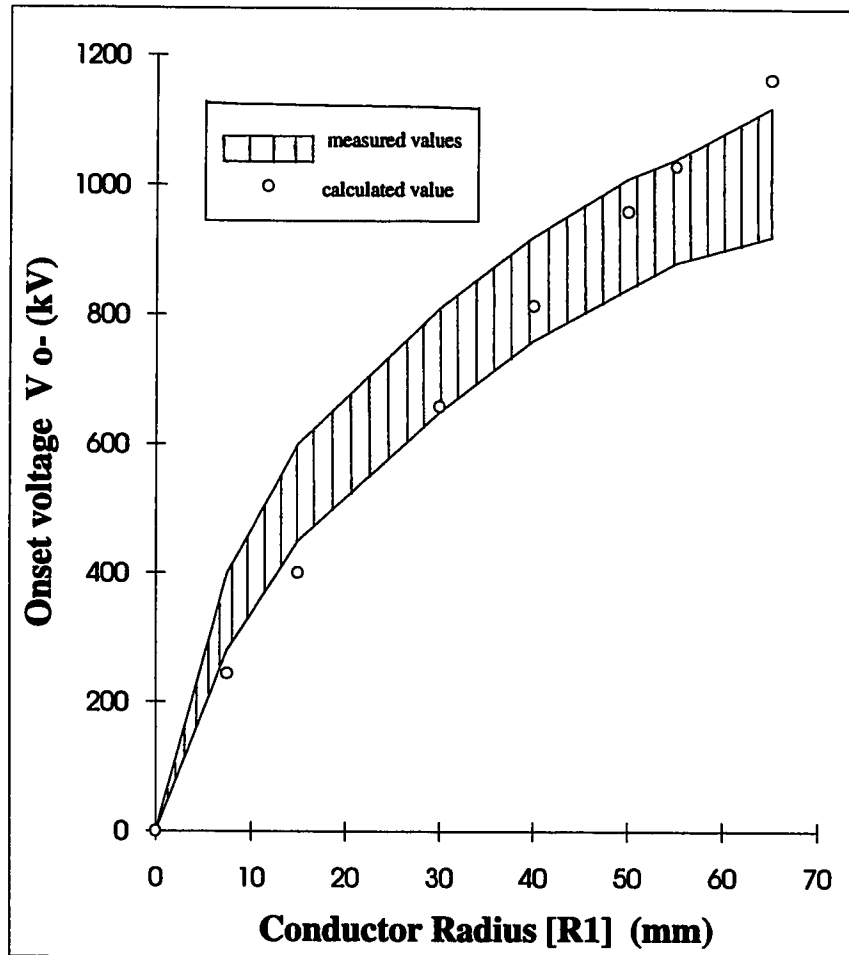


*Fig.(4.17) Measured and calculated negative onset voltages versus conductor radius*

# **CHAPTER 5**

## **RESULTS AND DISCUSSION**

### **5.1 Introduction**

The method proposed in chapter 4 for evaluating positive and negative corona onset voltages have been applied to coated and bare conductor-plane configurations . This chapter investigates the effect of different parameters on the onset voltage, the ionization-zone thickness and the growth of primary avalanche . A comparison between coated and bare conductors of the same outer radius is made to appreciate the effect of coating on improving the corona performance of the conductor .

At first, the effect of conductor radius on the ionization-zone thickness around both coated and bare conductors under positive and negative applied voltages is shown . After that, the effect of line parameters, conductor radius and height, on the positive and negative onset voltages is demonstrated . Then, the effect of dielectric permittivity and thickness of the coating layer on both the positive and negative onset voltages is evaluated .

## **5.2 Effect of line parameters on the onset voltage**

This section reports the effect of line parameters on the onset voltage of positive and negative coronas at different values of the thickness of the coating layer ( $\delta$ ). These line parameters are the conductor radius and the height above the ground plane.

### **5.2.1 Effect of Conductor Radius ( $R_1$ )**

In this sub-section, the effect of the coating-layer thickness ( $\delta$ ) on the onset voltage is evaluated when the conductor height ( $H$ ), and the relative permittivity( $\epsilon_r$ ) are kept constants at 12.5 m and 4.2 respectively.

Figures (5.1) and (5.2) depict the effect of the thickness  $\delta$  on the positive and negative onset voltages at different values of  $R_1$ , the radius of the metal conductor before being coated. The figures show that the positive and the negative onset voltages increase with the increase of the thickness of the coating layer. This is true for any value of the radius  $R_1$ . This increase of the onset voltage with the thickness  $\delta$  can be explained in the light of the fact that the electric field in conductor's vicinity assumes values less for coated conductors in comparison with those for bare conductors, Figs.(5.3)-(5.6). This decrease in the electric field values near the coated conductor results in an increase of the onset voltage with a subsequent decrease of corona

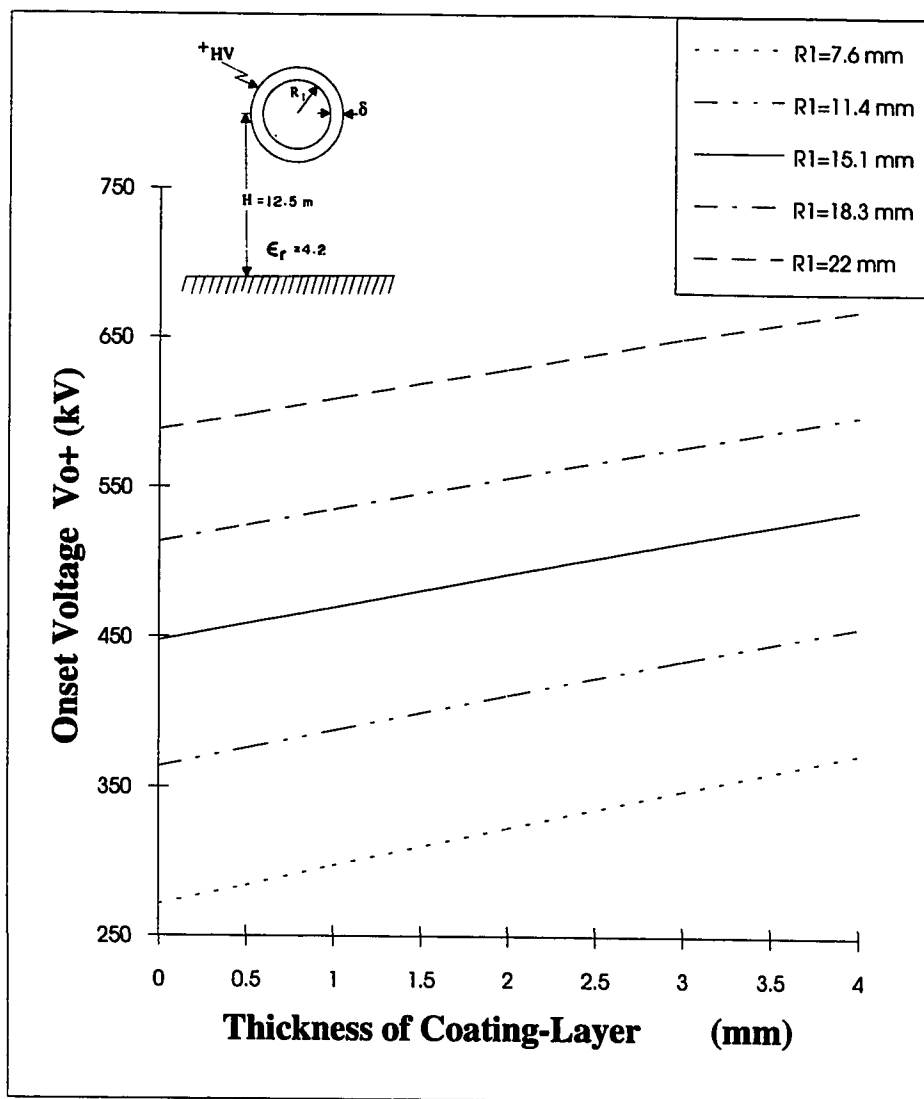
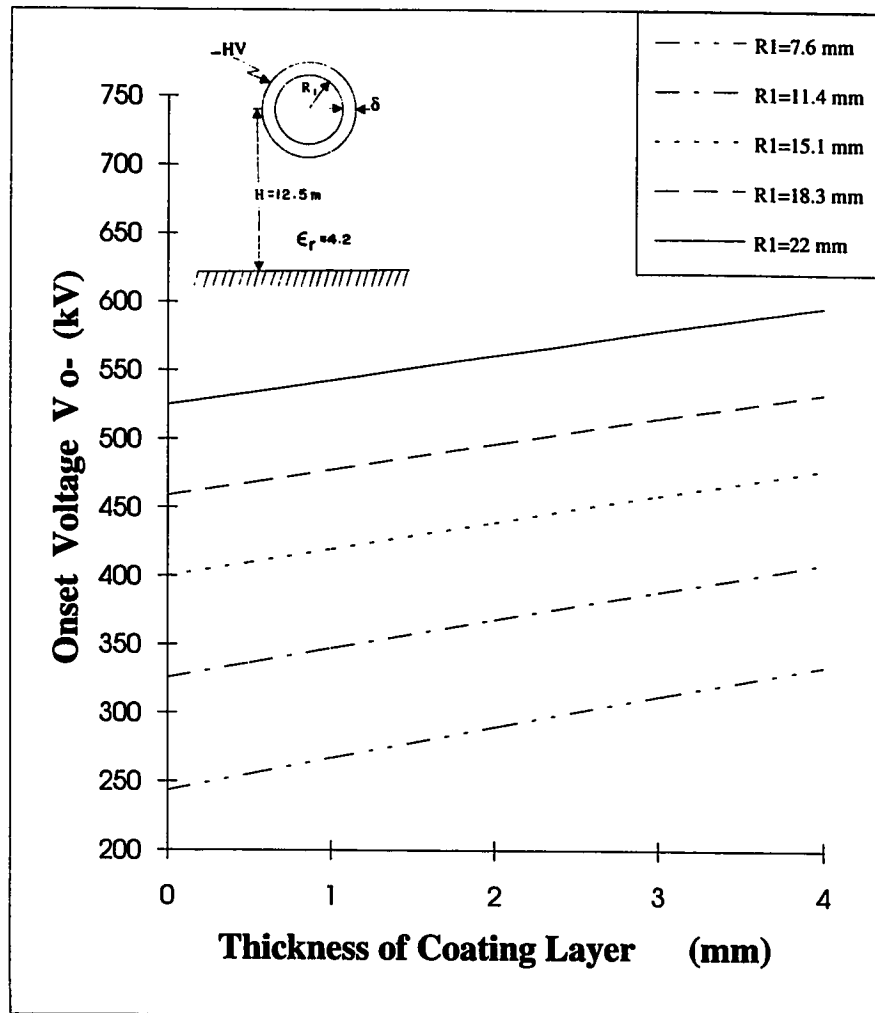


*Fig.(5.1) Effect of coating-layer thickness on positive onset voltage ( $V_{o+}$ ) for different values of  $R_1$*





*F(5.2) Effect of coating-layer thickness on negative onset voltage ( $V_o^-$ ) for different values of  $R1$*

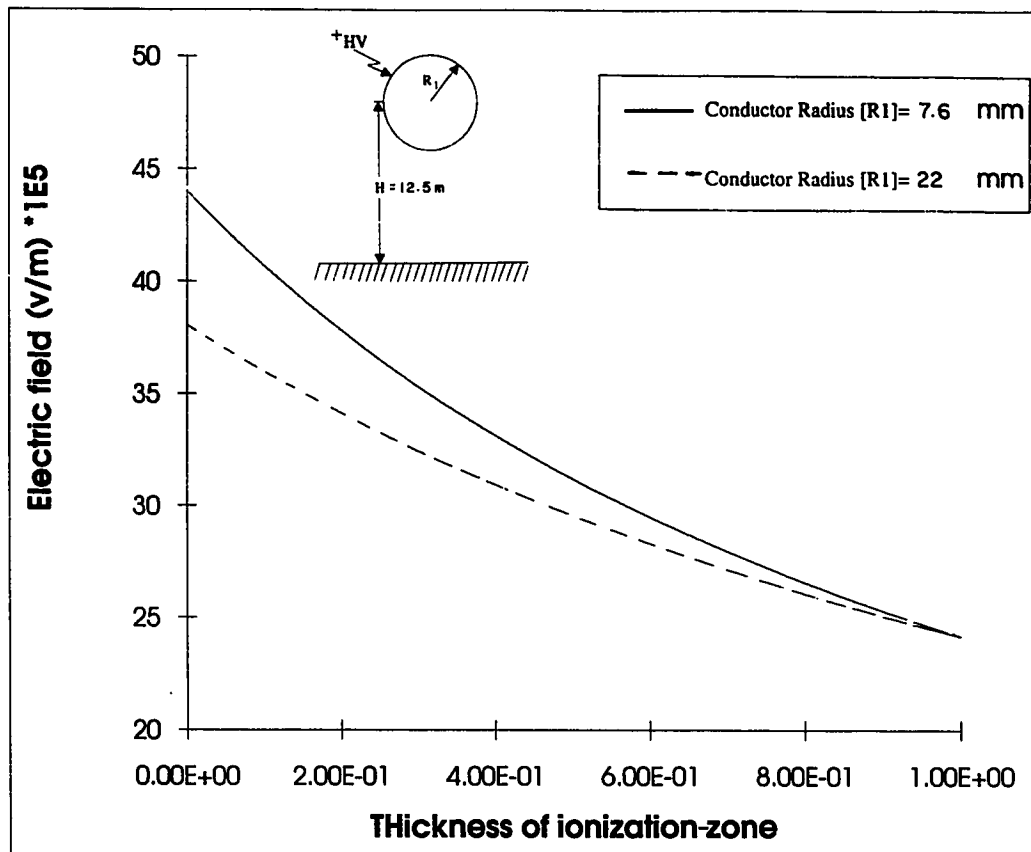


*Fig.(5.3) Electric field distribution across the ionization-zone for bare conductor stressed by voltage  $V_{0+} = 271.18$  and  $588.5$  kV.*

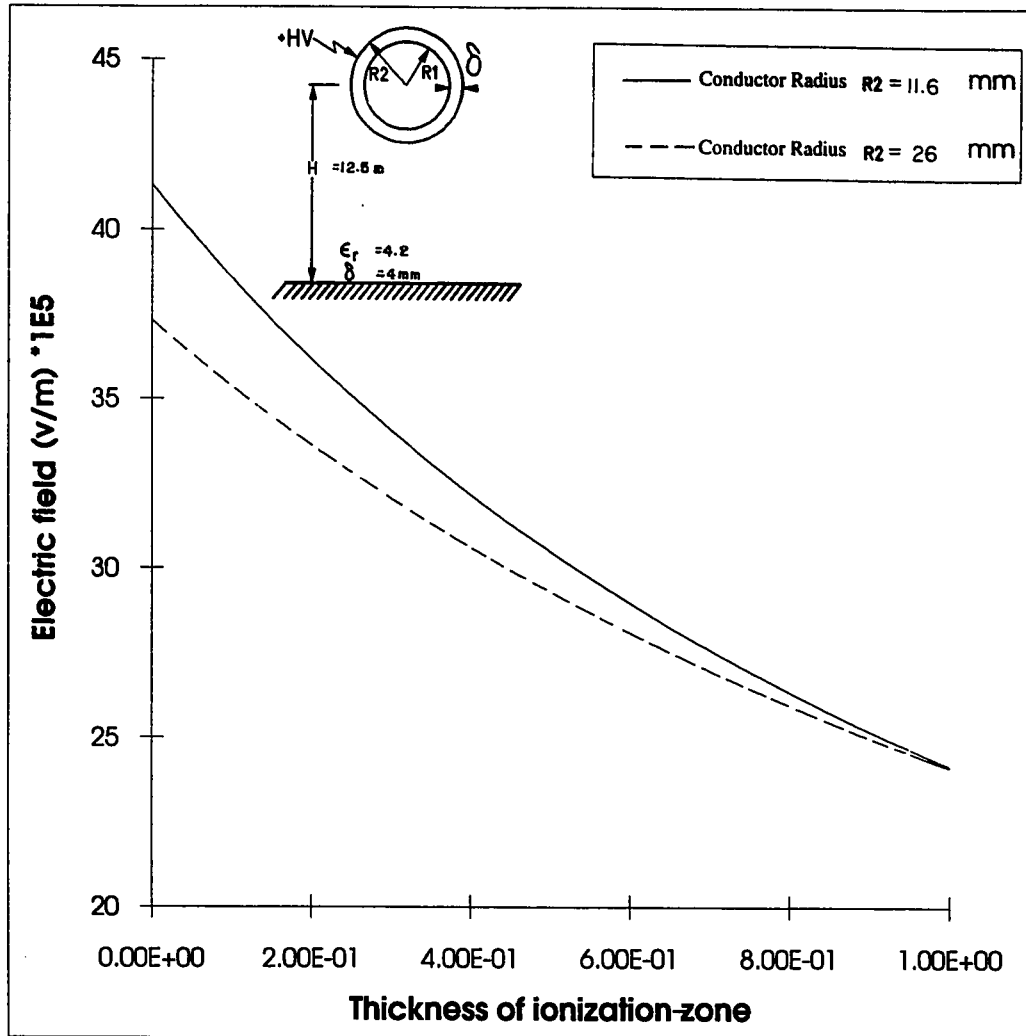


*Fig.(5.4) Electric field distribution across the ionization-zone for coated conductor stressed by voltage  $V_{0+} = 372.85$  and  $669.6 \text{ kV}$ .*

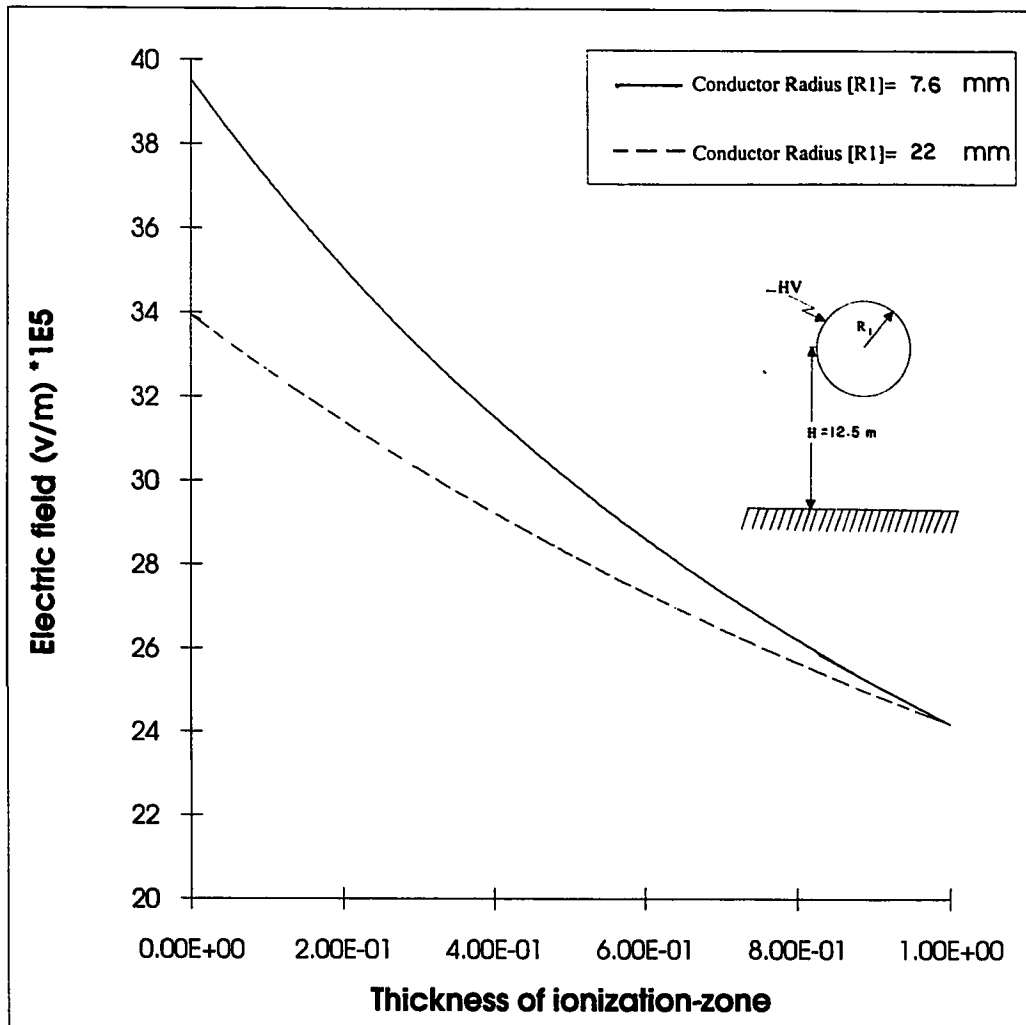


Fig.(5.5) Electric field distribution across the ionization-zone for bare conductor stressed by voltage  $V_{0.} = 243.5$  and  $525 \text{ kV}$ .

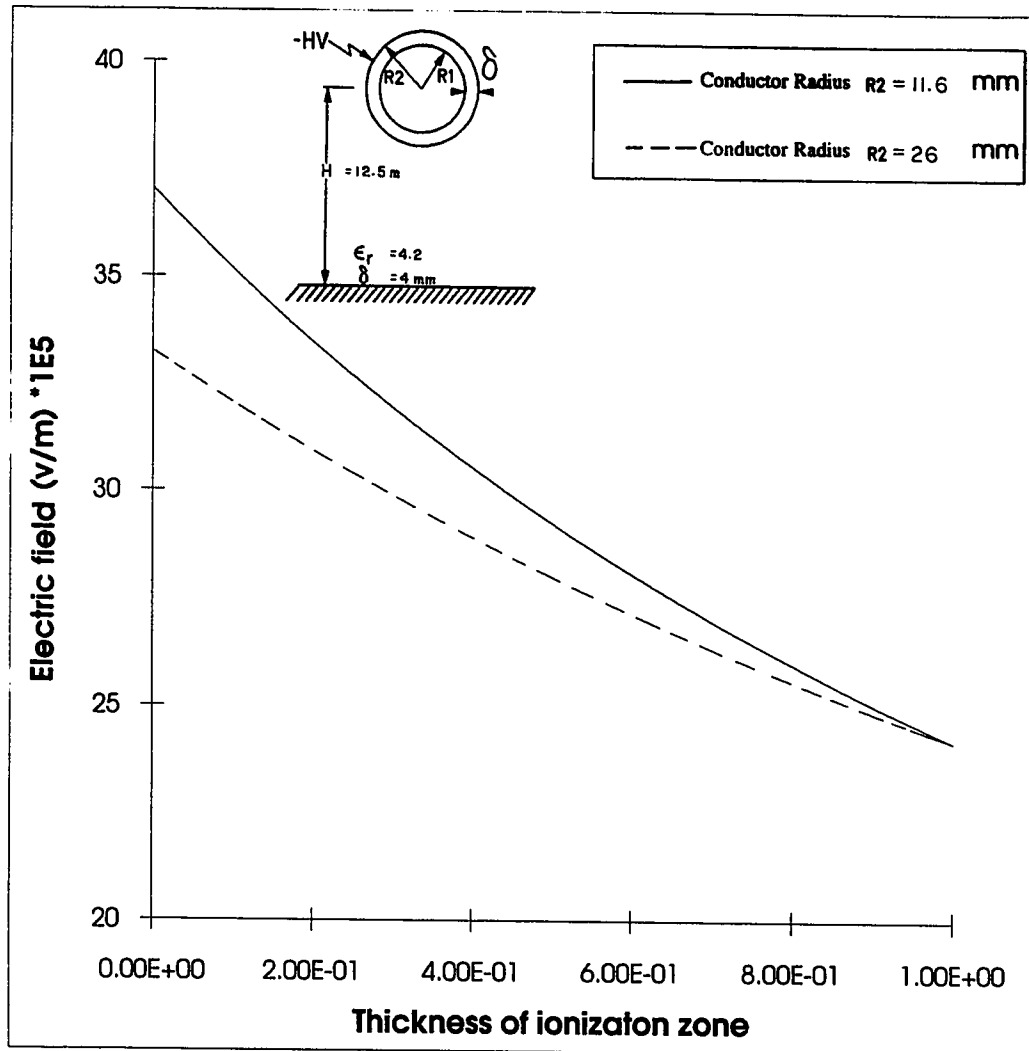


Fig.(5.6) Electric field distribution across the ionization-zone for coated conductor stressed by voltage  $V_{0.} = 334.1$  and  $596.6 \text{ kV}$ .

power loss and associated effect such as audible and TV noise . This confirms the improvement of corona performance of conductors when coated by a dielectric material .

The field values reported in Figs.(5.3)-(5.6) are for the same values of  $H$ ,  $\epsilon_r$  and  $\delta$ , i.e, 12.5 m, 4.2, and 4mm respectively.

### 5.2.2 Effect of Conductor Height (H)

The effect of conductor height on the positive and negative onset voltages is investigated in this sub-section . Five different values of conductor height ( $H$ ) are attempted with the radius  $R_1$  and relative permittivity  $\epsilon_r$  are maintained constants at 15.16 mm and 4.2 respectively . The thickness of coated layer is variable in the range 0-4 mm .

Figures (5.7) and (5.8) show that the positive and the negative onset voltages (  $V_{0+}$  and  $V_{0-}$  ) increase with the increase of the conductor height . Also, the onset voltages  $V_{0+}$  and  $V_{0-}$  increase with the increase of the thickness  $\delta$  of coated layer for any particular conductor height . However, the increase of  $V_{0\pm}$  with  $\delta$  is more pronounced than the increase of  $H$  . As conductor height increases the electric field in the conductor's vicinity decreases with a subsequent increase of the onset voltage whatever for positive or negative coronas.

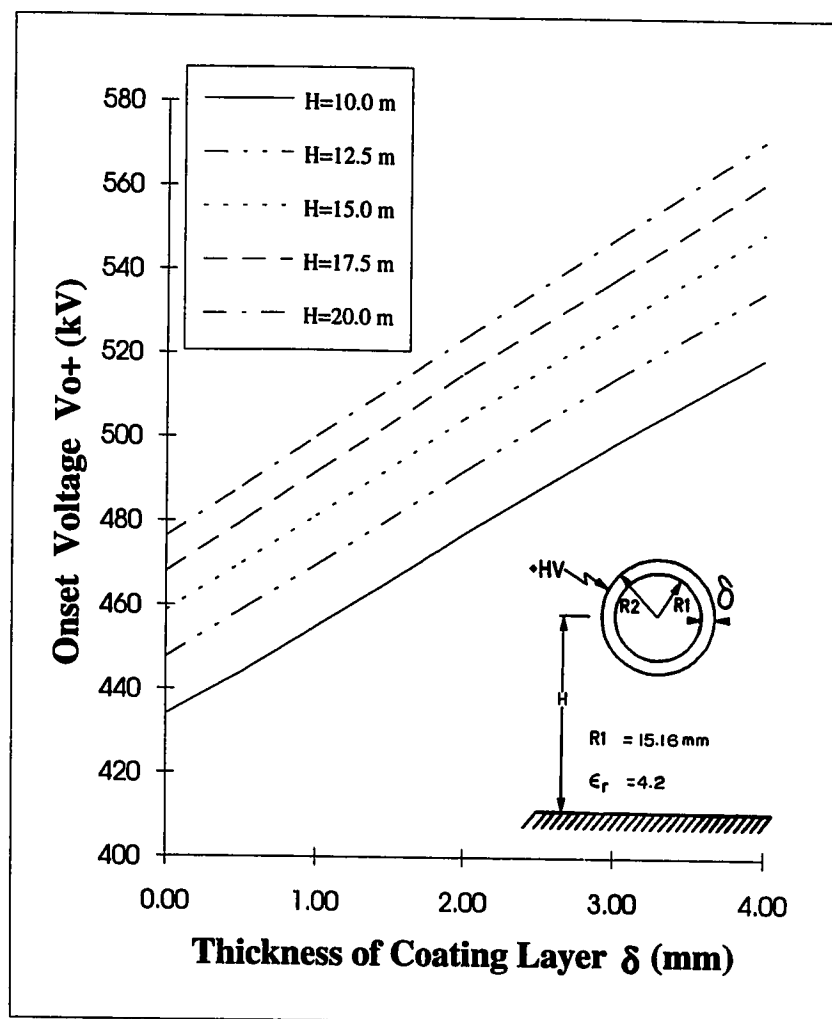
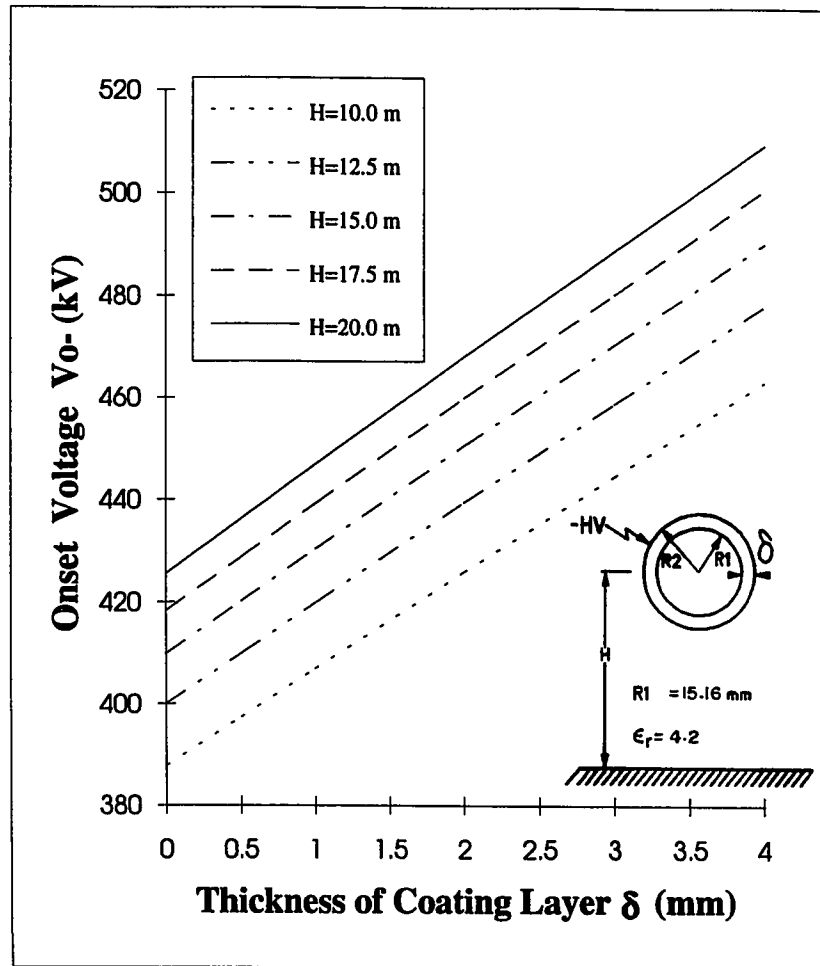


Fig.(5.7) Effect of coating-layer thickness on the positive onset voltage for different conductor heights



*Fig.(5.8) Effect of coating-layer thickness on the negative onset voltage for different conductor heights*



### 5.3 Effect of Dielectric Permittivity on the Onset Voltage

This section presents the effect of dielectric permittivity  $\epsilon_r$  on the positive and negative onset voltages for different values of coated layer thickness  $\delta$ . The effect of dielectric permittivity is computed for four different values of  $\epsilon_r$  and are attempted with the radius  $R_1$  and the conductor height  $H$  are kept constant at 15.16 mm and 12.5 m respectively.

Figures (5.9) and (5.10) show the increase of positive and negative onset voltages with the increase of  $\delta$ . For one and the same value of  $\delta$ , the positive and the negative onset voltages show a slight decrease with the increase of the relative permittivity from 2.3 to 6. This conforms with the fact that partial replacement of a given gaseous dielectric (air film around the conductor) by a solid dielectric of higher permittivity (coating layer) decreases the "effective gap distance", [9]. The effective gap distance decreases with the increase of  $\epsilon_r$  of the coating layer. This reflects itself in an increase of the field in the air film surrounding the coated conductor with a subsequent decrease of the onset voltages as depicted in Figs.(5.9) and (5.10).

### 5.4 Effect of Conductor Radius on Ionization-Zone Thickness

Figures (5.11) and (5.12) show how the ionization-zone thickness changes with the conductor radius for coated and bare conductors stressed by a voltage equal to the negative or positive onset value  $V_{0\pm}$ .

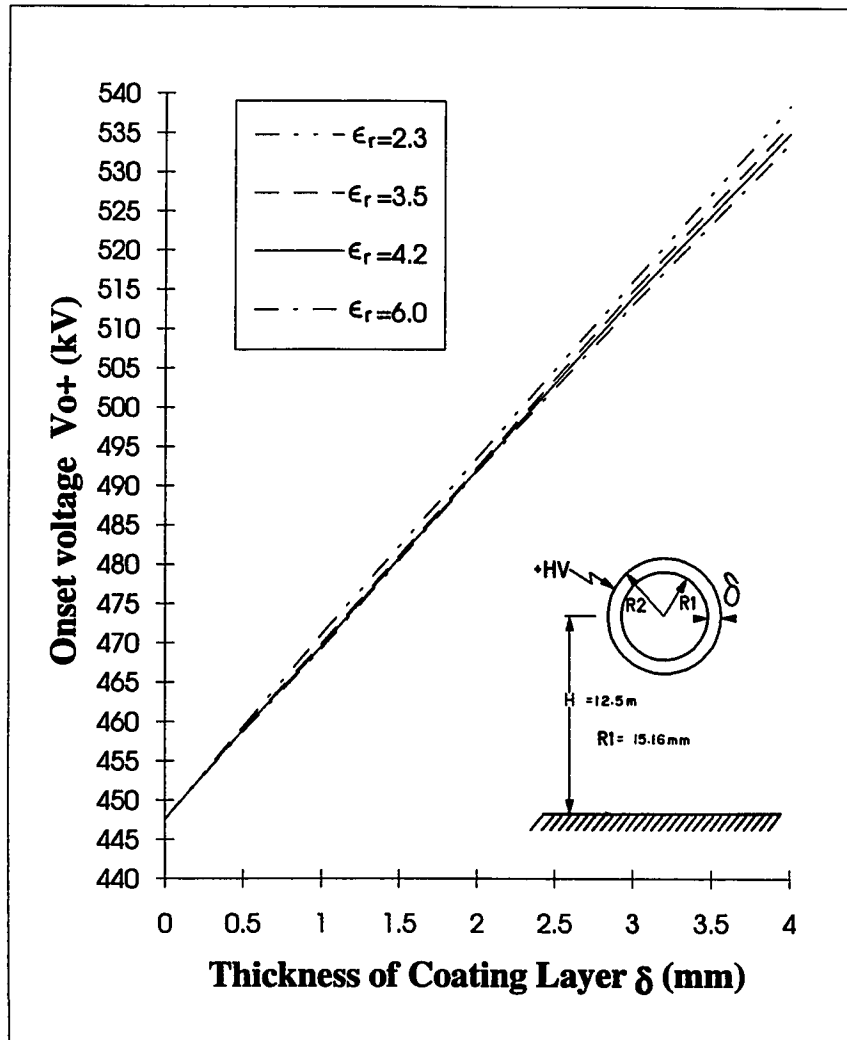


*Fig.(5.9) Effect of coating-layer thickness on the positive onset voltage for different permittivities of coating layer*

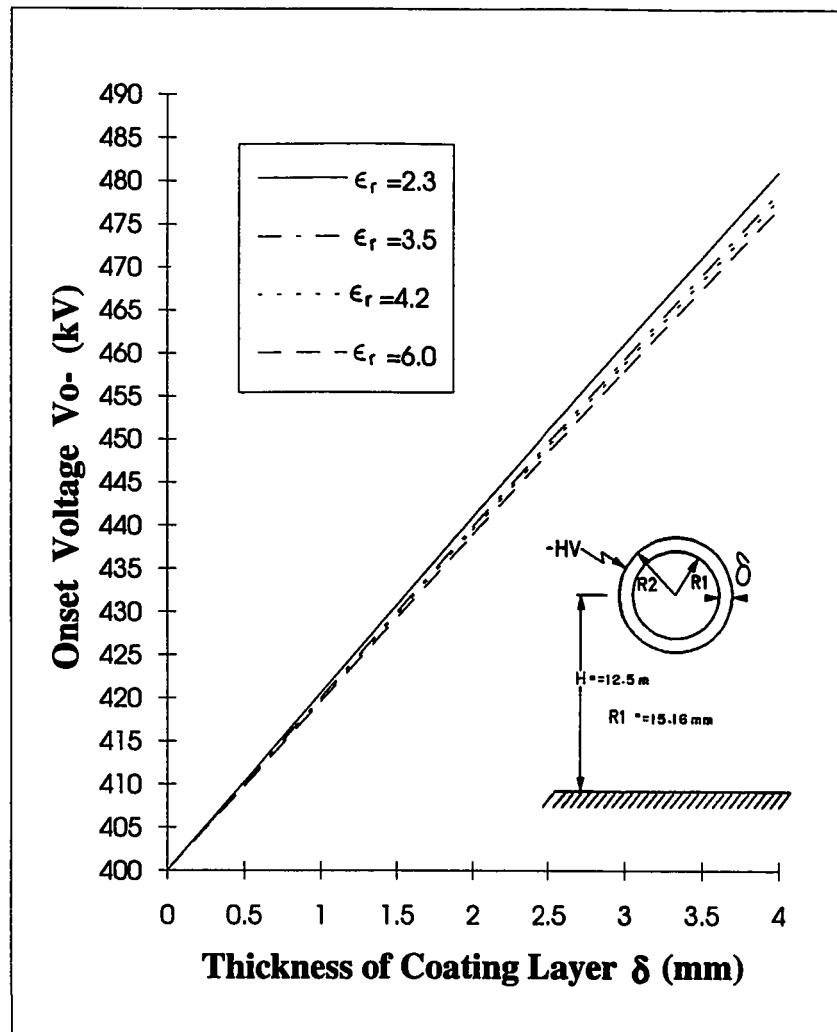


*Fig.(5.10) Effect of coating-layer thickness on the negative onset voltage for different permittivity of the coating layer*

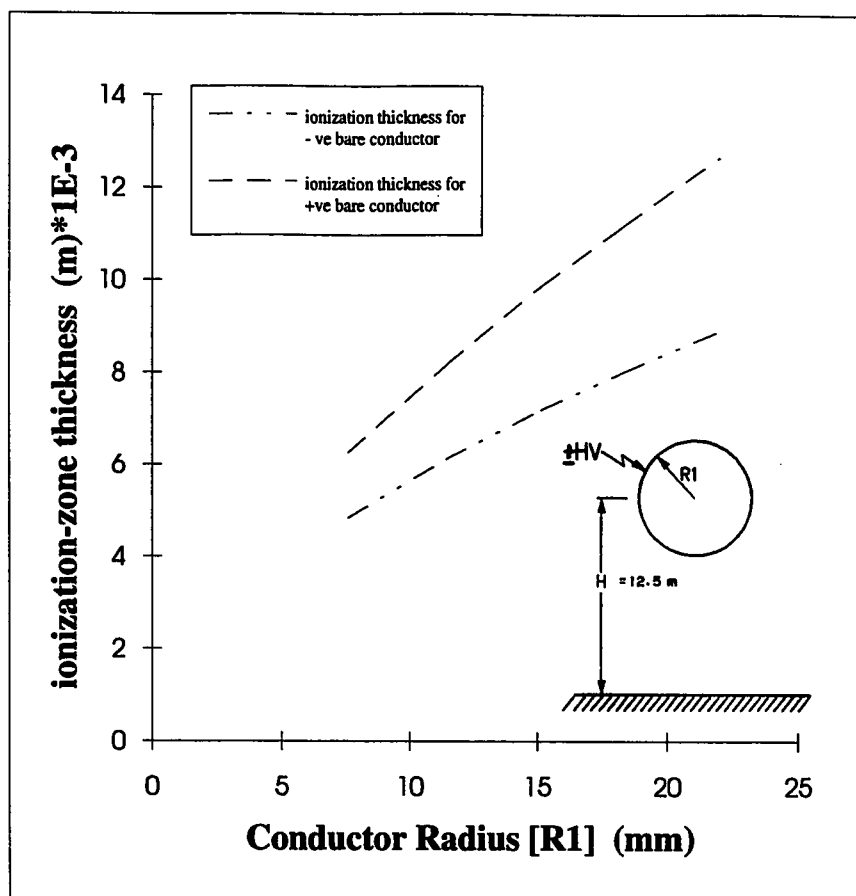


*Fig.(5.11) Effect of conductor radius on the ionization-zone thickness for bare conductor stressed by the onset voltage (  $V_{o+}$  /  $V_{o-}$  )*

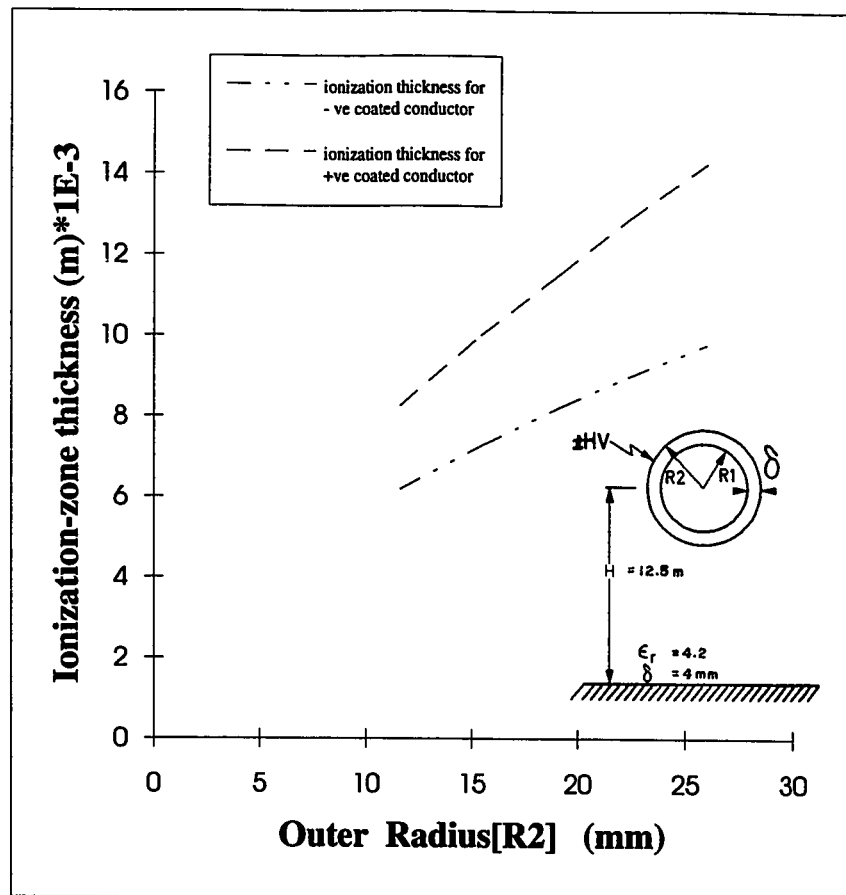


*Fig.(5.12) Effect of conductor radius on the ionization-zone thickness for coated conductor stressed by the onset voltage ( $V_{o+}$  /  $V_{o-}$ )*

The thickness values given in Figs.(5.11) and (5.12) have been computed for conductor height (H), relative permittivity ( $\epsilon_r$ ) and thickness of coated layer ( $\delta$ ) equal to 12.5 m, 4.2, 4 mm respectively.

The two figures indicate that the ionization zone thickness increases with the increase of the conductor radius for conductors stressed by negative or positive onset voltages. This is true and can be explained in the light of the fact that the electric field decreases as the conductor radius increases. This is in conformity with Figs.(5.3) and (5.4) for bare and coated conductors stressed by voltage  $V_{0+}$  and Figs.(5.5) and (5.6) for bare and coated conductors stressed by voltage  $V_{0-}$ . As a final result, the onset voltage should increase with the conductor radius increase. with a subsequent increase of the ionization zone thickness.

Also, it is quite clear from Figs.(5.11) and (5.12) that ionization-zone thickness values under positive voltage  $V_{0+}$  is higher than those under  $V_{0-}$  voltage whether the conductor is bare or coated. This is simply attributed to the fact that the positive onset voltage  $V_{0+}$  is always higher than the negative onset voltage  $V_{0-}$ .

## **5.5 Effect of Line Parameters on The Primary Avalanche Size**

The effect of line parameters on the primary avalanche size is presented in this section. These parameters are conductor radius and height above the ground plane.

### 5.5.1 Effect of Conductor Radius ( $R_1$ )

The effect of conductor radius on the size of the primary avalanche at the onset of positive and negative coronas is shown in Figs.(5.13) and (5.14) respectively. In the two figures, conductor height  $H$  and relative permittivity  $\epsilon_r$  are kept constant at 12.5 m and 4.2 respectively.

Figure (5.13) shows that the primary avalanche size at the onset of positive corona increases with increase of the thickness  $\delta$  of coating layer. On the contrary, the avalanche size at the onset of negative corona decreases with the increase of  $\delta$ . This can be explained by the fact that the onset voltage of positive and negative coronas increase with the increase of the thickness of the coating layer, Figs.(5.1) and (5.2). However, the onset voltage assumes smaller values for negative corona in comparison with those of positive corona, Figs.(5.1)-(5.2) and Figs.(5.7)-(5.10). This is why the avalanche size values are smaller for negative corona than those of positive corona, Figs(5.13) and (5.14). However, one has to recognize that the avalanche in positive corona starts its growth in a weak field at the ionization-zone boundary, so the retarding effect of the avalanche self-space-charge becomes effective only at later stage of the avalanche growth. This is why the avalanche size increases with the increase in the ionization-zone thickness achieved by the increase of either the radius  $R_1$  or the thickness  $\delta$ , Fig(5.13).

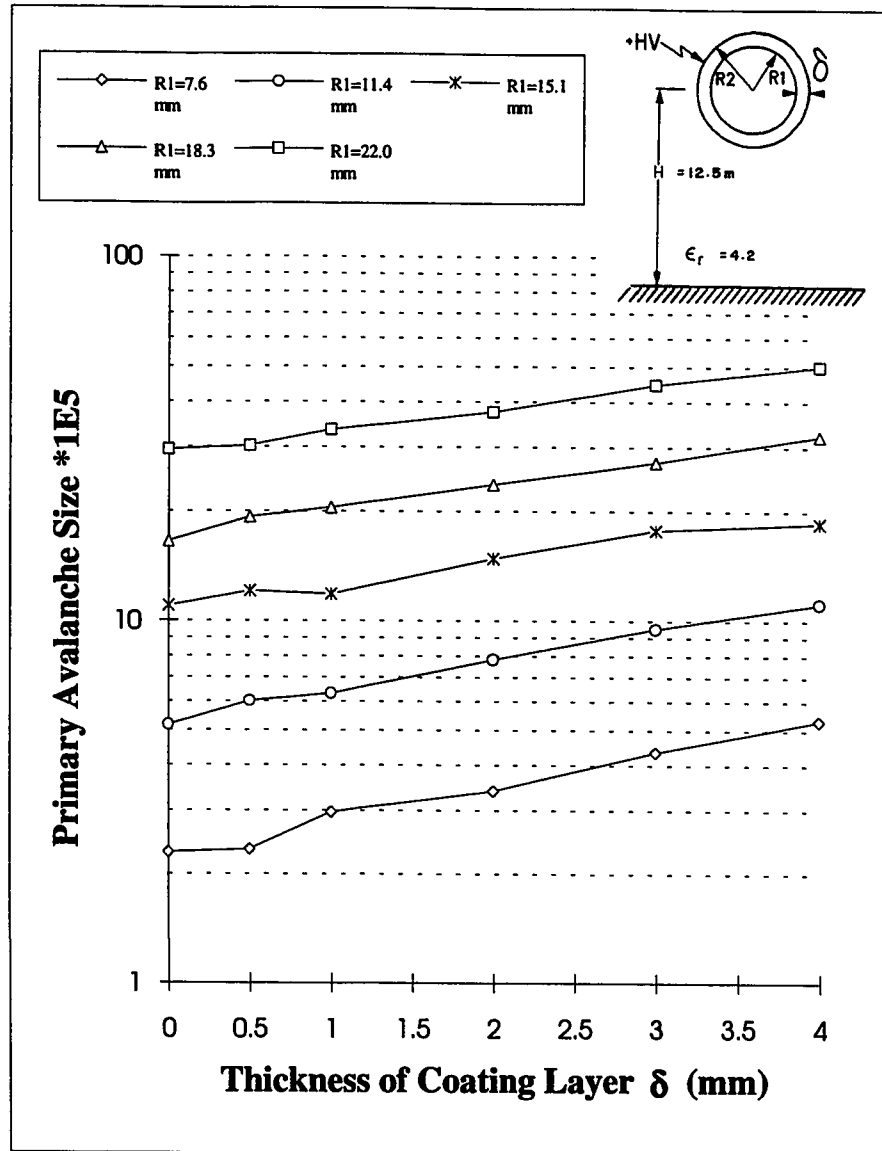
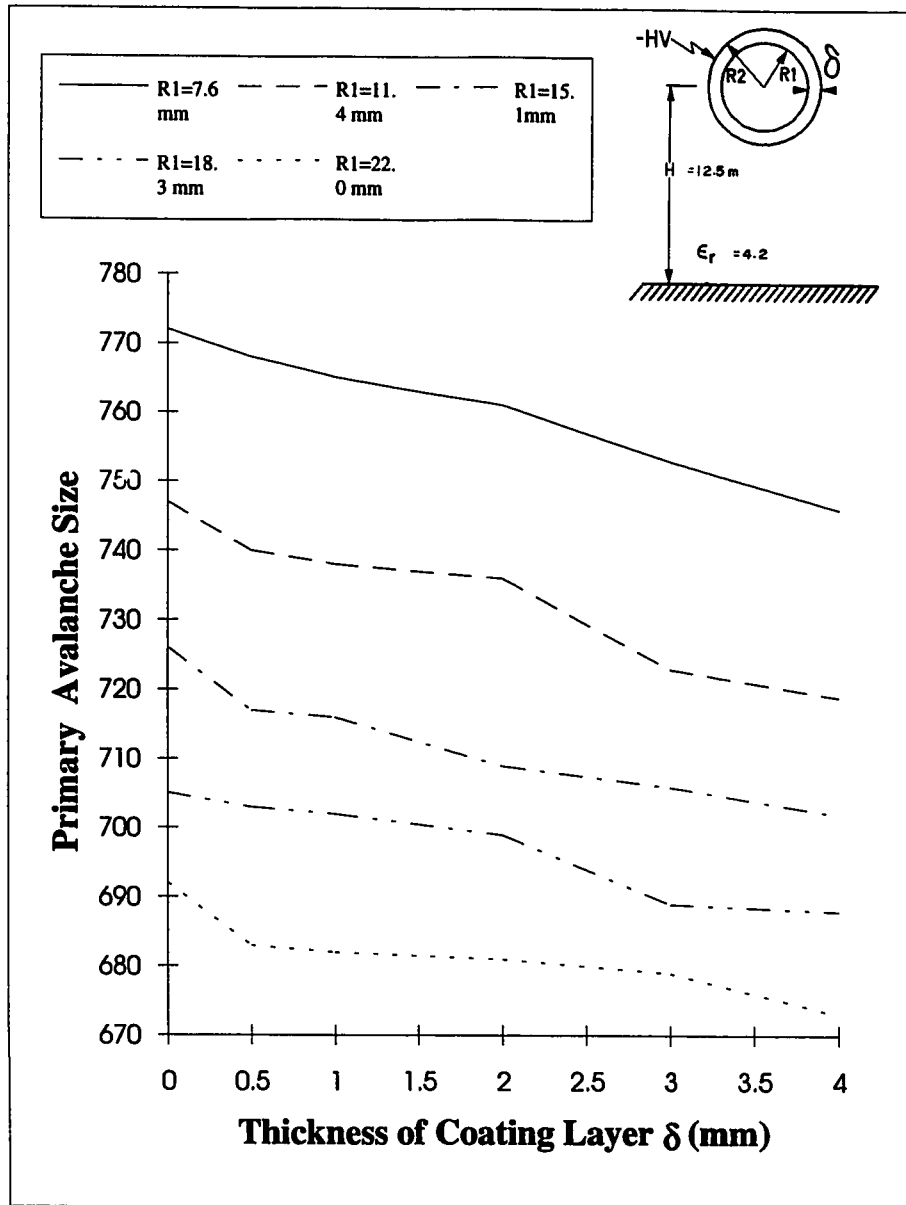


Fig.(5.13) Primary avalanche size at the positive onset voltage versus the thickness of coating layer for different values of  $R1$





*Fig.(5.14) Primary avalanche size at the negative onset voltage versus the thickness of coating layer for different values of  $R_i$*

The opposite is true for negative corona where the primary avalanche starts its growth in the highest field in the ionization-zone ( at the conductor's surface ). Thus, the self-space-charge field becomes effective early in the avalanche growth . This explains why the avalanche size decreases with the increase of the ionization-zone resulted from the increase of either  $R_1$  or  $\delta$ , Fig.(5.14) .

### 5.5.2 Effect of Conductor Height

Figures (5.15) and (5.16) represent the effect of conductor height on the primary avalanche size at the onset voltage of positive and negative coronas where the radius  $R_1$  and relative permittivity  $\epsilon_r$  are kept constant at 15.16 mm and 4.2 respectively. Increasing the conductor height in the range 10-20 m has no effect on the primary avalanche size at the onset voltage of positive and negative coronas , Figs.(5.15) and (5.16) . This is simply explained by the negligible effect of the conductor height on the electric field values inside the ionization-zone around the stressed conductor. The increase / decrease of the avalanche size with the increase of the coating-layer thickness at the onset voltage of positive / negative coronas , Figs.(5.15) and (5.16), is well described in section 5.5.1 .

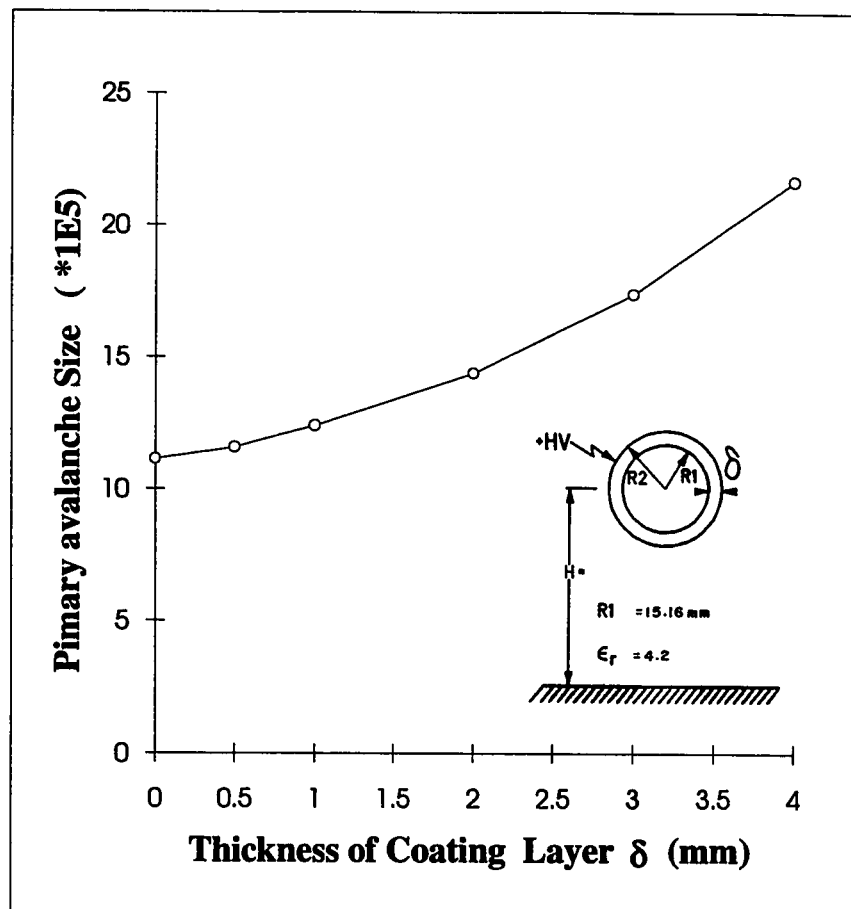


*Fig.(5.15) Primary avalanche size at the positive onset voltage versus the thickness of coating layer for different conductor heights in the range 10-20 m*

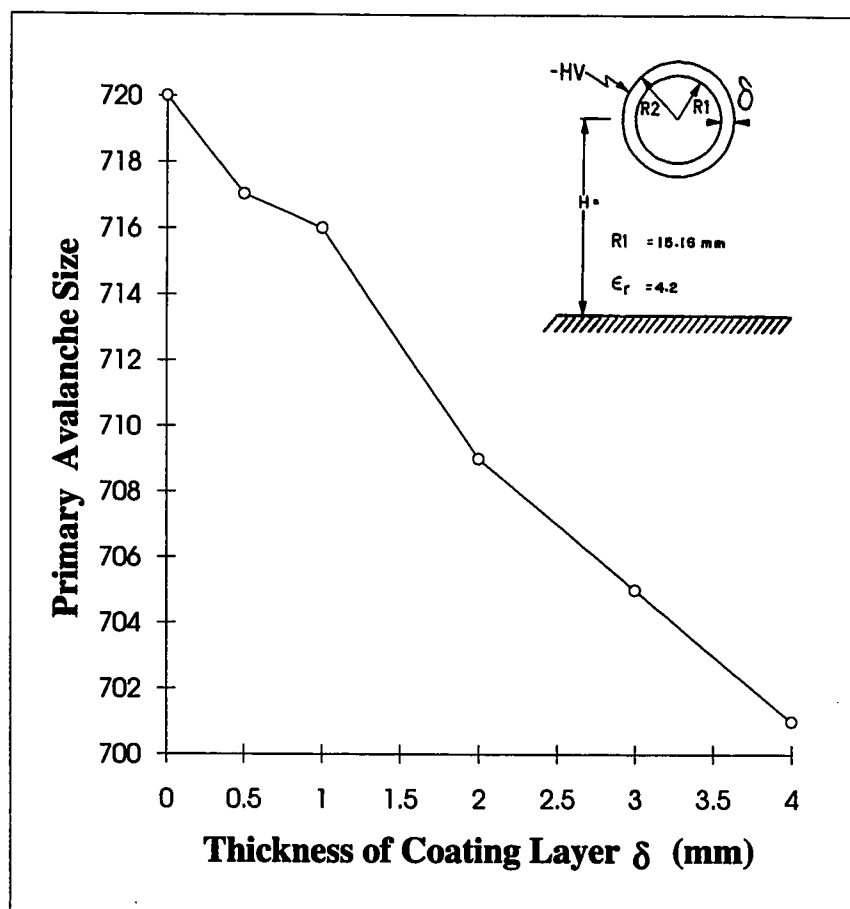


*Fig.(5.16) Primary avalanche size at the negative onset voltage versus the thickness of coating layer for different conductor heights in the range 10-20 m*

## **5.6 Effect of Dielectric Permittivity on Primary avalanche Size**

Figures (5.17) and (5.18) present the effect of dielectric permittivity on the primary avalanche size at the onset voltage of positive and negative coronas where the conductor height  $H$ , and radius  $R_1$  are kept constants at 12.5 m and 15.16 mm respectively.

Figures (5.17) and (5.18) show that the dielectric permittivity has no effect on the primary avalanche size at the onset voltage of positive and negative coronas. This is due to the fact that the onset voltage doesn't change significantly with the increase of dielectric permittivity as shown in Figs.(5.11) and (5.12). This increase / decrease of the avalanche size with the increase of the coating layer thickness at the onset voltage of positive / negative coronas, Figs.(5.17) and (5.18), is well explained in section 5.5.1.

## **5.7 Comparison Between Coated and Bare Conductors of the Same Outer Radius**

A comparison between coated and bare conductor of the same outer radius is made to appreciate the effect of coating on the corona performance of the conductor. This comparison is done based on the effect of conductor radius, conductor height, dielectric permittivity.

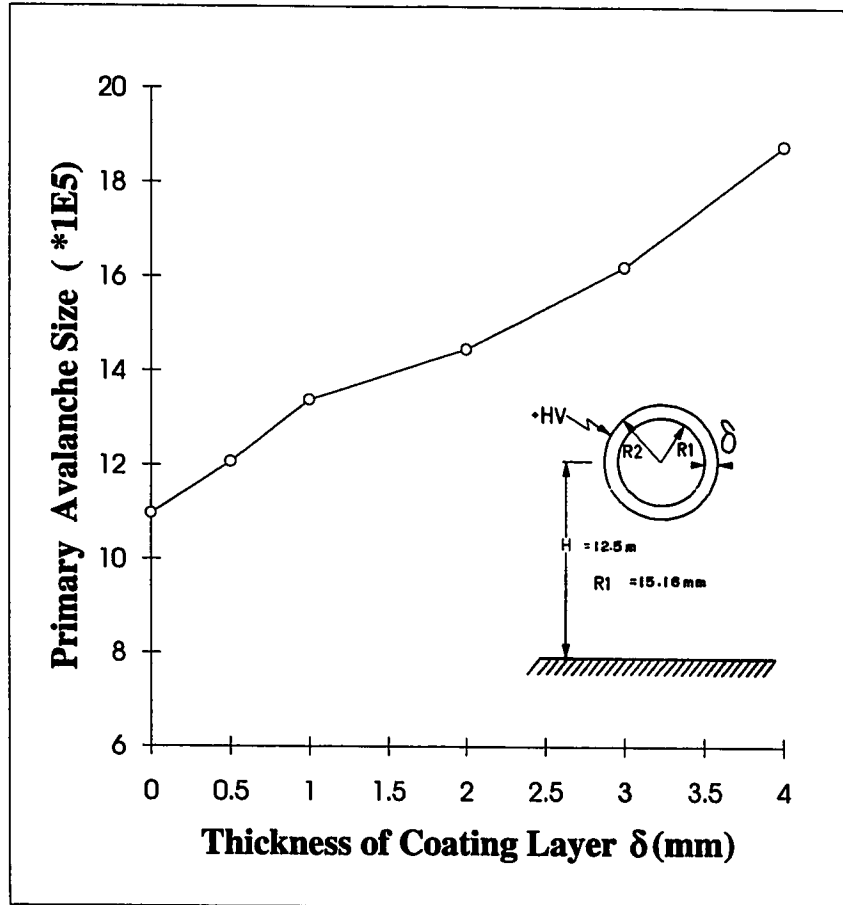


*Fig.(5.17) Primary avalanche size at the positive onset voltage versus the thickness of coating layer for different relative permittivities in the range 2.3-6.0*

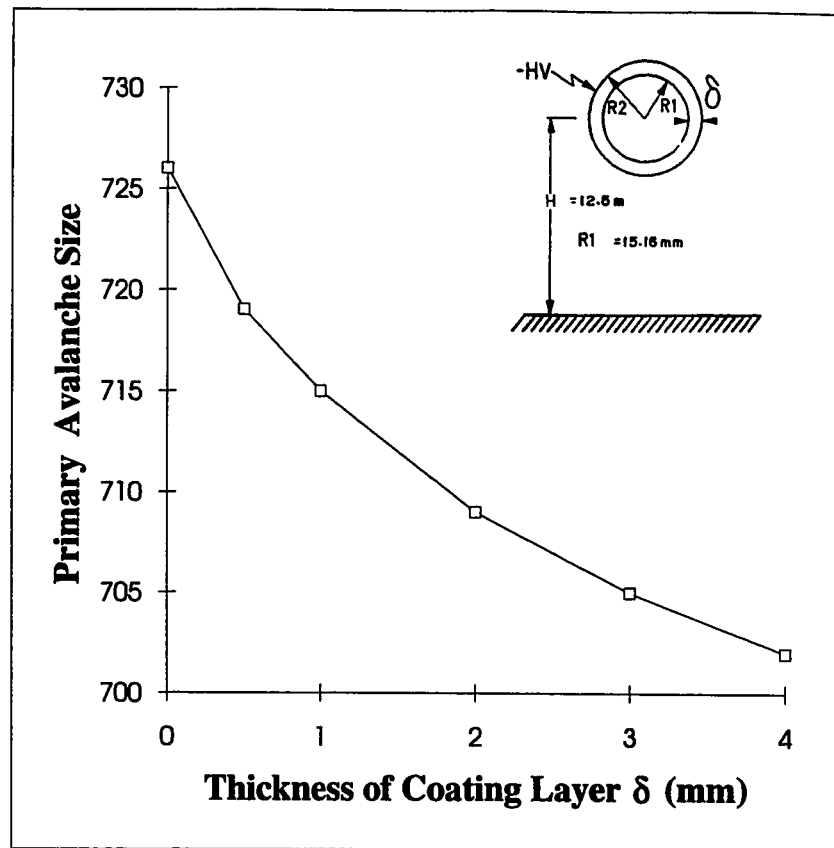


*Fig.(5.18) Primary avalanche size at the negative onset voltage versus the thickness of coating layer for different relative permittivities in the range 2.3-6.0*

### 5.7.1 Effect of Conductor Radius

This section reports a comparison between the computed onset voltage values for coated and bare conductors of the same outer radius for two values of the radius  $R_1$  ( 22 mm and 15.16 mm). This comparison is made for the positive and the negative corona. The conductor height  $H$  and relative permittivity  $\epsilon_r$  are kept constants at 12.5 m and 4.2 respectively .

Figures (5.19)-(5.22) show that the corona onset takes place at a higher voltage for a coated conductor than that for a bare conductor of the same radius for positive and negative coronas . This means that there are two options to increase the onset voltage, one is by increasing the radius of bare conductor and the other is by coating a conductor of smaller radius than the bare one . From the economical point of view , the last option is recommended as the coating material is cheaper than the conductor material itself .

### 5.7.2 Effect of Conductor Height

In this subsection, a comparison is made between the computed onset voltage values for coated and bare conductors of the same outer radius for two values of conductor height  $H$  (12.5 m and 20 m). This comparison is reported for positive and negative coronas. The relative permittivity  $\epsilon_r$  is kept constant at 4.2 .



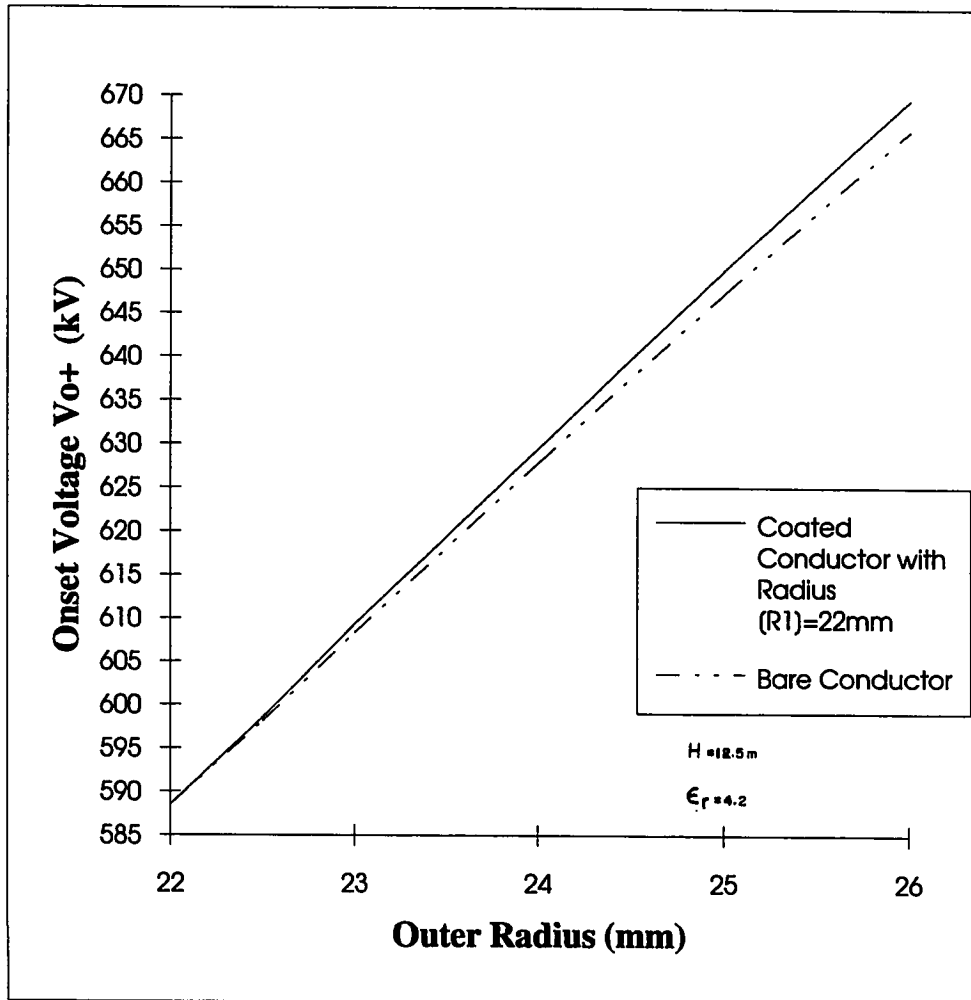


*Fig.(5.19) Positive onset voltage for coated and bare conductors of the same outer radius with  $R_1 = 22$  mm*

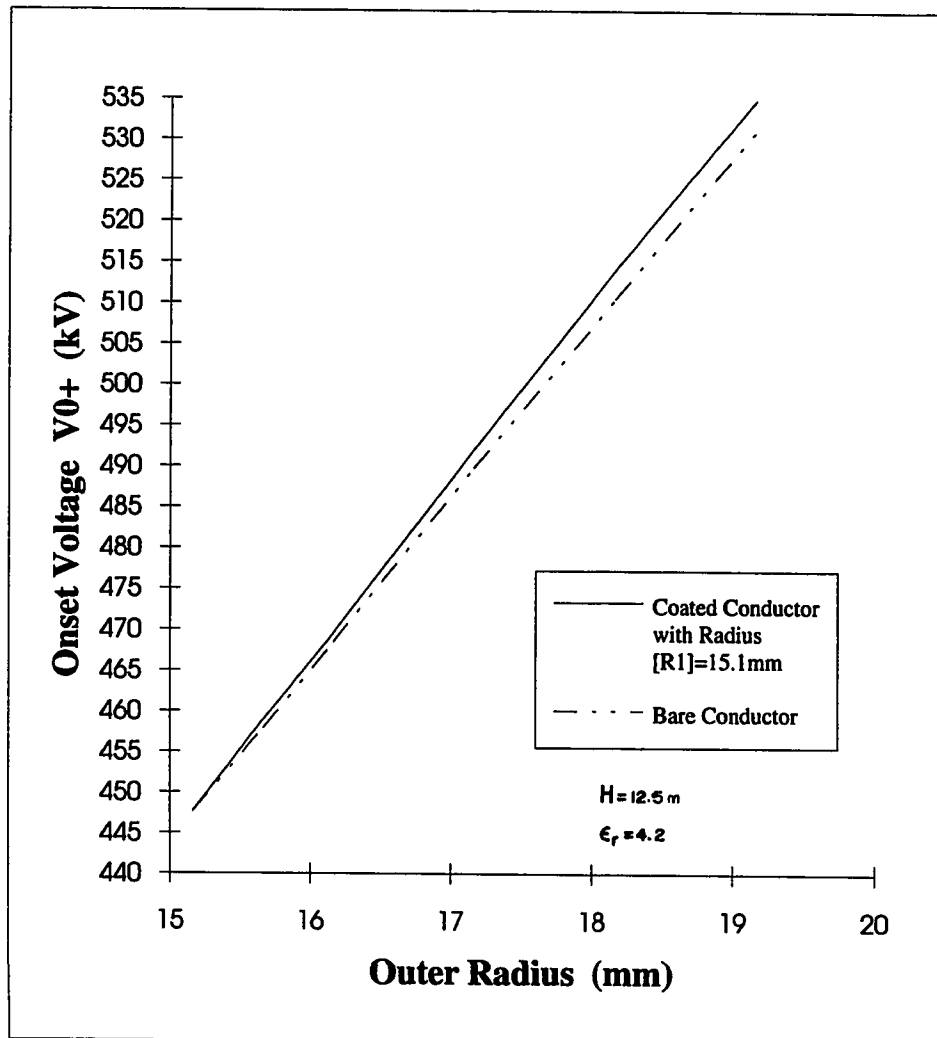


*Fig.(5.20) Positive onset voltage for coated and bare conductors of the same outer radius with  $R_1=15.16\text{ mm}$*

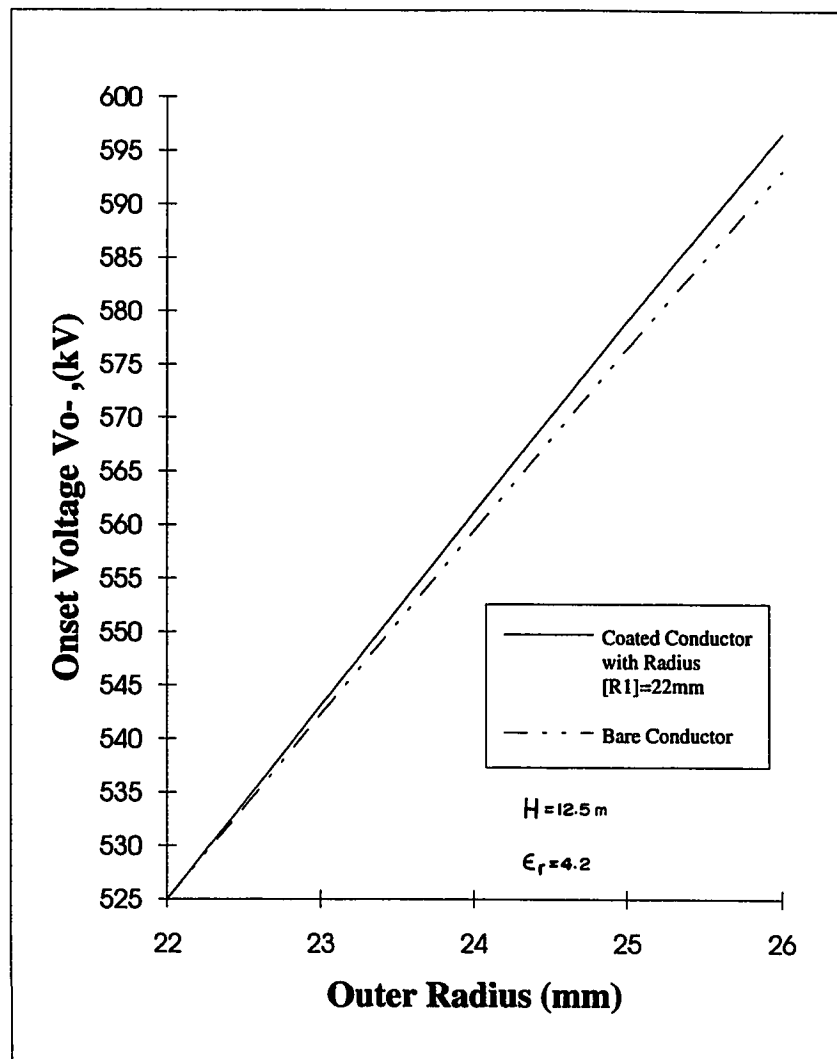


*Fig.(5.21) Negative onset voltage for coated and bare conductors of the same outer radius with  $R_1 = 22$  mm*

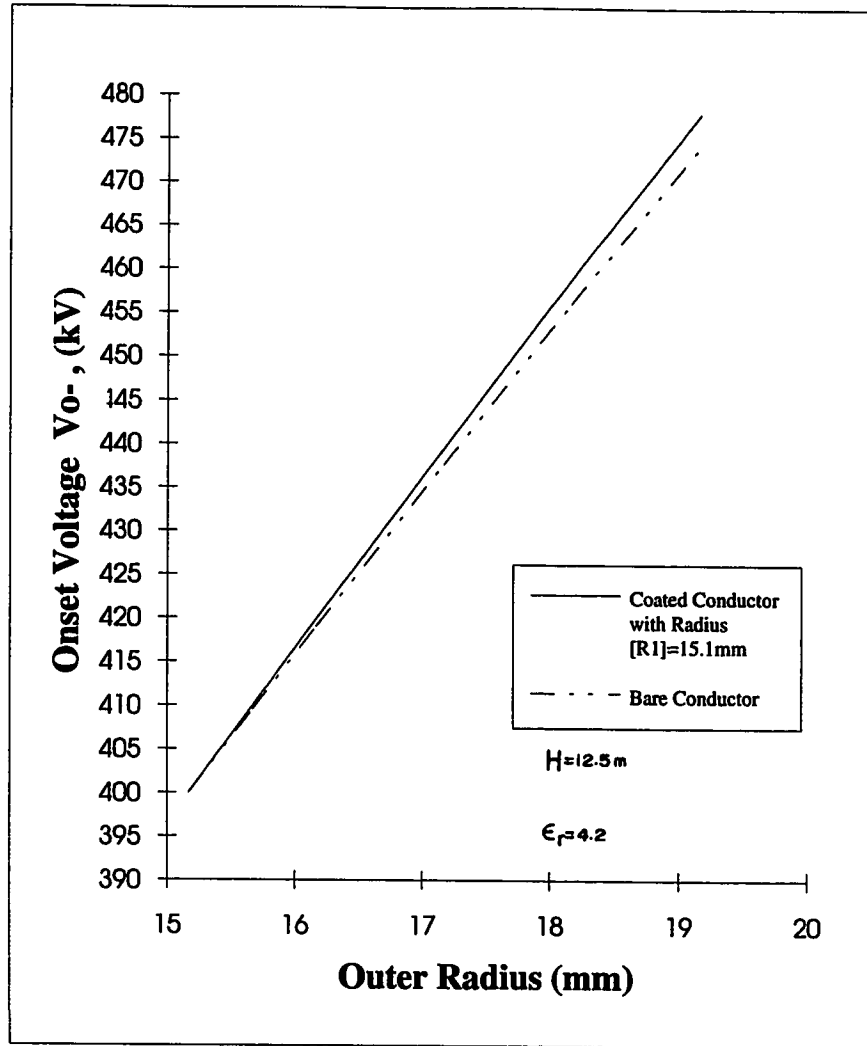


*Fig.(5.22) Negative onset voltage for coated and bare conductors of the same outer radius with  $R1=15.16$  mm*

Figures (5.23) and (5.24) indicate that the corona onset takes place at a voltage higher for coated conductor than that for bare conductor of the same radius whatever the corona polarity . This conforms with the discussion reported in the previous section .

### **5.7.3 Effect of Dielectric Permittivity**

In this subsection , a comparison is made between the computed onset voltage values for coated and bare conductors of the same outer radius . The comparison is done for positive and negative coronas . Two values of the relative permittivity  $\epsilon_r$  , 2.3 and 6 , are attempted . The conductor height is kept constant at 12.5 m .

Figures (5.25) and (5.26), show that the corona onset takes place at a higher voltage for coated conductor than that for bare conductor of the same radius irrespective of the corona polarity . The onset voltages decrease with the increase of  $\epsilon_r$  as described before . This conforms with the discussion reported in section 5.7.1 .

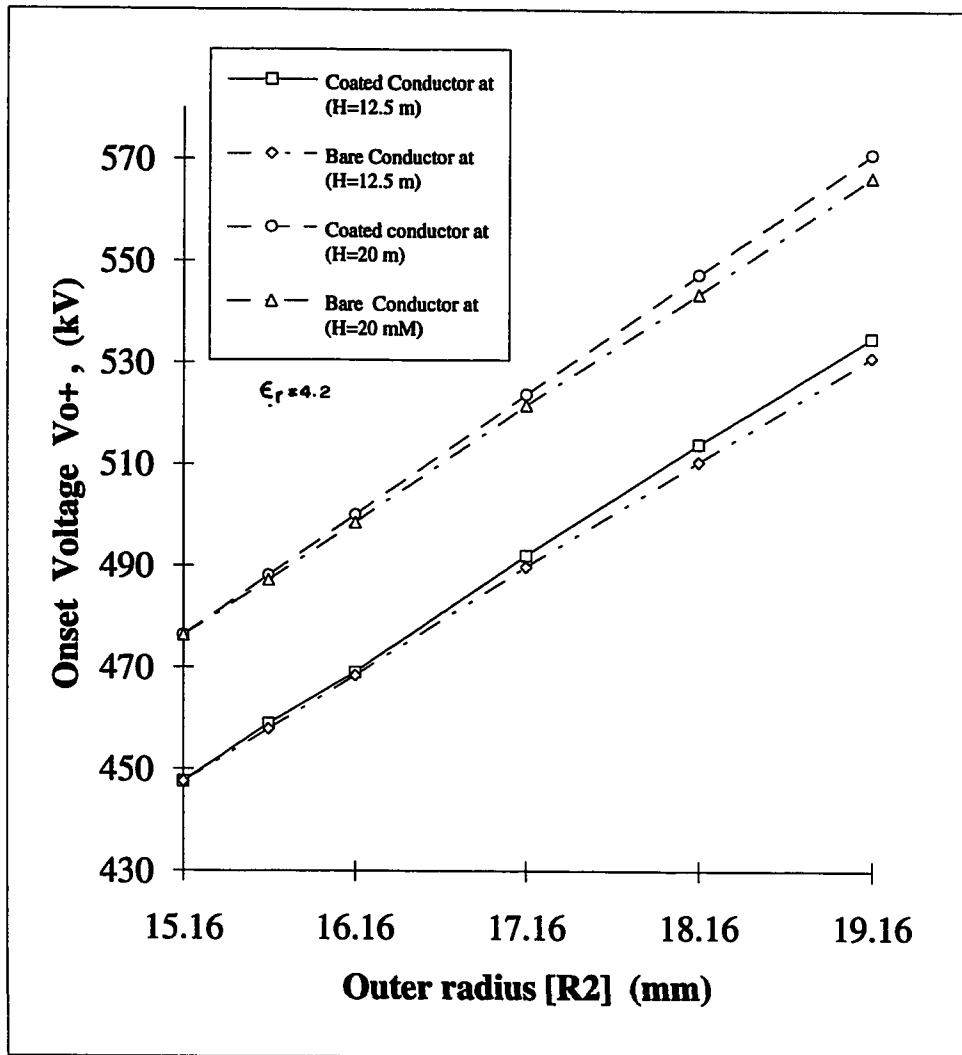


*Fig.(5.23) Positive onset voltage for coated and bare conductors of the same outer radius at heights(12.5 m and 20 m)*

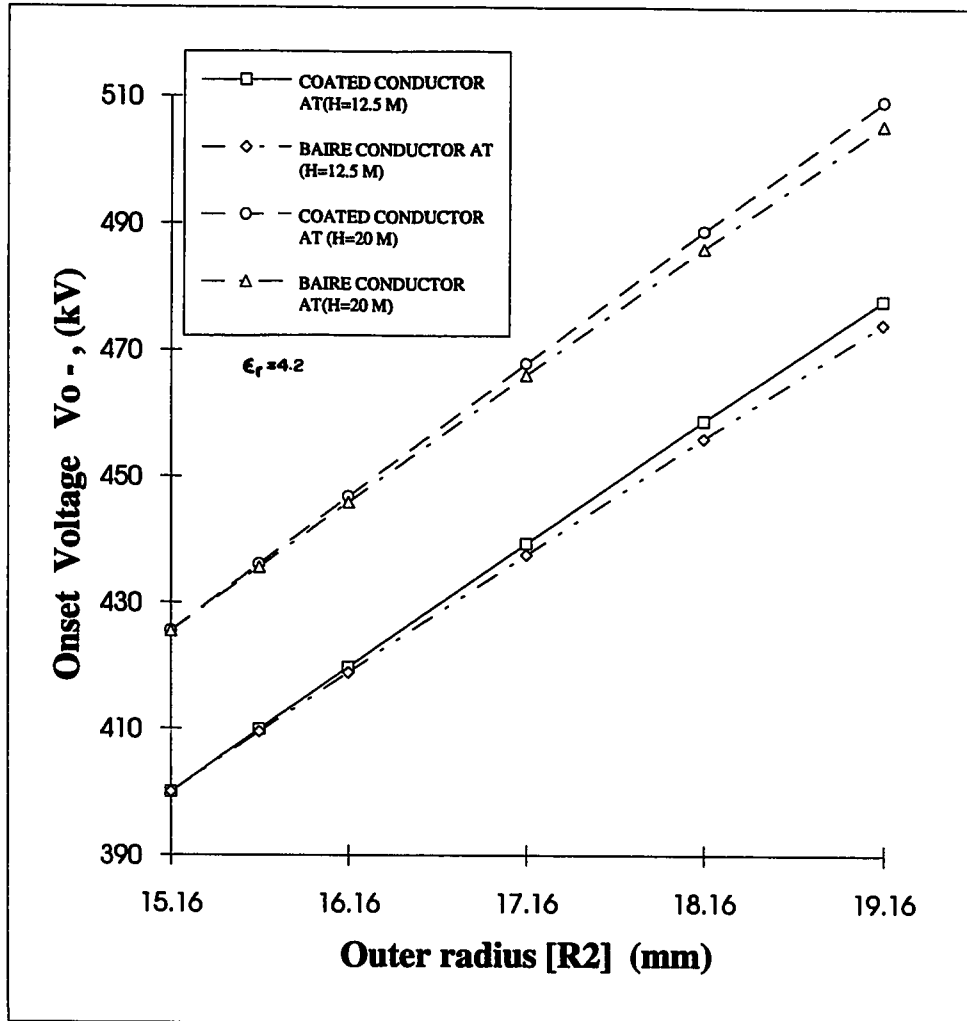


*Fig.(5.24) Negative onset voltage for coated and bare conductors of the same outer radius at heighs(12.5 m and 20 m)*

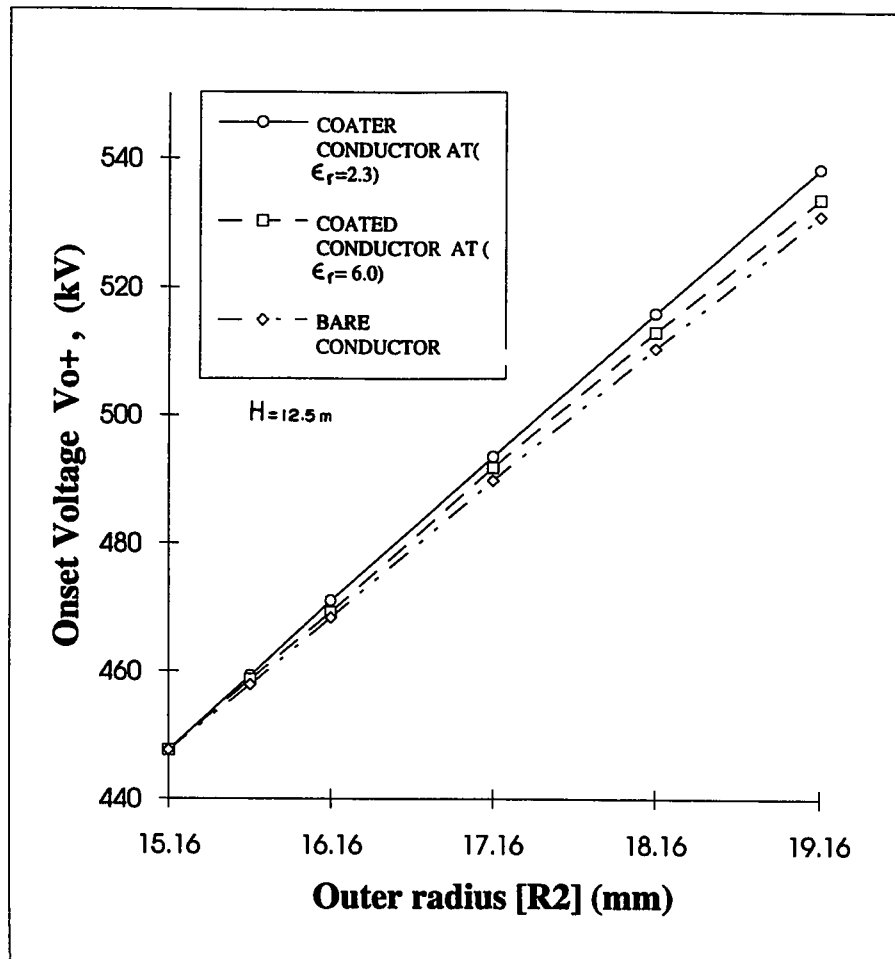


*Fig.(5.25) Positiv onset voltage for coated and bare conductors of the same outer radius at relative permittivities (2.3 and 6.0)*



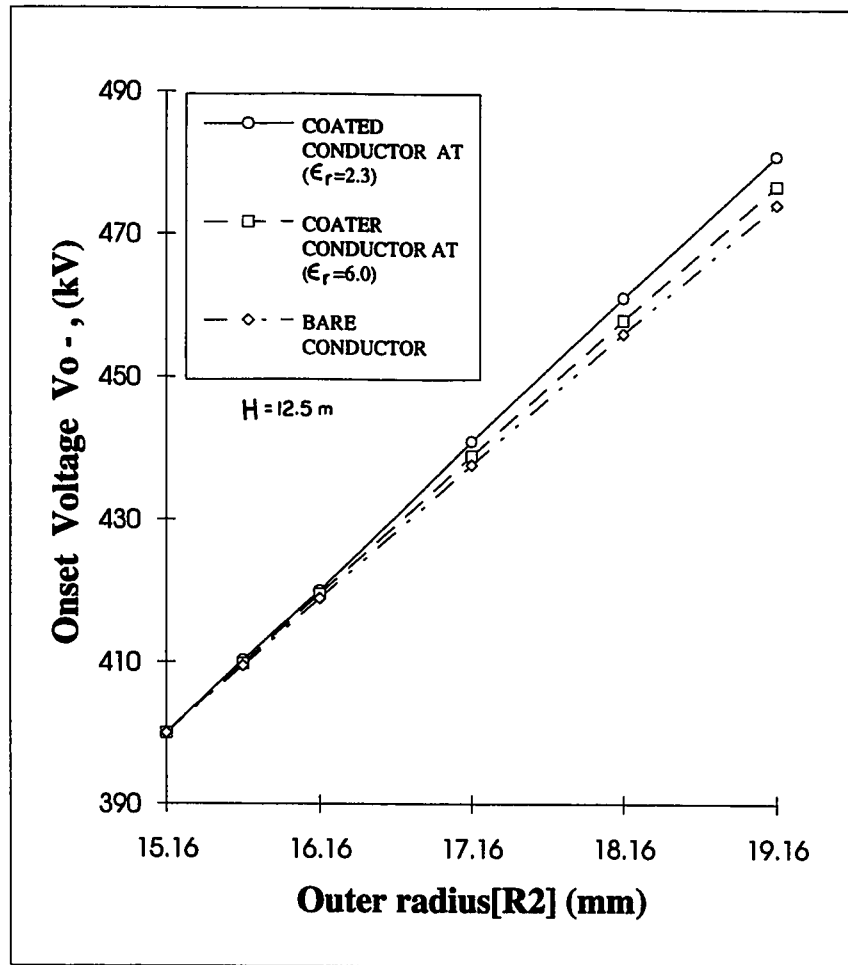


*Fig.(5.26) Negative onset voltage for coated and bare conductors of the same outer radius at relative permittivities (2.3 and 6.0)*

## **CHAPTER 6**

### **CONCLUSIONS AND SUGGESTIONS FOR FUTURE WORK**

Increased prospects of transmitting electric power by high - voltage AC have created a growing interest in the study of corona on AC transmission lines . The problems associated with corona are power loss , audible noise and radio interference . A systematic investigation [4,5] has shown that the problems associated with corona increase in wet weather and especially from water drop hanging underneath the conductor due to the rainfall . One of the suggested solutions for the above mentioned problems associated with corona [4,5,6] is to apply a coating material on a solid bare conductor .

The effect of coating has been studied for both positive and negative coronas during the respective half cycles. Several line parameters such as conductor radius , conductor height , coating layer permittivity and thickness of coating layer are investigated.

## 6.1 Conclusions

Based on the analysis of the results presented in this thesis , the following conclusions my be drawn :

- 1- A method is developed for calculating the electric field in the near vicinity of a coated conductor . This computation is performed by using charge simulation technique which shows very high accuracy .
- 2- The coated layer suppresses the electric field in the vicinity of the conductor surface in comparison with the bare conductor.
- 3- Positive and negative corona onset criteria are formulated for both coated and bare conductors . The calculated positive and negative onset voltages for bare conductor at different conductors radius are checked against the measured values [21]. It was found that the calculated values are close to those measured .
- 4- It was found that the ionization zone thickness increases with the conductor radius for bare and coated conductors . The ionization zone thickness at positive onset voltage is higher than that at the negative onset voltage .
- 5- Line parameters (conductor radius and height ) have an effect on the onset voltage for positive and negative coronas for bare and coated

conductors . The effect of conductor radius is more remarkable than that of the conductor height .

a- Increasing the conductor radius at any thickness of coated layer will result in an increase of the positive as well as the negative onset voltages . Also, increasing the thickness of coated layer will lead to an increase in both the positive and negative onset voltages .

b- Increasing the conductor height will result in an increase in both the positive and negative onset voltage at any particular thickness of coated layer.

6- Coating-layer permittivity does not have a significant effect on both the positive and negative onset voltages .

7- The line parameters ( conductor radius and height ) have a noticeable effect on the primary avalanche size for both positive and negative coronas at the onset voltage .

a- The primary avalanche size at positive onset voltage increase with the conductor radius. However , the primary avalanche size at negative onset voltage decreases with the increase of the conductor radius .

b- Increasing the height of conductor has no effect on the primary avalanche size at positive and negative onset voltages .

- 8- Increasing the coating-layer permittivity has no effect on the primary avalanche size at positive and negatives onset voltages .
- 9- A comparison between coated and bare conductors of the same outer radius is done . The onset voltage is higher for the coated conductor than that of the bare conductor of the same outer radius .

## **6.2 Suggestions for Future Work**

For future work , the following directions of research are recommended :

- 1- Calculation of electric field for stranded coated conductors .
- 2- Calculation of positive and negative corona onset voltages for stranded coated conductor and comparison with those for smooth coated conductors .
- 3- Analysis of AC corona modes on smooth and stranded coated conductors at voltages higher than the onset value .

# APPENDIX -A

## FOUR COMPUTER PROGRAMS FOR CALCULATING POSITIVE AND NEGATIVE ONSET VOLTAGES

### PROGRAM 1

#### CALCULATE POSITIVE ONSET VOLTAGE FOR COATED CONDUCTOR :

```

* *****
* * This computer program calculate the following
* * 1.The potential in the air and the coating-layer
* * 2.The electric field in the air and the coating-layer
* * 3.The positive onset voltage
* *
* *****
PARAMETER (M=150)
IMPLICIT DOUBLE PRECISION (A-H,O-Z)
DIMENSION XB(M),YB(M),XCK(M),YCK(M),TH(M),YAS(4000)
COMMON /COM1/ XC(M),YC(M)
COMMON /COM2/ Q(M)
COMMON /COM3/ AV(M,M),BV(M)
COMMON /COM4/ XIZ(180),YIZ(180),CX(180),CY(180),NSX(180)
COMMON /COM5/ AREA(900)
OPEN (UNIT = 5,FILE ='EZA.DAT',STATUS='OLD')
OPEN (UNIT = 6,FILE ='EZA.OUT',STATUS='OLD')

READ(5,*)N1,N2,N3,A,B,V,RF1,RF2,RF3,H,EPSR,STEPI,STEPE
PI=4*DATAN(1.0D0)
EPS=1E-9/(36*PI)
* *****
* * THIS SECTION FINDS CHARGES LOCATION
* *****
* WRITE(6,*)'CHARGE 1---- N1'
DTHET=PI/N1
THET=DTHET/2.0
DO 10 I=1,N1
XC(I)=RF1*B*DSIN(THET)
YC(I)=H+RF1*B*DCOS(THET)
THET=THET+DTHET
* WRITE(6,510)XC(I),YC(I)
10 CONTINUE
* *****
* WRITE(6,*)'CHARGE N1+1---N1+N2'
DTHET=PI/N2
THET=DTHET/2.0
DO 20 I=N1+1,N1+N2
XC(I)=RF2*A*DSIN(THET)
YC(I)=H+RF2*A*DCOS(THET)
THET=THET+DTHET

```

```

* WRITE(6,510)XC(I),YC(I)
20 CONTINUE
* *****
* WRITE(6,*)'CHARGE  N1+N2+1----N1+N2+N3'
DTHET=PI/N3
THET=DTHET/2.0
DO 30 I=N1+N2+1,N1+N2+N3
XC(I)=RF3*A*DSIN(THET)
YC(I)=H+RF3*A*DCOS(THET)
THET=THET+DTHET
* WRITE(6,510)XC(I),YC(I)
30 CONTINUE
* *****
* * THIS SECTION FINDS BOUNDARY POINTS LOCATION
* *****
* WRITE(6,*)'BOUNDARY  1---- N1'
DTHET=PI/N1
THET=DTHET/2.0
DO 40 I=1,N1
XB(I)=B*DSIN(THET)
YB(I)=H+B*DCOS(THET)
THET=THET+DTHET
TH(I)=THET
* WRITE(6,510)XB(I),YB(I)
40 CONTINUE
* *****
* WRITE(6,*)'BOUNDARY  N1+1---N1+N2'
DTHET=PI/N2
THET=DTHET/2.0
DO 50 I=N1+1,N1+N2
XB(I)=A*DSIN(THET)
YB(I)=H+A*DCOS(THET)
THET=THET+DTHET
TH(I)=THET
* WRITE(6,510)XB(I),YB(I)
50 CONTINUE
* *****
* WRITE(6,*)'BOUNDARY  N1+N2+1----N1+N2+N3'
DTHET=PI/N3
THET=DTHET/2.0
DO 60 I=N1+N2+1,N1+N2+N3
XB(I)=A*DSIN(THET)
YB(I)=H+A*DCOS(THET)
THET=THET+DTHET
TH(I)=THET
* WRITE(6,510)XB(I),YB(I)
60 CONTINUE
* *****
* * THIS SECTION MAKES POTENTIAL COEFFICIENT MATRIX
* *****
DO 70 I=1,N1+N2+N3
DO 70 J=1,N1+N2+N3
AV(I,J)=0.0
70 CONTINUE

DO 75 I=1,N1+N2+N3
BV(I)=0.0
75 CONTINUE

DO 80 I=1,N1
DO 80 J=1,N1

```

```

DC1=DSQRT((XB(I)-XC(J))**2+(YB(I)-YC(J))**2)
DI1=DSQRT((XB(I)-XC(J))**2+(YB(I)+YC(J))**2)

DC2=DSQRT((XB(I)+XC(J))**2+(YB(I)-YC(J))**2)
DI2=DSQRT((XB(I)+XC(J))**2+(YB(I)+YC(J))**2)
AV(I,J)=DLOG((DI1*DI2)/(DC1*DC2))
80 CONTINUE

DO 90 I=1,N1
DO 90 J=N1+N2+1,N1+N2+N3
DC1=DSQRT((XB(I)-XC(J))**2+(YB(I)-YC(J))**2)
DI1=DSQRT((XB(I)-XC(J))**2+(YB(I)+YC(J))**2)

DC2=DSQRT((XB(I)+XC(J))**2+(YB(I)-YC(J))**2)
DI2=DSQRT((XB(I)+XC(J))**2+(YB(I)+YC(J))**2)
AV(I,J)=DLOG((DI1*DI2)/(DC1*DC2))
90 CONTINUE

DO 100 I=N1+1,N1+N2
DO 100 J=N1+1,N1+N2
DC1=DSQRT((XB(I)-XC(J))**2+(YB(I)-YC(J))**2)
DI1=DSQRT((XB(I)-XC(J))**2+(YB(I)+YC(J))**2)

DC2=DSQRT((XB(I)+XC(J))**2+(YB(I)-YC(J))**2)
DI2=DSQRT((XB(I)+XC(J))**2+(YB(I)+YC(J))**2)
AV(I,J)=DLOG((DI1*DI2)/(DC1*DC2))
100 CONTINUE

DO 110 I=N1+1,N1+N2
DO 110 J=N1+N2+1,N1+N2+N3
DC1=DSQRT((XB(I)-XC(J))**2+(YB(I)-YC(J))**2)
DI1=DSQRT((XB(I)-XC(J))**2+(YB(I)+YC(J))**2)

DC2=DSQRT((XB(I)+XC(J))**2+(YB(I)-YC(J))**2)
DI2=DSQRT((XB(I)+XC(J))**2+(YB(I)+YC(J))**2)
AV(I,J)=(-1)*DLOG((DI1*DI2)/(DC1*DC2))
110 CONTINUE

DO 120 I=N1+N2+1,N1+N2+N3
DO 120 J=1,N1
I1=I-N1-N2
TH1=PI/2-(DTHET/2+DTHET*(I1-1))
RAD1=DSQRT((XB(I)-XC(J))**2+(YB(I)-YC(J))**2)
RAD2=DSQRT((XB(I)+XC(J))**2+(YB(I)-YC(J))**2)
RAD3=DSQRT((XB(I)-XC(J))**2+(YB(I)+YC(J))**2)
RAD4=DSQRT((XB(I)+XC(J))**2+(YB(I)+YC(J))**2)

XCOMP1=(XB(I)-XC(J))/RAD1**2
XCOMP2=(XB(I)+XC(J))/RAD2**2
XCOMP3=(XB(I)-XC(J))/RAD3**2
XCOMP4=(XB(I)+XC(J))/RAD4**2

XCOMP=XCOMP1+XCOMP2-XCOMP3-XCOMP4

YCOMP1=(YB(I)-YC(J))/RAD1**2
YCOMP2=(YB(I)-YC(J))/RAD2**2
YCOMP3=(YB(I)+YC(J))/RAD3**2
YCOMP4=(YB(I)+YC(J))/RAD4**2

YCOMP=YCOMP1+YCOMP2-YCOMP3-YCOMP4

```



```

      AV(I,J)=(EPSR-1)*(XCOMP*DCOS(TH1)+YCOMP*DSIN(TH1))
120 CONTINUE

```

```

      DO 130 I=N1+N2+1,N1+N2+N3
      DO 130 J=N1+1,N1+N2
      I1=I-N1-N2
      TH1=PI/2-(DTHET/2+DTHET*(I1-1))
      RAD1=DSQRT((XB(I)-XC(J))**2+(YB(I)-YC(J))**2)
      RAD2=DSQRT((XB(I)+XC(J))**2+(YB(I)-YC(J))**2)
      RAD3=DSQRT((XB(I)-XC(J))**2+(YB(I)+YC(J))**2)
      RAD4=DSQRT((XB(I)+XC(J))**2+(YB(I)+YC(J))**2)

```

```

      XCOMP1=(XB(I)-XC(J))/RAD1**2
      XCOMP2=(XB(I)+XC(J))/RAD2**2
      XCOMP3=(XB(I)-XC(J))/RAD3**2
      XCOMP4=(XB(I)+XC(J))/RAD4**2

```

```

      XCOMP=XCOMP1+XCOMP2-XCOMP3-XCOMP4

```

```

      YCOMP1=(YB(I)-YC(J))/RAD1**2
      YCOMP2=(YB(I)-YC(J))/RAD2**2
      YCOMP3=(YB(I)+YC(J))/RAD3**2
      YCOMP4=(YB(I)+YC(J))/RAD4**2

```

```

      YCOMP=YCOMP1+YCOMP2-YCOMP3-YCOMP4

```

```

      AV(I,J)=(-1)*(XCOMP*DCOS(TH1)+YCOMP*DSIN(TH1))
130 CONTINUE

```

```

      DO 140 I=N1+N2+1,N1+N2+N3
      DO 140 J=N1+N2+1,N1+N2+N3
      I1=I-N1-N2
      TH1=PI/2-(DTHET/2+DTHET*(I1-1))
      RAD1=DSQRT((XB(I)-XC(J))**2+(YB(I)-YC(J))**2)
      RAD2=DSQRT((XB(I)+XC(J))**2+(YB(I)-YC(J))**2)
      RAD3=DSQRT((XB(I)-XC(J))**2+(YB(I)+YC(J))**2)
      RAD4=DSQRT((XB(I)+XC(J))**2+(YB(I)+YC(J))**2)

```

```

      XCOMP1=(XB(I)-XC(J))/RAD1**2
      XCOMP2=(XB(I)+XC(J))/RAD2**2
      XCOMP3=(XB(I)-XC(J))/RAD3**2
      XCOMP4=(XB(I)+XC(J))/RAD4**2

```

```

      XCOMP=XCOMP1+XCOMP2-XCOMP3-XCOMP4

```

```

      YCOMP1=(YB(I)-YC(J))/RAD1**2
      YCOMP2=(YB(I)-YC(J))/RAD2**2
      YCOMP3=(YB(I)+YC(J))/RAD3**2
      YCOMP4=(YB(I)+YC(J))/RAD4**2

```

```

      YCOMP=YCOMP1+YCOMP2-YCOMP3-YCOMP4

```

```

      AV(I,J)=(EPSR)*(XCOMP*DCOS(TH1)+YCOMP*DSIN(TH1))
140 CONTINUE

```

```

      DO 150 I=1,N1
      BV(I)=V
150 CONTINUE

```

```

* *****

```

```

      N=N1+N2+N3
C   DO 220 I=1,N1+N2+N3
C   WRITE(6,510)(AV(I,J),J=1,N1+N2+N3)
C220 CONTINUE

      CALL NGAUSS(N)
      DTHET= PI/N1
      THET=0.0
      DO 160 I=1,N1
      XCK(I)=B*DSIN(THET)
      YCK(I)=H+B*DCOS(THET)
      THET=THET+DTHET
160 CONTINUE
      WRITE(6,*)' CONDUCTOR POTENTIAL'
      DO 170 I=1,N1
      X=XCK(I)
      Y=YCK(I)
      CALL POTI(N1,N2,N3,X,Y,POT)
      WRITE(6,510)X,Y,POT
170 CONTINUE

      DTHET= PI/N2
      THET=0.0
      DO 180 I=1,N2
      XCK(I)=A*DSIN(THET)
      YCK(I)=H+A*DCOS(THET)
      THET=THET+DTHET
180 CONTINUE
      YAA=0.0
c   WRITE(6,*)'POTENTIAL AT ENTERFACE'
      DO 190 I=1,N2
      X=XCK(I)
      Y=YCK(I)
      CALL POTI(N1,N2,N3,X,Y,POT)
      V1=POT
      YAA=YAA+V1
      CALL POTE(N1,N2,N3,X,Y,POT)
      V2=POT
C   WRITE(6,510)X,Y,V1,V2
190 CONTINUE
      YAA=YAA/N2
C   WRITE(6,*)'AVERAGE VLTAGE',YAA
C   WRITE(6,*)'FIELD AT ENTERFACE'

      DO 210 I=1,N2
      X=XCK(I)
      Y=YCK(I)
      CALL FELDI(N1,N2,N3,X,Y,EX,EY,E,EPSR,H)
      E1=E
      CALL FELDE(N1,N2,N3,X,Y,EX,EY,E,EPSR,H)
      E2=E
C   WRITE(6,510)X,Y,E1,E2,E2/E1
210 CONTINUE

510 FORMAT(08(E12.5,2X))
C   WRITE(6,*)'*****'
      DV=(V-YAA)/STEPI
      X=0.0
      Y=H-B
      DO 500 I=1,STEPI+3
      RX=DSQRT(X**2+(H-Y)**2)

```

```

IF(RX.GT.A) THEN
  GOTO111
ELSE
  CALL POTI(N1,N2,N3,X,Y,POT)
  CALL FELDI(N1,N2,N3,X,Y,EX,EY,E,EPSR,H)
C  WRITE(6,510)X,Y,POT,EX,EY,E
C  WRITE(6,*)Y,E
  DY=DV/E
  Y=Y-DY
ENDIF
500 CONTINUE
111 WRITE(6,*)'*****'
C  DV=YAA/STEPE
  X=0.0
  Y=H-A
  DY=Y/STEPE
  DO 501 I=1,STEPE
    CALL POTE(N1,N2,N3,X,Y,POT)
    CALL FELDE(N1,N2,N3,X,Y,EX,EY,E,EPSR,H)
C  WRITE(6,510)X,Y,POT,EX,EY,E
C  WRITE(6,*)Y,E
C  DY=DV/E
  Y=Y-DY
501 CONTINUE
C  stop

```

```

* *****
*  * THIS PART FINDS THE IONIZATION ZONE
* *****
  IN=1
  LL=1
  DS=100.0*A
  DO 502 I=0,180,10
    THET=I*PI/180.0
    X=A*DSIN(THET)
    Y=H+A*DCOS(THET)
* *****
  DO 503 L=1,4000
    CALL FELDE(N1,N2,N3,X,Y,EX,EY,E,EPSR,H)
    IF(I.EQ.180)THEN
c  WRITE(6,*)E
    YAS(IN)=Y
    IN=IN+1
    ENDIF

    E=E/100.0
    ATT=(0.01298-0.541E-3*(E/760.0)+0.87E-5*(E/760.0)**2)*760.0
    IF(E/760.0.GE.25.AND.E/760.0.LE.60.0) THEN
C  WRITE(6,*)E/760.0,'IONIZATION BET. 25--60'
    FION=(4.7786*EXP(-221*760.0/E))*760.0
    ELSEIF (E/760.0.GE.60.0.AND.E/760.0.LE.240.0) THEN
C  WRITE(6,*)E/760.0,'IONIZATION BET.60--240'
    FION=(9.682*EXP(-264.2*760.0/E))*760.0
    ELSE
    WRITE(6,*)E/760.0,'IONIZATION OUT OF THE RANGE',i,l
    GOTO 987
    ENDIF
    DIF=FION-ATT
    IF(ABS(DIF).LT.0.01*FION) GOTO 560

```

```

RZ=.01*FION
DL=DS/E
Y=Y+DL*DCOS(THET)
X=X+DL*DSIN(THET)
C  WRITE(6,*)FION,ATT,DIF,RZ
503  CONTINUE
    WRITE(6,*)'STEPE IS NOT INAF'
    GOTO 987
C560 WRITE(6,*)'THE IONIZATION AND THE ATTACHEMENT WHEN ION=ATT'

560 IF(I.LE.180) THEN
    EI=E/100.0
C  CALL ATTION(EI,FION,ATT,DIF)
    XIZ(LL)=X
    YIZ(LL)=Y
    WRITE(6,*)XIZ(LL),YIZ(LL),'IONIZATION ',LL,FION,ATT
    LL=LL+1
ENDIF

C  WRITE(6,*)X,Y
502  CONTINUE
* *****
*  * THIS PART DRAWS THE CONDUCTOR
* *****
561  KK=1
    DO 504 I=0,180,10
        THET=I*PI/180.0
        X=A*DSIN(THET)
        Y=H+A*DCOS(THET)
        IF(I.LE.180) THEN
            CX(KK)=X
            CY(KK)=Y
            WRITE(6,*)CX(KK),CY(KK),'CONDUCTOR',KK,I
            KK=KK+1
        ENDIF
    *  WRITE(6,*)X,Y
504  CONTINUE
C987 stop
* *****
*  * THIS PART FINDS NUMBER OF SECTIONS IN EACH LEVEL
* *****
    FAK=.002
    KK=KK-1
    LL=LL-1
    DO 301 I=2,LL
        IF(I.LE.(LL/2+1)) THEN
            NSX(I)=XIZ(I)/FAK+1
            IF(YIZ(I).LT.CY(1).AND.YIZ(I).GT.CY(KK)) THEN
                THET=DACOS((YIZ(I)-H)/A)
                X=A*DSIN(THET)
                NSX(I)=ABS(XIZ(I)-X)/FAK+1
            ENDIF
        ELSE
            NSX(I)=XIZ(I-1)/FAK+1
            IF(YIZ(I).LT.CY(1).AND.YIZ(I).GT.CY(KK)) THEN
                THET=DACOS((YIZ(I-1)-H)/A)
                X=A*DSIN(THET)
                NSX(I)=ABS(XIZ(I-1)-X)/FAK+1
            ENDIF
        ENDIF
    WRITE(6,*)I,NSX(I)

```

```

301 CONTINUE
* *****
* * THIS PART FINDS THE PRIMARY AVALANCHE
* *****
DO 33 I=1,IN-1
  DF=((H-A)-YAS(I))/(CY(KK)-YIZ(LL))
c WRITE(6,*)DF
33 CONTINUE
  TAW=0.0
  NOA=50
  NINTG=150
  SUM=0.0
  ISAV=1
  TL=CY(KK)-YIZ(LL)
  write(6,*)tl='tl
  YL=TL/(NOA*1.0)
  STEIN=YL/(NINTG*1.0)
  NINTG=NINTG+1
  DO 302 K=1,NOA
  DO 303 NN=ISAV,NINTG
    Y=YIZ(LL)+(NN-1)*STEIN
    X=0.0
    CALL FELDE(N1,N2,N3,X,Y,EX,EY,E,EPSR,H)
    IF(NN.EQ.1) THEN
      ET=E/100.0
    ELSE
      ESC=1.6E-19*(EXP(SUM)-1.0)/(4.0*PI*EPS*XSC**2)
      ET=(E-ESC)/100.0
    ENDIF
    CALL ATTION(ET,FION,ATT,DIF)
    XSC=1.0/(FION*100.0)
    SUM=SUM+STEIN*DIF*100.0
    CALL EMOBS(ET,EMOB)
    TAW=TAW+STEIN/(EMOB*(ET*100.0))
    IF(K.EQ.NOA.AND.NN.EQ.NINTG) THEN
      CALL EMOBS(ET,EMOB)
      CALL RADPAV(ET,TAW,EMOB,RPA)
    ENDIF
  303 CONTINUE

  EIONS=EXP(SUM)
  YTAV=Y
  XTAV=X
  WRITE(6,*)EIONS,K,YTAV
  CALL FAREA(YTAV,XTAV,LL,KK,PI,N1,N2,N3,H,EIONS,A)
  ISAV=NINTG+1
  NINTG=NINTG+150
302 CONTINUE
  AVPR=EIONS
* *****
* * CALCULATION OF THE SECONDARY AVALANCHES SIZE
* *****
  SAVAL=0.0
  NAA=1
  DO 401 I=2,LL
    IF(I.LE.(LL/2+1)) THEN
      THIX=XIZ(I)/(NSX(I)*1.0)
      IF(YIZ(I).LT.CY(1).AND.YIZ(I).GT.CY(KK)) THEN
        THET=DACOS((YIZ(I)-H)/A)
        X=A*DSIN(THET)
        THIX=ABS(XIZ(I)-X)/(NSX(I)*1.0)

```

```

ENDIF
ELSE
THIX=XIZ(I-1)/(NSX(I)*1.0)
IF(YIZ(I).LT.CY(1).AND.YIZ(I).GT.CY(KK)) THEN
THET=DACOS((YIZ(I-1)-H)/A)
X=A*DSIN(THET)
THIX=ABS(XIZ(I-1)-X)/(NSX(I)*1.0)
ENDIF
ENDIF
NZ=5
DO 402 J=1,NSX(I)
IF(I.LE.(LL/2+1)) THEN
COIX=XIZ(I)-(J-1)*THIX
ELSE
COIX=XIZ(I-1)-(J-1)*THIX
ENDIF
Z=0.0
THIZ=((CY(KK)-YIZ(LL))*DTAN(80*PI/180))/NZ
DO 403 K=1,NZ
DELT=.00004
SUMS=0.0
Z=Z+(K-1)*THIZ
X=COIX
Y=YIZ(I)
DO 404 MS=1,300
CALL FELDE(N1,N2,N3,X,Y,EX,EY,E,EPSR,H)
SCP=SQRT((Y-(CY(KK)-RPA))**2+X**2+Z**2)
ESCP=1.6E-19*(AVPR-1.0)/(4.0*PI*EPS*SCP**2)
c  write(6,*)'avpr=',avpr,escp
c  stop
IF(Z.EQ.0.0) THEN
EXSCP=(X/SCP)*ESCP
EYSCP=(Y-(CY(KK)-RPA))/SCP*ESCP
EZSCP=0.0
ELSE
THTY=DACOS((Y-(CY(KK)-RPA))/SCP)
EYSCP=ESCP*DCOS(THTY)
EXZ=ESCP*DSIN(THTY)
THTX=DACOS(X/SQRT(X**2+Z**2))
EXSCP=EXZ*DCOS(THTX)
EZSCP=EXZ*DSIN(THTX)
ENDIF
IF(MS.GT.1) THEN
ESSC=1.6E-19*(EXP(SUMS)-1.0)/(4.0*PI*EPS*SSC**2)
EXSSC=-ESSC*(EX+EXSCP)/ETS
EYSSC=-ESSC*(EY+EYSCP)/ETS
EZSSC=-ESSC*(EZSCP/ETS)
ELSE
ESSC=0.0
EXSSC=0.0
EYSSC=0.0
EZSSC=0.0
ENDIF
ETS=SQRT((EX+EXSCP+EXSSC)**2+(EY+EYSCP+EYSSC)**2+
+(EZSCP+EZSSC)**2)
ETTS=ETS/100.0
CALL ATTION(ETTS,FION,ATT,DIF)
SUMS=SUMS+DIF*DELT*100.0
SSC=1.0/(FION*100.0)
DELT=1.0/(10.0*FION*100.0)
IF(Z.EQ.0.0) THEN

```

```

X=X-DELT*(EX+EXSCP+EXSSC)/ETS
Y=Y-DELT*(EY+EYSCP+EYSSC)/ETS
Z=0.0
ELSE
X=X-DELT*(EX+EXSCP+EXSSC)/ETS
Y=Y-DELT*(EY+EYSCP+EYSSC)/ETS
Z=Z-DELT*(EZSCP+EZSSC)/ETS
ENDIF
DBCP=SQRT(X**2+(Y-(CY(KK)-RPA))**2+Z**2)
CAPC=SQRT(X**2+(Y-H)**2+Z**2)
IF(Z.EQ.0.0) THEN
IF(DBCP.LE.RPA) GOTO 45
IF(CAPC.LE.A) GOTO 45
ELSE
CAPC=SQRT(X**2+(Y-H)**2)
IF(CAPC.LE.A) GOTO 45
ENDIF
404 CONTINUE
45 SEION=EXP(SUMS)
SAVAL=SAVAL+AREA(NAA)*SEION
NAA=NAA+1
403 CONTINUE
402 CONTINUE
401 CONTINUE
WRITE(6,87)X,Y,SAVAL,I,J,K,MS
87 FORMAT(1X,'X=',F12.10,1X,'Y=',F12.10,1X,'SAVAL=',F12.6,1X,'I='
+,I3,1X,'J=',I3,1X,'K=',I2,1X,'MS=',I3)
TOTSA=SAVAL*4.0
WRITE(6,*)'SECONDARY=',TOTSA
987 STOP
END
* ***** END OF NAIM PROGRAM *****
* *****
* * THIS SUBROUTINE FINDS POTENTIAL IN THE COATING-LAYER
* *****
SUBROUTINE POTI(N1,N2,N3,X,Y,POT)
PARAMETER (M=150)
IMPLICIT DOUBLE PRECISION (A-H,O-Z)
COMMON /COM1/ XC(M),YC(M)
COMMON /COM2/ Q(M)
SUMV=0.0
DO 200 J=1,N1
DC1=DSQRT((X-XC(J))**2+(Y-YC(J))**2)
DI1=DSQRT((X-XC(J))**2+(Y+YC(J))**2)

DC2=DSQRT((X+XC(J))**2+(Y-YC(J))**2)
DI2=DSQRT((X+XC(J))**2+(Y+YC(J))**2)
SUMV=SUMV+Q(J)*DLOG((DI1*DI2)/(DC1*DC2))
200 CONTINUE

DO 300 J=N1+N2+1,N1+N2+N3
DC1=DSQRT((X-XC(J))**2+(Y-YC(J))**2)
DI1=DSQRT((X-XC(J))**2+(Y+YC(J))**2)

DC2=DSQRT((X+XC(J))**2+(Y-YC(J))**2)
DI2=DSQRT((X+XC(J))**2+(Y+YC(J))**2)
SUMV=SUMV+Q(J)*DLOG((DI1*DI2)/(DC1*DC2))
300 CONTINUE
POT=SUMV
RETURN
END

```

```
* *****
* * THIS SUBROUTINE FINDS POTENTIAL IN THE AIR
* *****
```

```
SUBROUTINE POTE(N1,N2,N3,X,Y,POT)
PARAMETER (M=150)
IMPLICIT DOUBLE PRECISION (A-H,O-Z)
COMMON /COM1/ XC(M),YC(M)
COMMON /COM2/ Q(M)
SUMV=0.0
DO 200 J=1,N1+N2
DC1=DSQRT((X-XC(J))**2+(Y-YC(J))**2)
DI1=DSQRT((X-XC(J))**2+(Y+YC(J))**2)

DC2=DSQRT((X+XC(J))**2+(Y-YC(J))**2)
DI2=DSQRT((X+XC(J))**2+(Y+YC(J))**2)
SUMV=SUMV+Q(J)*DLOG((DI1*DI2)/(DC1*DC2))
200 CONTINUE
POT=SUMV
RETURN
END
```

```
* *****
* * THIS SUBROUTINE FINDS ELECTRIC FIELD IN THE COATING-LAYER
* *****
```

```
SUBROUTINE FELDI(N1,N2,N3,X,Y,EX,EY,E,EPSR,H)
PARAMETER (M=150)
IMPLICIT DOUBLE PRECISION (A-H,O-Z)
COMMON /COM1/ XC(M),YC(M)
COMMON /COM2/ Q(M)
PI=4*DATAN(1.0D0)
SUMX=0.0
SUMY=0.0
DO 200 J=1,N1
IF(Y.GT.H)TH1=PI-DATAN(X/(Y-H))-PI/2
IF(Y.LT.H)TH1=DATAN(X/(H-Y))-PI/2
IF(Y.EQ.H)TH1=0

RAD1=DSQRT((X-XC(J))**2+(Y-YC(J))**2)
RAD2=DSQRT((X+XC(J))**2+(Y-YC(J))**2)
RAD3=DSQRT((X-XC(J))**2+(Y+YC(J))**2)
RAD4=DSQRT((X+XC(J))**2+(Y+YC(J))**2)

XCOMP1=(X-XC(J))/RAD1**2
XCOMP2=(X+XC(J))/RAD2**2
XCOMP3=(X-XC(J))/RAD3**2
XCOMP4=(X+XC(J))/RAD4**2

XCOMP=XCOMP1+XCOMP2-XCOMP3-XCOMP4

YCOMP1=(Y-YC(J))/RAD1**2
YCOMP2=(Y-YC(J))/RAD2**2
YCOMP3=(Y+YC(J))/RAD3**2
YCOMP4=(Y+YC(J))/RAD4**2

YCOMP=YCOMP1+YCOMP2-YCOMP3-YCOMP4

SUMX=SUMX+Q(J)*XCOMP
SUMY=SUMY+Q(J)*YCOMP
200 CONTINUE
```



```

DO 300 J=N1+N2+1,N1+N2+N3
IF(Y.GT.H)TH1=PI-DATAN(X/(Y-H))-PI/2
IF(Y.LT.H)TH1=DATAN(X/(H-Y))-PI/2
IF(Y.EQ.H)TH1=0
RAD1=DSQRT((X-XC(J))**2+(Y-YC(J))**2)
RAD2=DSQRT((X+XC(J))**2+(Y-YC(J))**2)
RAD3=DSQRT((X-XC(J))**2+(Y+YC(J))**2)
RAD4=DSQRT((X+XC(J))**2+(Y+YC(J))**2)

XCOMP1=(X-XC(J))/RAD1**2
XCOMP2=(X+XC(J))/RAD2**2
XCOMP3=(X-XC(J))/RAD3**2
XCOMP4=(X+XC(J))/RAD4**2

XCOMP=XCOMP1+XCOMP2-XCOMP3-XCOMP4

YCOMP1=(Y-YC(J))/RAD1**2
YCOMP2=(Y-YC(J))/RAD2**2
YCOMP3=(Y+YC(J))/RAD3**2
YCOMP4=(Y+YC(J))/RAD4**2

YCOMP=YCOMP1+YCOMP2-YCOMP3-YCOMP4

SUMX=SUMX+Q(J)*XCOMP
SUMY=SUMY+Q(J)*YCOMP
300 CONTINUE
EX=SUMX
EY=SUMY
E=DSQRT(SUMX**2+SUMY**2)
RETURN
END
* *****
* * THIS SUBROUTINE FINDS ELECTRIC FIELD IN THE AIR
* *****
SUBROUTINE FELDE(N1,N2,N3,X,Y,EX,EY,E,EPSR,H)
PARAMETER (M=150)
IMPLICIT DOUBLE PRECISION (A-H,O-Z)
COMMON /COM1/ XC(M),YC(M)
COMMON /COM2/ Q(M)
PI=4*DATAN(1.0D0)
SUMX=0.0
SUMY=0.0
DO 200 J=1,N1+N2
IF(Y.GT.H)TH1=PI-DATAN(X/(Y-H))-PI/2
IF(Y.LT.H)TH1=DATAN(X/(H-Y))-PI/2
IF(Y.EQ.H)TH1=0
RAD1=DSQRT((X-XC(J))**2+(Y-YC(J))**2)
RAD2=DSQRT((X+XC(J))**2+(Y-YC(J))**2)
RAD3=DSQRT((X-XC(J))**2+(Y+YC(J))**2)
RAD4=DSQRT((X+XC(J))**2+(Y+YC(J))**2)

XCOMP1=(X-XC(J))/RAD1**2
XCOMP2=(X+XC(J))/RAD2**2
XCOMP3=(X-XC(J))/RAD3**2
XCOMP4=(X+XC(J))/RAD4**2

XCOMP=XCOMP1+XCOMP2-XCOMP3-XCOMP4

YCOMP1=(Y-YC(J))/RAD1**2
YCOMP2=(Y-YC(J))/RAD2**2

```

```

YCOMP3=(Y+YC(J))/RAD3**2
YCOMP4=(Y+YC(J))/RAD4**2

YCOMP=YCOMP1+YCOMP2-YCOMP3-YCOMP4

SUMX=SUMX+Q(J)*XCOMP
SUMY=SUMY+Q(J)*YCOMP
200 CONTINUE
EX=SUMX
EY=SUMY
E=DSQRT(SUMX**2+SUMY**2)
RETURN
END
* *****
* *THIS SUBROUTINE FINDS INVERSE OF MATRIX
* *****
SUBROUTINE NGAUSS(N)
PARAMETER (M=150)
IMPLICIT DOUBLE PRECISION (A-H,O-Z)
COMMON /COM2/ Q(M)
COMMON /COM3/ AV(M,M),BV(M)
DO 4 K=1,N-1
DO 3 I=K+1,N
XMULT=AV(I,K)/AV(K,K)
DO 2 J=K+1,N
AV(I,J)=AV(I,J)-XMULT*AV(K,J)
2 CONTINUE
AV(I,K)=XMULT
BV(I)=BV(I)-XMULT*BV(K)
3 CONTINUE
4 CONTINUE
Q(N)=BV(N)/AV(N,N)
DO 6 I=N-1,1,-1
SUM=BV(I)
DO 5 J=I+1,N
SUM=SUM-AV(I,J)*Q(J)
5 CONTINUE
Q(I)=SUM/AV(I,I)
6 CONTINUE
RETURN
END
* *****
* *THIS SUBROUTINE FINDS ATT & ION
* *****
SUBROUTINE ATTION(E,FION,ATT,DIF)
IMPLICIT DOUBLE PRECISION (A-H,O-Z)

ATT=(0.01298-0.541E-3*(E/760.0)+0.87E-5*(E/760.0)**2)*760.0
IF(E/760.0.GE.25.AND.E/760.0.LE.60.0) THEN
C WRITE(6,*)E/760.0,'IONIZATION BET. 25--60'
FION=(4.7786*EXP(-221*760.0/E))*760.0
ELSEIF (E/760.0.GE.60.0.AND.E/760.0.LE.240.0) THEN
C WRITE(6,*)E/760.0,'IONIZATION BET.60--240'
FION=(9.682*EXP(-264.2*760.0/E))*760.0
ELSE
WRITE(6,*)E/760.0,'IONIZATION OUT OF THE RANGE'
ENDIF
DIF=FION-ATT
RETURN
END

```

```

* *****
*  *THIS SUBROUTINE FINDS ABSORPTION COEFFICIENT (MU)
*  *****
SUBROUTINE ABSORP(E,AMU)
  IMPLICIT DOUBLE PRECISION (A-H,O-Z)

  E=E/100000.0
  IF(E.GE.19.0.AND.E.LE.190.0) THEN
    AMU=100*EXP(-31.568+6.785*LOG(E))
  ELSEIF(E.GT.190.0) THEN
    AMU=100.0*EXP(-11.743+2.78*LOG(E))
  ELSE
    WRITE(6,*)'AMU CAN NOT BE CALCULATED E='E,'KV/CM'
  ENDIF
  RETURN
END

* *****
*  *THIS SUBROUTINE DIVIDES THE IONIZATION ZONE AND STOR
*    PHOTOELECTRONS
*  *****
SUBROUTINE FAREA(YTAV,XTAV,LL,KK,PI,N1,N2,N3,H,EIONS,A)
  PARAMETER (M=150)
  IMPLICIT DOUBLE PRECISION (A-H,O-Z)
  COMMON /COM1/ XC(M),YC(M)
  COMMON /COM2/ Q(M)
  COMMON /COM4/ XIZ(180),YIZ(180),CX(180),CY(180),NSX(180)
  COMMON /COM5/ AREA(900)

  NAA=1
  DO 304 I=2,LL
    DRO=ABS(YIZ(I-1)-YIZ(I))
    IF(I.LE.(LL/2+1)) THEN
      THIX=XIZ(I)/(NSX(I)*1.0)
      IF(YIZ(I).LT.CY(1).AND.YIZ(I).GT.CY(KK)) THEN
        THET=DACOS((YIZ(I)-H)/A)
        X=A*DSIN(THET)
        THIX=ABS(XIZ(I)-X)/(NSX(I)*1.0)
      ENDIF
    ELSE
      THIX=XIZ(I-1)/(NSX(I)*1.0)
      IF(YIZ(I).LT.CY(1).AND.YIZ(I).GT.CY(KK)) THEN
        THET=DACOS((YIZ(I-1)-H)/A)
        X=A*DSIN(THET)
        THIX=ABS(XIZ(I-1)-X)/(NSX(I)*1.0)
      ENDIF
    ENDIF
    NZ=5
    DO 305 J=1,NSX(I)
      IF(I.LE.(LL/2+1)) THEN
        COIX=XIZ(I)-(J-1)*THIX
      ELSE
        COIX=XIZ(I-1)-(J-1)*THIX
      ENDIF
      Z=0.0
      THIZ=((CY(KK)-YIZ(LL))*DTAN(80*PI/180))/NZ
      DO 306 K=1,NZ
        RO=SQRT((XTAV-COIX)**2+(YTAV-YIZ(I))**2+Z**2)
        PAREA=THIZ*THIX
        TAREA=4*PI*RO**2
      END DO
    END DO
  END DO

```

```

IF(30590*RO.GE.150) THEN
F1F2=2.46*EXP(-696.92*RO)+28.3*EXP(-3002.0*RO)
ELSE
F1F2=2.46*EXP(-696.92*RO)+28.3*EXP(-3002.0*RO)+
+528.0*EXP(-30590.0*RO)
ENDIF
X=COIX
Y=YIZ(I)
CALL FELDE(N1,N2,N3,X,Y,EX,EY,E,EPSR,H)
CALL ABSORP(E,AMU)
AREA(NAA)=AREA(NAA)+EIONS*(PAREA/TAREA)*F1F2*AMU*EXP(-AMU*RO)*DRO
C IF(NAA.EQ.182) THEN
C WRITE(6,*)'AREA(',NAA,')',AREA(NAA),I,J,K
C ENDIF
Z=Z+THIZ
NAA=NAA+1

306 CONTINUE
305 CONTINUE
304 CONTINUE
RETURN
END
* *****
* * THIS SUBROUTINE FINDS THE ELECTRON MOBILITY (ke (m2/(s*v)))
* *****
SUBROUTINE EMOBS(E,EMOB)
IMPLICIT DOUBLE PRECISION (A-H,O-Z)
EMO=E/1000.0
IF(EMO.LE.76.0)EVELOC=1.217E4*EMO**0.715
IF(EMO.GT.76.0)EVELOC=1.837E4*EMO**0.62
EMOB=EVELOC/(EMO*100000.0)
RETURN
END
* *****
* * THIS SUBROUTINE FINDS THE RADIUS OF THE HEAD OF THE
* * PRIMARY AVALANCHE *
* *****
SUBROUTINE RADPAV(ET,TAW,EMOB,RPA)
IMPLICIT DOUBLE PRECISION (A-H,O-Z)
ERA=ET/1000.0
BK=1.37E-23
ECHA=1.6E-19
IF(ERA.LT.0.532)TR=12.267+3.16*LOG(ERA)
IF(ERA.GE.0.532)TR=20.632+14.29*LOG(ERA)
TG=298.0
DE=EMOB*(BK/ECHA)*TR*TG
RPA=SQRT(6.0*DE*TAW)
WRITE(6,*)'RPA=',RPA
RETURN
END

```

## PROGRAM 2

### CALCULATE POSITIVE ONSET VOLTAGE FOR A BARE CONDUCTOR:

```

* *****
* * This computer program calculate the following for a bare conductor:
* * 1.The potential & the electric field
* * 2.The postive onset voltage for a bare conductor
* *
* *****
PARAMETER (M=150)
IMPLICIT DOUBLE PRECISION (A-H,O-Z)
DIMENSION XB(M),YB(M),XCK(M),YCK(M),TH(M)
COMMON /COM1/ XC(M),YC(M)
COMMON /COM2/ Q(M)
COMMON /COM3/ AV(M,M),BV(M)
COMMON /COM4/ XIZ(180),YIZ(180),CX(180),CY(180),NSX(180)
COMMON /COM5/ AREA(900)
OPEN (UNIT = 5,FILE ='EZA2.DAT',STATUS='OLD')
OPEN (UNIT = 6,FILE ='EZA2.OUT',STATUS='OLD')

READ(5,*)N1,A,V,RF1,H,STEPE
PI=4*DATAN(1.0D0)
EPS=1E-9/(36*PI)
* *****
* * THIS SECTION FINDS CHARGES LOCATION
* *****
* WRITE(6,*)'CHARGE 1---- N1'
DTHET=PI/N1
THET=DTHET/2.0
DO 10 I=1,N1
XC(I)=RF1*A*DSIN(THET)
YC(I)=H+RF1*A*DCOS(THET)
THET=THET+DTHET
* WRITE(6,510)XC(I),YC(I)
10 CONTINUE
* *****
* * THIS SECTION FINDS BOUNDARY POINT LOCATION
* *****
* WRITE(6,*)'BOUNDARY 1---- N1'
DTHET=PI/N1
THET=DTHET/2.0
DO 40 I=1,N1
XB(I)=A*DSIN(THET)
YB(I)=H+A*DCOS(THET)
THET=THET+DTHET
TH(I)=THET
* WRITE(6,510)XB(I),YB(I)
40 CONTINUE
* *****
* * THIS SECTION MAKES POTENTIAL COEFFICIENT MATRIX
* *****

DO 75 I=1,N1
BV(I)=V
75 CONTINUE

```

```

DO 80 I=1,N1
DO 80 J=1,N1
DC1=DSQRT((XB(I)-XC(J))**2+(YB(I)-YC(J))**2)
DI1=DSQRT((XB(I)-XC(J))**2+(YB(I)+YC(J))**2)

DC2=DSQRT((XB(I)+XC(J))**2+(YB(I)-YC(J))**2)
DI2=DSQRT((XB(I)+XC(J))**2+(YB(I)+YC(J))**2)
AV(I,J)=DLOG((DI1*DI2)/(DC1*DC2))
80 CONTINUE

* *****
N=N1
CALL NGAUSS(N)
DTHET= PI/N1
THET=0.0
DO 160 I=1,N1
XCK(I)=A*DSIN(THET)
YCK(I)=H+A*DCOS(THET)
THET=THET+DTHET
160 CONTINUE
WRITE(6,*)' CONDUCTOR POTENTIAL'
DO 170 I=1,N1
X=XCK(I)
Y=YCK(I)
CALL POTE(N1,X,Y,POT)
C WRITE(6,510)X,Y,POT
WRITE(6,*)X,Y,POT
170 CONTINUE

510 FORMAT(08(E12.5,2X))
C STOP
WRITE(6,*)'*****'
C DV=V/STEPE
X=0.0
Y=H-A
DY=Y/STEPE
DO 501 I=1,STEPE
CALL POTE(N1,X,Y,POT)
CALL FELDE(N1,X,Y,EX,EY,E,H)
C WRITE(6,510)Y,E
C WRITE(6,510)X,Y,POT,EX,EY,E
c WRITE(6,*)Y,E
C DY=DV/E
Y=Y-DY
501 CONTINUE
C STOP
* *****
* * THIS PART FINDS THE IONIZATION ZONE
* *****
LL=1
DS=40.0*A
DO 502 I=0,180,10
THET=I*PI/180.0
X=A*DSIN(THET)
Y=H+A*DCOS(THET)
DO 503 L=1,1000
CALL FELDE(N1,X,Y,EX,EY,E,H)
E=E/100.0
ATT=(0.01298-0.541E-3*(E/760.0)+0.87E-5*(E/760.0)**2)*760.0
IF(E/760.0.GE.25.AND.E/760.0.LE.60.0) THEN

```

```

C  WRITE(6,*)E/760.0,'IONIZATION BET. 25--60'
   FION=(4.7786*EXP(-221*760.0/E))*760.0
   ELSEIF (E/760.0.GE.60.0.AND.E/760.0.LE.240.0) THEN
C  WRITE(6,*)E/760.0,'IONIZATION BET.60--240'
   FION=(9.682*EXP(-264.2*760.0/E))*760.0
   ELSE
   WRITE(6,*)E/760.0,'IONIZATION OUT OF THE RANGE',L
   GOTO 561
   ENDIF
   DIF=FION-ATT
   IF(ABS(DIF).LT.0.01*FION) GOTO 560
   RZ=.01*FION
   DL=DS/E
   Y=Y+DL*DCOS(THET)
   X=X+DL*DSIN(THET)
C  WRITE(6,*)FION,ATT,DIF,RZ
503  CONTINUE
   WRITE(6,*)'STEPE IS NOT INAF'
   GOTO 561
C560 WRITE(6,*)'THE IONIZATION AND THE ATTACHEMENT WHEN ION=ATT'

560 IF(I.LE.180) THEN
   XIZ(LL)=X
   YIZ(LL)=Y
   WRITE(6,*)XIZ(LL),YIZ(LL),'IONIZATION ',I
   LL=LL+1
   ENDIF
C  WRITE(6,*)X,Y
502  CONTINUE
*  *****
*  * THIS PART DRAWS THE CONDUCTOR
*  *****
561  KK=1
   DO 504 I=0,180,10
   THET=I*PI/180.0
   X=A*DSIN(THET)
   Y=H+A*DCOS(THET)

   IF(I.LE.180) THEN
   CX(KK)=X
   CY(KK)=Y
   WRITE(6,*)CX(KK),CY(KK),'CONDUCTOR',KK,I
   KK=KK+1
   ENDIF

*  WRITE(6,*)X,Y
504  CONTINUE
c  STOP
*  *****
*  * THIS PART FINDS NUMBER OF SECTIONS IN EACH LEVEL
*  *****
   FAK=.002
   KK=KK-1
   LL=LL-1
   DO 301 I=2,LL
   IF(I.LE.(LL/2+1)) THEN
   NSX(I)=XIZ(I)/FAK+1
   IF(YIZ(I).LT.CY(I).AND.YIZ(I).GT.CY(KK)) THEN
   THET=DACOS((YIZ(I)-H)/A)
   X=A*DSIN(THET)
   NSX(I)=ABS(XIZ(I)-X)/FAK+1

```

```

ENDIF
ELSE
NSX(I)=XIZ(I-1)/FAK+1
IF(YIZ(I).LT.CY(1).AND.YIZ(I).GT.CY(KK)) THEN
THET=DACOS((YIZ(I-1)-H)/A)
X=A*DSIN(THET)
NSX(I)=ABS(XIZ(I-1)-X)/FAK+1
ENDIF
ENDIF
WRITE(6,*)I,NSX(I)
301 CONTINUE
* *****
* * THIS PART FINDS THE PRIMARY AVALANCHE
* *****
TAW=0.0
NOA=50
NINTG=150
SUM=0.0
ISAV=1
TL=CY(KK)-YIZ(LL)
YL=TL/(NOA*1.0)
STEIN=YL/(NINTG*1.0)
NINTG=NINTG+1
DO 302 K=1,NOA
DO 303 NN=ISAV,NINTG
Y=YIZ(LL)+(NN-1)*STEIN
X=0.0
CALL FELDE(N1,X,Y,EX,EY,E,H)
IF(NN.EQ.1) THEN
ET=E/100.0
ELSE
ESC=1.6E-19*(EXP(SUM)-1.0)/(4.0*PI*EPS*XSC**2)
ET=(E-ESC)/100.0
ENDIF
CALL ATTION(ET,FION,ATT,DIF)
XSC=1.0/(FION*100.0)
SUM=SUM+STEIN*DIF*100.0
CALL EMOBS(ET,EMOB)
TAW=TAW+STEIN/(EMOB*(ET*100.0))
IF(K.EQ.NOA.AND.NN.EQ.NINTG) THEN
CALL EMOBS(ET,EMOB)
CALL RADPAV(ET,TAW,EMOB,RPA)
ENDIF
C IF(K.LE.2) THEN
C WRITE(6,*)Y,FION,'OK'
C ENDIF
303 CONTINUE
EIONS=EXP(SUM)
YTAV=Y
XTAV=X
WRITE(6,*)EIONS,K,YTAV
CALL FAREA(YTAV,XTAV,LL,KK,PI,N1,H,EIONS,A)
ISAV=NINTG+1
NINTG=NINTG+150
302 CONTINUE
C STOP
C END
* *****
* * CALCULATION OF THE SECONDARY AVALANCHES SIZE
* *****
SAVAL=0.0

```



```

NAA=1
DO 401 I=2,LL
  IF(I.LE.(LL/2+1)) THEN
    THIX=XIZ(I)/(NSX(I)*1.0)
    IF(YIZ(I).LT.CY(1).AND.YIZ(I).GT.CY(KK)) THEN
      THET=DACOS((YIZ(I)-H)/A)
      X=A*DSIN(THET)
      THIX=ABS(XIZ(I)-X)/(NSX(I)*1.0)
    ENDIF
  ELSE
    THIX=XIZ(I-1)/(NSX(I)*1.0)
    IF(YIZ(I).LT.CY(1).AND.YIZ(I).GT.CY(KK)) THEN
      THET=DACOS((YIZ(I-1)-H)/A)
      X=A*DSIN(THET)
      THIX=ABS(XIZ(I-1)-X)/(NSX(I)*1.0)
    ENDIF
  ENDIF
NZ=5
DO 402 J=1,NSX(I)
  IF(I.LE.(LL/2+1)) THEN
    COIX=XIZ(I)-(J-1)*THIX
  ELSE
    COIX=XIZ(I-1)-(J-1)*THIX
  ENDIF
Z=0.0
THIZ=((CY(KK)-YIZ(LL))*DTAN(80*PI/180))/NZ
DO 403 K=1,NZ
  DELT=.00004
  SUMS=0.0
  Z=Z+(K-1)*THIZ
  X=COIX
  Y=YIZ(I)
DO 404 MS=1,300
  CALL FELDE(N1,X,Y,EX,EY,E,H)
  SCP=SQRT((Y-(CY(KK)-RPA))**2+X**2+Z**2)
  ESCP=1.6E-19*(AVPR-1.0)/(4.0*PI*EPS*SCP**2)
  IF(Z.EQ.0.0) THEN
    EXSCP=(X/SCP)*ESCP
    EYSCP=(Y-(CY(KK)-RPA))/SCP*ESCP
    EZSCP=0.0
  ELSE
    THTY=DACOS((Y-(CY(KK)-RPA))/SCP)
    EYSCP=ESCP*DCOS(THTY)
    EXZ=ESCP*DSIN(THTY)
    THTX=DACOS(X/SQRT(X**2+Z**2))
    EXSCP=EXZ*DCOS(THTX)
    EZSCP=EXZ*DSIN(THTX)
  ENDIF
  IF(MS.GT.1) THEN
    ESSC=1.6E-19*(EXP(SUMS)-1.0)/(4.0*PI*EPS*SSC**2)
    EXSSC=-ESSC*(EX+EXSCP)/ETS
    EYSSC=-ESSC*(EY+EYSCP)/ETS
    EZSSC=-ESSC*(EZSCP/ETS)
  ELSE
    ESSC=0.0
    EXSSC=0.0
    EYSSC=0.0
    EZSSC=0.0
  ENDIF
  ETS=SQRT((EX+EXSCP+EXSSC)**2+(EY+EYSCP+EYSSC)**2+
    +(EZSCP+EZSSC)**2)

```

```

      ETTS=ETS/100.0
c  IF(I.EQ.7.AND.J.EQ.3.AND.K.EQ.4.AND.MS.EQ.40) THEN
C  WRITE(6,*)'ETTS=',ETTS,MS
C  WRITE(6,87)X,Y,ETTS,I,J,K,MS
C 87 FORMAT(1X,'X=',F12.10,1X,'Y=',F12.10,1X,'ETTS=',F12.6,1X,'I='
C  +,I3,1X,'J=',I3,1X,'K=',I2,1X,'MS=',I3)
c  ENDIF
      CALL ATTION(ETTS,FION,ATT,DIF)
      SUMS=SUMS+DIF*DELT*100.0
      SSC=1.0/(FION*100.0)
      DELT=1.0/(10.0*FION*100.0)
      IF(Z.EQ.0.0) THEN
        X=X-DELT*(EX+EXSCP+EXSSC)/ETS
        Y=Y-DELT*(EY+EYSCP+EYSSC)/ETS
        Z=0.0
      ELSE
        X=X-DELT*(EX+EXSCP+EXSSC)/ETS
        Y=Y-DELT*(EY+EYSCP+EYSSC)/ETS
        Z=Z-DELT*(EZSCP+EZSSC)/ETS
      ENDIF
      DBCP=SQRT(X**2+(Y-(CY(KK)-RPA))**2+Z**2)
      CAPC=SQRT(X**2+(Y-H)**2+Z**2)
      IF(Z.EQ.0.0) THEN
        IF(DBCP.LE.RPA) GOTO 45
        IF(CAPC.LE.A) GOTO 45
      ELSE
        CAPC=SQRT(X**2+(Y-H)**2)
        IF(CAPC.LE.A) GOTO 45
      ENDIF
404 CONTINUE
45 SEION=EXP(SUMS)
   SAVAL=SAVAL+AREA(NAA)*SEION
   NAA=NAA+1
403 CONTINUE
402 CONTINUE
401 CONTINUE
   WRITE(6,87)X,Y,SAVAL,I,J,K,MS
C 87 FORMAT(1X,'X=',F12.10,1X,'Y=',F12.10,1X,'SAVAL=',F12.6,1X,'I='
C  +,I3,1X,'J=',I3,1X,'K=',I2,1X,'MS=',I3)
   TOTS=SAVAL*4.0
   WRITE(6,*)'SECONDARY=',TOTS
   STOP
   END
* ***** END OF NAIM PROGRAM *****

```

```

* *****
*  * THIS SUBROUTINE FINDS POTENTIAL IN THE AIR
* *****

```

```

SUBROUTINE POTE(N1,X,Y,POT)
PARAMETER (M=150)
IMPLICIT DOUBLE PRECISION (A-H,O-Z)
COMMON /COM1/ XC(M),YC(M)
COMMON /COM2/ Q(M)
SUMV=0.0
DO 200 J=1,N1
  DC1=DSQRT((X-XC(J))**2+(Y-YC(J))**2)
  DI1=DSQRT((X-XC(J))**2+(Y+YC(J))**2)

  DC2=DSQRT((X+XC(J))**2+(Y-YC(J))**2)
  DI2=DSQRT((X+XC(J))**2+(Y+YC(J))**2)

```

```

SUMV=SUMV+Q(J)*DLOG((DI1*DI2)/(DC1*DC2))
200 CONTINUE
POT=SUMV
RETURN
END

* *****
* * THIS SUBROUTINE FINDS ELECTRIC FIELD IN THE AIR
* *****
SUBROUTINE FELDE(N1,X,Y,EX,EY,E,H)
PARAMETER (M=150)
IMPLICIT DOUBLE PRECISION (A-H,O-Z)
COMMON /COM1/ XC(M),YC(M)
COMMON /COM2/ Q(M)
PI=4*DATAN(1.0D0)
SUMX=0.0
SUMY=0.0
DO 200 J=1,N1
RAD1=DSQRT((X-XC(J))**2+(Y-YC(J))**2)
RAD2=DSQRT((X+XC(J))**2+(Y-YC(J))**2)
RAD3=DSQRT((X-XC(J))**2+(Y+YC(J))**2)
RAD4=DSQRT((X+XC(J))**2+(Y+YC(J))**2)

XCOMP1=(X-XC(J))/RAD1**2
XCOMP2=(X+XC(J))/RAD2**2
XCOMP3=(X-XC(J))/RAD3**2
XCOMP4=(X+XC(J))/RAD4**2

XCOMP=XCOMP1+XCOMP2-XCOMP3-XCOMP4

YCOMP1=(Y-YC(J))/RAD1**2
YCOMP2=(Y-YC(J))/RAD2**2
YCOMP3=(Y+YC(J))/RAD3**2
YCOMP4=(Y+YC(J))/RAD4**2

YCOMP=YCOMP1+YCOMP2-YCOMP3-YCOMP4

SUMX=SUMX+Q(J)*XCOMP
SUMY=SUMY+Q(J)*YCOMP
200 CONTINUE
EX=SUMX
EY=SUMY
E=DSQRT(SUMX**2+SUMY**2)
RETURN
END

* *****
* * THIS SUBROUTINE FINDS INVERS OF MATRICE
* *****
SUBROUTINE NGAUSS(N)
PARAMETER (M=150)
IMPLICIT DOUBLE PRECISION (A-H,O-Z)
COMMON /COM2/ Q(M)
COMMON /COM3/ AV(M,M),BV(M)
DO 4 K=1,N-1
DO 3 I=K+1,N
XMULT=AV(I,K)/AV(K,K)
DO 2 J=K+1,N
AV(I,J)=AV(I,J)-XMULT*AV(K,J)
2 CONTINUE
AV(I,K)=XMULT
BV(I)=BV(I)-XMULT*BV(K)

```

```

3 CONTINUE
4 CONTINUE
  Q(N)=BV(N)/AV(N,N)
  DO 6 I=N-1,1,-1
    SUM=BV(I)
    DO 5 J=I+1,N
      SUM=SUM-AV(I,J)*Q(J)
5 CONTINUE
  Q(I)=SUM/AV(I,I)
6 CONTINUE
  RETURN
  END
* *****
* *THIS SUBROUTINE FINDS ATT & ION
* *****
  SUBROUTINE ATTION(E,FION,ATT,DIF)
  IMPLICIT DOUBLE PRECISION (A-H,O-Z)

  ATT=(0.01298-0.541E-3*(E/760.0)+0.87E-5*(E/760.0)**2)*760.0
  IF(E/760.0.GE.25.AND.E/760.0.LE.60.0) THEN
C  WRITE(6,*)E/760.0,'IONIZATION BET. 25--60'
    FION=(4.7786*EXP(-221*760.0/E))*760.0
  ELSEIF (E/760.0.GE.60.0.AND.E/760.0.LE.240.0) THEN
C  WRITE(6,*)E/760.0,'IONIZATION BET.60--240'
    FION=(9.682*EXP(-264.2*760.0/E))*760.0
  ELSE
    WRITE(6,*)E/760.0,'IONIZATION OUT OF THE RANGE'
  ENDIF
  DIF=FION-ATT
  RETURN
  END
* *****
* *THIS SUBROUTINE FINDS ABSORPTION COEFFICIENT (MU)
* *****
  SUBROUTINE ABSORP(E,AMU)
  IMPLICIT DOUBLE PRECISION (A-H,O-Z)

  E=E/100000.0
  IF(E.GE.19.0.AND.E.LE.190.0) THEN
    AMU=100*EXP(-31.568+6.785*LOG(E))
  ELSEIF(E.GT.190.0) THEN
    AMU=100.0*EXP(-11.743+2.78*LOG(E))
  ELSE
    WRITE(6,*)'AMU CAN NOT BE CALCULATED E=',E,'KV/CM'
  ENDIF
  RETURN
  END

* *****
* *THIS SUBROUTINE DIVIDES THE IONIZATION ZONE AND STOR
  PHOTOELECTRONS
* *****
  SUBROUTINE FAREA(YTAV,XTAV,LL,KK,PI,N1,H,EIONS,A)
  PARAMETER (M=150)
  IMPLICIT DOUBLE PRECISION (A-H,O-Z)
  COMMON /COM1/ XC(M),YC(M)
  COMMON /COM2/ Q(M)
  COMMON /COM4/ XIZ(180),YIZ(180),CX(180),CY(180),NSX(180)
  COMMON /COM5/ AREA(900)

```

```

NAA=1
DO 304 I=2,LL
C  WRITE(6,*)'YAHYA ABU-SHAL'
DRO=ABS(YIZ(I-1)-YIZ(I))
IF(I.LE.(LL/2+1)) THEN
THIX=XIZ(I)/(NSX(I)*1.0)
IF(YIZ(I).LT.CY(1).AND.YIZ(I).GT.CY(KK)) THEN
THET=DACOS((YIZ(I)-H)/A)
X=A*DSIN(THET)
THIX=ABS(XIZ(I)-X)/(NSX(I)*1.0)
ENDIF
ELSE
THIX=XIZ(I-1)/(NSX(I)*1.0)
IF(YIZ(I).LT.CY(1).AND.YIZ(I).GT.CY(KK)) THEN
THET=DACOS((YIZ(I-1)-H)/A)
X=A*DSIN(THET)
THIX=ABS(XIZ(I-1)-X)/(NSX(I)*1.0)
ENDIF
ENDIF
NZ=5
DO 305 J=1,NSX(I)
IF(I.LE.(LL/2+1)) THEN
COIX=XIZ(I)-(J-1)*THIX
ELSE
COIX=XIZ(I-1)-(J-1)*THIX
ENDIF
Z=0.0
C  WRITE(*,*)LL,KK
C  WRITE(*,*)CY(KK),YIZ(LL),PI,NZ
THIZ=((CY(KK)-YIZ(LL))*DTAN(80*PI/180))/NZ
DO 306 K=1,NZ
RO=SQRT((XTAV-COIX)**2+(YTAV-YIZ(I))**2+Z**2)
PAREA=THIZ*THIX
TAREA=4*PI*RO**2
C  WRITE(6,*)RO,DRO,I
IF(30590*RO.GE.150) THEN
F1F2=2.46*EXP(-696.92*RO)+28.3*EXP(-3002.0*RO)
ELSE
F1F2=2.46*EXP(-696.92*RO)+28.3*EXP(-3002.0*RO)+
+528.0*EXP(-30590.0*RO)
ENDIF
C  WRITE(6,*)F1F2,I
X=COIX
Y=YIZ(I)
CALL FELDE(N1,X,Y,EX,EY,E,H)
C  WRITE(6,*)'E=',E,I,J,K
CALL ABSORP(E,AMU)
c  WRITE(6,*)'AMU',AMU
AREA(NAA)=AREA(NAA)+EIONS*(PAREA/TAREA)*F1F2*AMU*EXP(-AMU*RO)*DRO
c  IF(NAA.EQ.182) THEN
c  WRITE(6,*)X,Y,Z
c  WRITE(6,*)'AREA(',NAA,')',AREA(NAA),I,J,K
c  ENDIF
Z=Z+THIZ
NAA=NAA+1

306 CONTINUE
305 CONTINUE
304 CONTINUE
RETURN
END

```

```

* *****
*  * THIS SUBROUTINE FINDS THE ELECTRON MOBILITY (ke (m2/(s*v)))
*  *****
SUBROUTINE EMOBS(E,EMOB)
IMPLICIT DOUBLE PRECISION (A-H,O-Z)
EMO=E/1000.0
IF(EMO.LE.76.0)EVELOC=1.217E4*EMO**0.715
IF(EMO.GT.76.0)EVELOC=1.837E4*EMO**0.62
EMOB=EVELOC/(EMO*100000.0)
RETURN
END
* *****
*  * THIS SUBROUTINE FINDS THE RADIUS OF THE HEAD OF THE
*  * PRIMARY AVALANCHE
*  *****
SUBROUTINE RADPAV(ET,TAW,EMOB,RPA)
IMPLICIT DOUBLE PRECISION (A-H,O-Z)
ERA=ET/1000.0
BK=1.37E-23
ECHA=1.6E-19
IF(ERA.LT.0.532)TR=12.267+3.16*LOG(ERA)
IF(ERA.GE.0.532)TR=20.632+14.29*LOG(ERA)
TG=298.0
DE=EMOB*(BK/ECHA)*TR*TG
RPA=SQRT(6.0*DE*TAW)
WRITE(6,*)'RPA=',RPA
RETURN
END

```

## PROGRAM 3

### CALCULATE NEGATIVE ONSET VOLTAGE FOR COATED CONDUCTOR:

```

* *****
* * This computer program calculates the following for a coated conductor:
* * 1.The potential and electric field
* * 2.The negative onset voltage
* *****

PARAMETER (M=180)
IMPLICIT DOUBLE PRECISION (A-H,O-Z)
DIMENSION XB(M),YB(M),XCK(M),YCK(M),TH(M),yas(4000)
COMMON /COM1/ XC(M),YC(M)
COMMON /COM2/ Q(M)
COMMON /COM3/ AV(M,M),BV(M)
COMMON /COM4/ XIZ(180),YIZ(180),CX(180),CY(180),NSX(180)
COMMON /COM5/ AREA(900)

OPEN(UNIT = 5,FILE ='EZA.DAT',STATUS ='OLD')
OPEN(UNIT = 6,FILE ='EZA.OUT',STATUS ='OLD')

READ(5,*)N1,N2,N3,A,B,V,RF1,RF2,RF3,H,EPSR,STEPI,STEPE
PI=4*DATAN(1.0D0)
EPS=1E-9/(36.0*PI)
* *****
* * THIS SECTION FINDS CHARGES LOCATION
* *****
* WRITE(6,*)'CHARGE 1---- N1'
DTHET=PI/N1
THET=DTHET/2.0
DO 10 I=1,N1
XC(I)=RF1*B*DSIN(THET)
YC(I)=H+RF1*B*DCOS(THET)
THET=THET+DTHET
* WRITE(6,510)XC(I),YC(I)
10 CONTINUE
* *****
* WRITE(6,*)'CHARGE N1+1---N1+N2'
DTHET=PI/N2
THET=DTHET/2.0
DO 20 I=N1+1,N1+N2
XC(I)=RF2*A*DSIN(THET)
YC(I)=H+RF2*A*DCOS(THET)
THET=THET+DTHET
* WRITE(6,510)XC(I),YC(I)
20 CONTINUE
* *****
* WRITE(6,*)'CHARGE N1+N2+1----N1+N2+N3'
DTHET=PI/N3
THET=DTHET/2.0
DO 30 I=N1+N2+1,N1+N2+N3
XC(I)=RF3*A*DSIN(THET)
YC(I)=H+RF3*A*DCOS(THET)
THET=THET+DTHET
* WRITE(6,510)XC(I),YC(I)
30 CONTINUE

```

```

* *****
* * THIS SECTION FINDS BOUNDARY POINTS LOCATION
* *****
* WRITE(6,*)'BOUNDARY  1---- N1'
  DTHET=PI/N1
  THET=DTHET/2.0
  DO 40 I=1,N1
    XB(I)=B*DSIN(THET)
    YB(I)=H+B*DCOS(THET)
    THET=THET+DTHET
    TH(I)=THET
*   WRITE(6,510)XB(I),YB(I)
40  CONTINUE
* *****
* WRITE(6,*)'BOUNDARY  N1+1---N1+N2'
  DTHET=PI/N2
  THET=DTHET/2.0
  DO 50 I=N1+1,N1+N2
    XB(I)=A*DSIN(THET)
    YB(I)=H+A*DCOS(THET)
    THET=THET+DTHET
    TH(I)=THET
*   WRITE(6,510)XB(I),YB(I)
50  CONTINUE
* *****
* WRITE(6,*)'BOUNDARY  N1+N2+1---N1+N2+N3'
  DTHET=PI/N3
  THET=DTHET/2.0
  DO 60 I=N1+N2+1,N1+N2+N3
    XB(I)=A*DSIN(THET)
    YB(I)=H+A*DCOS(THET)
    THET=THET+DTHET
    TH(I)=THET
*   WRITE(6,510)XB(I),YB(I)
60  CONTINUE
* *****
* * THIS SECTION MAKES POTENTIAL COEFFICIENT MATRIX
* *****
  DO 70 I=1,N1+N2+N3
    DO 70 J=1,N1+N2+N3
      AV(I,J)=0.0
70  CONTINUE

  DO 75 I=1,N1+N2+N3
    BV(I)=0.0
75  CONTINUE

  DO 80 I=1,N1
    DO 80 J=1,N1
      DC1=DSQRT((XB(I)-XC(J))**2+(YB(I)-YC(J))**2)
      DI1=DSQRT((XB(I)-XC(J))**2+(YB(I)+YC(J))**2)

      DC2=DSQRT((XB(I)+XC(J))**2+(YB(I)-YC(J))**2)
      DI2=DSQRT((XB(I)+XC(J))**2+(YB(I)+YC(J))**2)
      AV(I,J)=DLOG((DI1*DI2)/(DC1*DC2))
80  CONTINUE

  DO 90 I=1,N1
    DO 90 J=N1+N2+1,N1+N2+N3
      DC1=DSQRT((XB(I)-XC(J))**2+(YB(I)-YC(J))**2)
      DI1=DSQRT((XB(I)-XC(J))**2+(YB(I)+YC(J))**2)

```



```

DC2=DSQRT((XB(I)+XC(J))**2+(YB(I)-YC(J))**2)
DI2=DSQRT((XB(I)+XC(J))**2+(YB(I)+YC(J))**2)
AV(I,J)=DLOG((DI1*DI2)/(DC1*DC2))
90 CONTINUE

DO 100 I=N1+1,N1+N2
DO 100 J=N1+1,N1+N2
DC1=DSQRT((XB(I)-XC(J))**2+(YB(I)-YC(J))**2)
DI1=DSQRT((XB(I)-XC(J))**2+(YB(I)+YC(J))**2)

DC2=DSQRT((XB(I)+XC(J))**2+(YB(I)-YC(J))**2)
DI2=DSQRT((XB(I)+XC(J))**2+(YB(I)+YC(J))**2)
AV(I,J)=DLOG((DI1*DI2)/(DC1*DC2))

100 CONTINUE

DO 110 I=N1+1,N1+N2
DO 110 J=N1+N2+1,N1+N2+N3
DC1=DSQRT((XB(I)-XC(J))**2+(YB(I)-YC(J))**2)
DI1=DSQRT((XB(I)-XC(J))**2+(YB(I)+YC(J))**2)

DC2=DSQRT((XB(I)+XC(J))**2+(YB(I)-YC(J))**2)
DI2=DSQRT((XB(I)+XC(J))**2+(YB(I)+YC(J))**2)
AV(I,J)=(-1)*DLOG((DI1*DI2)/(DC1*DC2))
110 CONTINUE

DO 120 I=N1+N2+1,N1+N2+N3
DO 120 J=1,N1
I1=I-N1-N2
TH1=PI/2-(DTHET/2+DTHET*(I1-1))
RAD1=DSQRT((XB(I)-XC(J))**2+(YB(I)-YC(J))**2)
RAD2=DSQRT((XB(I)+XC(J))**2+(YB(I)-YC(J))**2)

RAD3=DSQRT((XB(I)-XC(J))**2+(YB(I)+YC(J))**2)
RAD4=DSQRT((XB(I)+XC(J))**2+(YB(I)+YC(J))**2)

XCOMP1=(XB(I)-XC(J))/RAD1**2
XCOMP2=(XB(I)+XC(J))/RAD2**2
XCOMP3=(XB(I)-XC(J))/RAD3**2
XCOMP4=(XB(I)+XC(J))/RAD4**2

XCOMP=XCOMP1+XCOMP2-XCOMP3-XCOMP4

YCOMP1=(YB(I)-YC(J))/RAD1**2
YCOMP2=(YB(I)-YC(J))/RAD2**2
YCOMP3=(YB(I)+YC(J))/RAD3**2
YCOMP4=(YB(I)+YC(J))/RAD4**2

YCOMP=YCOMP1+YCOMP2-YCOMP3-YCOMP4

AV(I,J)=(EPSR-1)*(XCOMP*DCOS(TH1)+YCOMP*DSIN(TH1))
120 CONTINUE

DO 130 I=N1+N2+1,N1+N2+N3
DO 130 J=N1+1,N1+N2
I1=I-N1-N2
TH1=PI/2-(DTHET/2+DTHET*(I1-1))
RAD1=DSQRT((XB(I)-XC(J))**2+(YB(I)-YC(J))**2)
RAD2=DSQRT((XB(I)+XC(J))**2+(YB(I)-YC(J))**2)
RAD3=DSQRT((XB(I)-XC(J))**2+(YB(I)+YC(J))**2)

```

```

RAD4=DSQRT((XB(I)+XC(J))**2+(YB(I)+YC(J))**2)

XCOMP1=(XB(I)-XC(J))/RAD1**2
XCOMP2=(XB(I)+XC(J))/RAD2**2
XCOMP3=(XB(I)-XC(J))/RAD3**2
XCOMP4=(XB(I)+XC(J))/RAD4**2

XCOMP=XCOMP1+XCOMP2-XCOMP3-XCOMP4

YCOMP1=(YB(I)-YC(J))/RAD1**2
YCOMP2=(YB(I)-YC(J))/RAD2**2
YCOMP3=(YB(I)+YC(J))/RAD3**2
YCOMP4=(YB(I)+YC(J))/RAD4**2

YCOMP=YCOMP1+YCOMP2-YCOMP3-YCOMP4

AV(I,J)=(-1)*(XCOMP*DCOS(TH1)+YCOMP*DSIN(TH1))
130 CONTINUE

DO 140 I=N1+N2+1,N1+N2+N3
DO 140 J=N1+N2+1,N1+N2+N3
I1=I-N1-N2
TH1=PI/2-(DTHET/2+DTHET*(I1-1))
RAD1=DSQRT((XB(I)-XC(J))**2+(YB(I)-YC(J))**2)
RAD2=DSQRT((XB(I)+XC(J))**2+(YB(I)-YC(J))**2)
RAD3=DSQRT((XB(I)-XC(J))**2+(YB(I)+YC(J))**2)
RAD4=DSQRT((XB(I)+XC(J))**2+(YB(I)+YC(J))**2)

XCOMP1=(XB(I)-XC(J))/RAD1**2
XCOMP2=(XB(I)+XC(J))/RAD2**2
XCOMP3=(XB(I)-XC(J))/RAD3**2
XCOMP4=(XB(I)+XC(J))/RAD4**2

XCOMP=XCOMP1+XCOMP2-XCOMP3-XCOMP4

YCOMP1=(YB(I)-YC(J))/RAD1**2
YCOMP2=(YB(I)-YC(J))/RAD2**2
YCOMP3=(YB(I)+YC(J))/RAD3**2
YCOMP4=(YB(I)+YC(J))/RAD4**2

YCOMP=YCOMP1+YCOMP2-YCOMP3-YCOMP4

C  AV(I,J)=(EPSR)*DSQRT(XCOMP**2+YCOMP**2)
  AV(I,J)=(EPSR)*(XCOMP*DCOS(TH1)+YCOMP*DSIN(TH1))
140 CONTINUE

DO 150 I=1,N1
  BV(I)=V
150 CONTINUE
* *****
  N=N1+N2+N3

C  DO 220 I=1,N1+N2+N3
C  WRITE(6,510)(AV(I,J),J=1,N1+N2+N3)
C220 CONTINUE

CALL NGAUSS(N)
DTHET= PI/N1
THET=0.0
DO 160 I=1,N1

```

```

      XCK(I)=B*DSIN(THET)
      YCK(I)=H+B*DCOS(THET)
      THET=THET+DTHET
160  CONTINUE
      WRITE(6,*)'CNDUCTOR POTENTIAL'
      DO 170 I=1,N1
      X=XCK(I)
      Y=YCK(I)
      CALL POTI(N1,N2,N3,X,Y,POT)
      WRITE(6,510)X,Y,POT

170  CONTINUE

      DTHET= PI/N2
      THET=0.0
      DO 180 I=1,N2
      XCK(I)=A*DSIN(THET)
      YCK(I)=H+A*DCOS(THET)
      THET=THET+DTHET
180  CONTINUE
      YAA=0.0
      WRITE(6,*)'POTENTIAL AT ENTERFACE'
      DO 190 I=1,N2
      X=XCK(I)
      Y=YCK(I)
      CALL POTI(N1,N2,N3,X,Y,POT)
      V1=POT
      YAA=YAA+V1
      CALL POTE(N1,N2,N3,X,Y,POT)
      V2=POT
      WRITE(6,510)X,Y,V1,V2
190  CONTINUE
      YAA=YAA/N2
      WRITE(6,*)'AVERAGE VLTAGE',YAA

      WRITE(6,*)'FIELD AT ENTERFACE'
      DO 210 I=1,N2
      X=XCK(I)
      Y=YCK(I)
      CALL FELDI(N1,N2,N3,X,Y,EX,EY,E,EPSR,H)
      E1=E
      CALL FELDE(N1,N2,N3,X,Y,EX,EY,E,EPSR,H)
      E2=E
      WRITE(6,510)X,Y,E1,E2,E2/E1
210  CONTINUE

510  FORMAT(08(E12.5,2X))
      WRITE(6,*)'*****'
      DV=(1.0-YAA)/STEPI
      X=0.0
      Y=H-B
      DO 500 I=1,STEPI+3
      RX=DSQRT(X**2+(H-Y)**2)
      IF(RX.GT.A) THEN
      GOTO111
      ELSE
      CALL POTI(N1,N2,N3,X,Y,POT)
      CALL FELDI(N1,N2,N3,X,Y,EX,EY,E,EPSR,H)
c  WRITE(6,510)Y,E
C  WRITE(6,510)X,Y,POT,EX,EY,E
      DY=DV/E

```

```

      Y=Y-DY
    ENDIF
500 CONTINUE
111 WRITE(6,*)'*****'
      DV=YAA/STEPE
      X=0.0
      Y=H-A
      DO 501 I=1,STEPE
        CALL POTE(N1,N2,N3,X,Y,POT)
        CALL FELDE(N1,N2,N3,X,Y,EX,EY,E,EPSR,H)
C   WRITE(6,510)X,Y,POT,EX,EY,E
      DY=DV/E
      Y=Y-DY
501 CONTINUE
*   *****
*   * THIS PART FINDS THE IONIZATION ZONE
*   *****

      IN=1
      LL=1
      DS=40.0*A
      DO 502 I=0,180,10
        THET=I*PI/180.0
        X=A*DSIN(THET)
        Y=H+A*DCOS(THET)
        DO 503 L=1,2000
          CALL FELDE(N1,N2,N3,X,Y,EX,EY,E,EPSR,H)
          IF(I.EQ.180)THEN
C   WRITE(6,*)E
            YAS(IN)=Y
            IN=IN+1
          ENDIF

          E=E/100.0
          ATT=(0.01298-0.541E-3*(E/760.0)+0.87E-5*(E/760.0)**2)*760.0
          IF(E/760.0.GE.25.AND.E/760.0.LE.60.0) THEN
C   WRITE(6,*)E/760.0,'IONIZATION BET. 25--60'
            FION=(4.7786*EXP(-221*760.0/E))*760.0
            ELSEIF (E/760.0.GE.60.0.AND.E/760.0.LE.240.0) THEN
C   WRITE(6,*)E/760.0,'IONIZATION BET. 60--240'
            FION=(9.682*EXP(-264.2*760.0/E))*760.0
          ELSE
            WRITE(6,*)E/760.0,'IONIZATION OUT OF THE RANGE',L
            GOTO 561
          ENDIF
          DIF=FION-ATT
          IF(ABS(DIF).LT.0.01*FION) GOTO 560
          RZ=.01*FION
          DL=DS/E
          Y=Y+DL*DCOS(THET)
          X=X+DL*DSIN(THET)
C   WRITE(6,*)FION,ATT,DIF,RZ
503 CONTINUE
      WRITE(6,*)'STEPE IS NOT INAF'
      GOTO 561
c560 WRITE(6,*)'THE IONIZATION AND THE ATTACHEMENT WHEN ION=ATT'

560 IF(I.LE.180) THEN
      XIZ(LL)=X
      YIZ(LL)=Y
      WRITE(6,*)XIZ(LL),YIZ(LL),'IONIZATION ',I

```

```

LL=LL+1
ENDIF

C  WRITE(6,*)X,Y
502 CONTINUE
* *****
*  * THIS PART DRAWS THE CONDUCTOR
* *****
561 KK=1
DO 504 I=0,180,10
  THET=I*PI/180.0
  X=A*DSIN(THET)
  Y=H+A*DCOS(THET)

  IF(I.LE.180) THEN
    CX(KK)=X
    CY(KK)=Y
    WRITE(6,*)CX(KK),CY(KK),'CONDUCTOR',KK,I
    KK=KK+1
  ENDIF

*  WRITE(6,*)X,Y
504 CONTINUE
c  STOP
  KK=KK-1
  LL=LL-1
* *****
*  * THIS PART FINDS THE PRIMARY AVALANCHE
* *****
DO 33 I=1,IN-1
  DF=((H-A)-YAS(I))/(CY(KK)-YIZ(LL))
c  WRITE(6,*)DF
33 CONTINUE
c  STOP

SUM=0.0
TNAV=0.0
GP=3E-3
NINTG=300
TL=CY(KK)-YIZ(LL)
STEIN=TL/(NINTG*1.0)
NINTG=NINTG+1
DO 303 NN=1,NINTG
  Y=CY(KK)-(NN-1)*STEIN
  X=0.0
  CALL FELDE(N1,N2,N3,X,Y,EX,EY,E,EPSR,H)
  IF(NN.EQ.1) THEN
    ET=E/100.0
  ELSE
    ESC=1.6E-19*(EXP(SUM)-1.0)/(4.0*PI*EPS*XSC**2)
    ET=(E-ESC)/100.0
  ENDIF
  CALL ATTION(ET,FION,ATT,DIF)
  XSC=1.0/(FION*100.0)
  SUM=SUM+STEIN*DIF*100.0
  CALL ABSORP(ET,AMU)
  RX=H-Y
c  write(6,*)'rx',rx,'h',h,'y',y
  RMU=CY(KK)-Y
C  WRITE(6,*)RX,A,AMU,PI

```

```

c  WRITE(6,*)'res'
c  CALL ROMBERG(RX,A,AMU,RES,PI)
CALL RAD(RX,A,AMU,PI,GR)
CALL GAX(RX,A,AMU,PI,GX)
RES=GR*GX
C  stop
eion=exp(sum)
TNAV=TNAV+(GP*RES*(FION*100.0)*EXP(-AMU*RMU)*EXP(SUM))*STEIN
WRITE(6,*)TNAV,EION,SUM
303 CONTINUE

```

```

STOP
END

```

```

* *****END OF MAIN PROGRAM*****

```

```

*
* *****
* * THIS SUBROUTINE FINDS POTENTIAL IN THE COATING-LAYER
* *****

```

```

SUBROUTINE POTI(N1,N2,N3,X,Y,POT)
EZA03450
PARAMETER(M=180)
IMPLICIT DOUBLE PRECISION(A-H,O-Z)

COMMON /COM1/ XC(M),YC(M)
COMMON /COM2/ Q(M)
SUMV=0.0
DO 200 J=1,N1
DC1=DSQRT((X-XC(J))**2+(Y-YC(J))**2)
DI1=DSQRT((X-XC(J))**2+(Y+YC(J))**2)

DC2=DSQRT((X+XC(J))**2+(Y-YC(J))**2)
DI2=DSQRT((X+XC(J))**2+(Y+YC(J))**2)
SUMV=SUMV+Q(J)*DLOG((DI1*DI2)/(DC1*DC2))
200 CONTINUE

```

```

DO 300 J=N1+N2+1,N1+N2+N3
DC1=DSQRT((X-XC(J))**2+(Y-YC(J))**2)
DI1=DSQRT((X-XC(J))**2+(Y+YC(J))**2)

DC2=DSQRT((X+XC(J))**2+(Y-YC(J))**2)
DI2=DSQRT((X+XC(J))**2+(Y+YC(J))**2)
SUMV=SUMV+Q(J)*DLOG((DI1*DI2)/(DC1*DC2))
300 CONTINUE
POT=SUMV
RETURN
END

```

```

* *****
* * THIS SUBROUTINE FINDS POTENTIAL IN THE AIR
* *****

```

```

SUBROUTINE POTE(N1,N2,N3,X,Y,POT)
PARAMETER(M=180)
IMPLICIT DOUBLE PRECISION (A-H,O-Z)
* DIMENSION XC(M),YC(M),Q(M)

COMMON /COM1/ XC(M),YC(M)
COMMON /COM2/ Q(M)
SUMV=0.0
DO 200 J=1,N1+N2
DC1=DSQRT((X-XC(J))**2+(Y-YC(J))**2)

```

```

DI1=DSQRT((X-XC(J))**2+(Y+YC(J))**2)

DC2=DSQRT((X+XC(J))**2+(Y-YC(J))**2)
DI2=DSQRT((X+XC(J))**2+(Y+YC(J))**2)
SUMV=SUMV+Q(J)*DLOG((DI1*DI2)/(DC1*DC2))
200 CONTINUE
POT=SUMV
RETURN
END

* *****
* * THIS SUBROUTINE FINDS ELECTRIC FIELD IN THE COATING-LAYER
* *****
SUBROUTINE FELDI(N1,N2,N3,X,Y,EX,EY,E,EPSR,H)
PARAMETER(M=180)
IMPLICIT DOUBLE PRECISION (A-H,O-Z)

COMMON /COM1/ XC(M),YC(M)
COMMON /COM2/ Q(M)
PI=4*DATAN(1.0D0)
SUMX=0.0
SUMY=0.0
DO 200 J=1,N1
IF(Y.GT.H)TH1=PI-DATAN(X/(Y-H))-PI/2
IF(Y.LT.H)TH1=DATAN(X/(H-Y))-PI/2
IF(Y.EQ.H)TH1=0

RAD1=DSQRT((X-XC(J))**2+(Y-YC(J))**2)
RAD2=DSQRT((X+XC(J))**2+(Y-YC(J))**2)
RAD3=DSQRT((X-XC(J))**2+(Y+YC(J))**2)
RAD4=DSQRT((X+XC(J))**2+(Y+YC(J))**2)

XCOMP1=(X-XC(J))/RAD1**2
XCOMP2=(X+XC(J))/RAD2**2
XCOMP3=(X-XC(J))/RAD3**2
XCOMP4=(X+XC(J))/RAD4**2

XCOMP=XCOMP1+XCOMP2-XCOMP3-XCOMP4

YCOMP1=(Y-YC(J))/RAD1**2
YCOMP2=(Y-YC(J))/RAD2**2
YCOMP3=(Y+YC(J))/RAD3**2
YCOMP4=(Y+YC(J))/RAD4**2

YCOMP=YCOMP1+YCOMP2-YCOMP3-YCOMP4

SUMX=SUMX+Q(J)*XCOMP
SUMY=SUMY+Q(J)*YCOMP
200 CONTINUE

DO 300 J=N1+N2+1,N1+N2+N3
IF(Y.GT.H)TH1=PI-DATAN(X/(Y-H))-PI/2
IF(Y.LT.H)TH1=DATAN(X/(H-Y))-PI/2
IF(Y.EQ.H)TH1=0
RAD1=DSQRT((X-XC(J))**2+(Y-YC(J))**2)
RAD2=DSQRT((X+XC(J))**2+(Y-YC(J))**2)
RAD3=DSQRT((X-XC(J))**2+(Y+YC(J))**2)
RAD4=DSQRT((X+XC(J))**2+(Y+YC(J))**2)

XCOMP1=(X-XC(J))/RAD1**2
XCOMP2=(X+XC(J))/RAD2**2

```

```
XCOMP3=(X-XC(J))/RAD3**2
XCOMP4=(X+XC(J))/RAD4**2
```

```
XCOMP=XCOMP1+XCOMP2-XCOMP3-XCOMP4
```

```
YCOMP1=(Y-YC(J))/RAD1**2
YCOMP2=(Y-YC(J))/RAD2**2
YCOMP3=(Y+YC(J))/RAD3**2
YCOMP4=(Y+YC(J))/RAD4**2
```

```
YCOMP=YCOMP1+YCOMP2-YCOMP3-YCOMP4
```

```
SUMX=SUMX+Q(J)*XCOMP
SUMY=SUMY+Q(J)*YCOMP
```

```
300 CONTINUE
```

```
EX=SUMX
EY=SUMY
E=DSQRT(SUMX**2+SUMY**2)
RETURN
END
```

```
* *****
```

```
* * THIS SUBROUTINE FINDS ELECTRIC FIELD IN THE AIR
```

```
* *****
```

```
SUBROUTINE FELDE(N1,N2,N3,X,Y,EX,EY,E,EPSR,H)
PARAMETER(M=180)
IMPLICIT DOUBLE PRECISION (A-H,O-Z)
```

```
COMMON /COM1/ XC(M),YC(M)
COMMON /COM2/ Q(M)
PI=4*DATAN(1.0D0)
SUMX=0.0
SUMY=0.0
DO 200 J=1,N1+N2
IF(Y.GT.H)TH1=PI-DATAN(X/(Y-H))-PI/2
IF(Y.LT.H)TH1=DATAN(X/(H-Y))-PI/2
IF(Y.EQ.H)TH1=0
RAD1=DSQRT((X-XC(J))**2+(Y-YC(J))**2)
RAD2=DSQRT((X+XC(J))**2+(Y-YC(J))**2)
RAD3=DSQRT((X-XC(J))**2+(Y+YC(J))**2)
RAD4=DSQRT((X+XC(J))**2+(Y+YC(J))**2)
```

```
XCOMP1=(X-XC(J))/RAD1**2
XCOMP2=(X+XC(J))/RAD2**2
XCOMP3=(X-XC(J))/RAD3**2
XCOMP4=(X+XC(J))/RAD4**2
```

```
XCOMP=XCOMP1+XCOMP2-XCOMP3-XCOMP4
```

```
YCOMP1=(Y-YC(J))/RAD1**2
YCOMP2=(Y-YC(J))/RAD2**2
YCOMP3=(Y+YC(J))/RAD3**2
YCOMP4=(Y+YC(J))/RAD4**2
```

```
YCOMP=YCOMP1+YCOMP2-YCOMP3-YCOMP4
```

```
SUMX=SUMX+Q(J)*XCOMP
SUMY=SUMY+Q(J)*YCOMP
```

```
200 CONTINUE
```

```
EX=SUMX
EY=SUMY
E=DSQRT(SUMX**2+SUMY**2)
```



```

RETURN
END
* *****
* *THIS SUBROUTINE FINDS INVERSE OF MATRIX
* *****
SUBROUTINE NGAUSS(N)
PARAMETER(M=180)
IMPLICIT DOUBLE PRECISION (A-H,O-Z)
COMMON /COM3/ AV(M,M),BV(M)
COMMON /COM2/ Q(M)
write(6,*)'N=',N
DO 4 K=1,N-1

    DO 3 I=K+1,N
        XMULT=AV(I,K)/AV(K,K)
        DO 2 J=K+1,N
            AV(I,J)=AV(I,J)-XMULT*AV(K,J)
2        CONTINUE
        AV(I,K)=XMULT
        BV(I)=BV(I)-XMULT*BV(K)
3    CONTINUE
4    CONTINUE
    Q(N)=BV(N)/AV(N,N)
    DO 6 I=N-1,1,-1
        SUM=BV(I)
        DO 5 J=I+1,N
            SUM=SUM-AV(I,J)*Q(J)
5    CONTINUE
        Q(I)=SUM/AV(I,I)
6    CONTINUE
RETURN
END
* *****
* *THIS SUBROUTINE FINDS ATT & ION
* *****
SUBROUTINE ATTION(E,FION,ATT,DIF)
IMPLICIT DOUBLE PRECISION (A-H,O-Z)

ATT=(0.01298-0.541E-3*(E/760.0)+0.87E-5*(E/760.0)**2)*760.0
IF(E/760.0.GE.25.AND.E/760.0.LE.60.0) THEN
C  WRITE(6,*)E/760.0,'IONIZATION BET. 25--60'
    FION=(4.7786*EXP(-221*760.0/E))*760.0
ELSEIF (E/760.0.GE.60.0.AND.E/760.0.LE.240.0) THEN
C  WRITE(6,*)E/760.0,'IONIZATION BET.60--240'
    FION=(9.682*EXP(-264.2*760.0/E))*760.0
ELSE
    WRITE(6,*)E/760.0,'IONIZATION OUT OF THE RANGE'
ENDIF
DIF=FION-ATT
RETURN
END
* *****
* *THIS SUBROUTINE FINDS ABSORPTION COEFFICIENT (MU)
* *****
SUBROUTINE ABSORP(E,AMU)
IMPLICIT DOUBLE PRECISION (A-H,O-Z)

E=E/1000.0
IF(E.GE.19.0.AND.E.LE.190.0) THEN
    AMU=100*EXP(-31.568+6.785*LOG(E))
ELSEIF(E.GT.190.0) THEN

```

```

AMU=100.0*EXP(-11.743+2.78*LOG(E))
ELSE
WRITE(6,*)'AMU CAN NOT BE CALCULATED E=',E,'KV/CM'
ENDIF
RETURN
END
* *****
* *THIS SUBROUTINE FINDS THE GEOMETRY FACTOR (Grad*Gax)
* *****
SUBROUTINE ROMBERG(RX,R,AMU,RES,PI)
IMPLICIT DOUBLE PRECISION (A-H,O-Z)
DIMENSION T1(15),T2(15)
C F(X)=EXP(X)
NI=15
X01=0.0
X02=0.0
XZ=R/RX
IF(XZ.GT.1.0)THEN
H01=DASIN(1.0)
ELSE
H01=DASIN(XZ)
ENDIF
H02=PI/2*(88.0/90.0)
XEPS=1.0D-6
DO 7 K=1,NI
HK1=H01/(2**(K-1))
Y1=0.0
HK2=H02/(2**(K-1))
Y2=0.0
DO 9 I=1,(2**(K-1))-1
X1=X01+I*HK1
XE1=-AMU*DSQRT(RX**2+R**2-2*RX*R*DCOS(X1))
IF(XE1.LT.-100.0)XE1=-100.0
Y1=Y1+EXP(XE1)
X2=X02+I*HK2
XE2=-AMU*(RX-R)/DCOS(X2)
IF(XE2.LT.-100.0)XE2=-100.0
Y2=Y2+EXP(XE2)
9 CONTINUE
X1=X01+H01
Z1=(RX**2+R**2-2.0*RX*R*DCOS(X1))
Z2=(RX**2+R**2-2.0*RX*R*DCOS(X01))
IF(Z1.LT.0.0) THEN
XE1=-AMU*DSQRT(0.0)
ELSE
XE1=-AMU*DSQRT(Z1)
ENDIF
IF(Z2.LT.0.0) THEN
YE1=-AMU*DSQRT(0.0)
ELSE
YE1=-AMU*DSQRT(Z2)
ENDIF
IF(XE1.LT.-100.0)XE1=-100.0
IF(YE1.LT.-100.0)YE1=-100.0
T1(K)=HK1/2.0*(EXP(YE1)+2.0*Y1+EXP(XE1))
X2=X02+H02
XE2=-AMU*(RX-R)/DCOS(X2)
YE2=-AMU*(RX-R)/DCOS(X02)
IF(XE2.LT.-100.0)XE2=-100.0
IF(YE2.LT.-100.0)YE2=-100.0
T2(K)=HK2/2.0*(EXP(YE2)+2.0*Y2+EXP(XE2))

```

```

IF(K.GT.1)THEN
  DIF1=DABS(1-T1(K-1)/T1(K))
  DIF2=DABS(1-T2(K-1)/T2(K))
  IF(DIF1.LT.XEPS.AND.DIF2.LT.XEPS)THEN
    RES1=T1(K)/(PI*EXP(-AMU*(RX-R)))
    RES2=2*T2(K)/(PI*EXP(-AMU*(RX-R)))
    RES=RES1*RES2
    GOTO 999
  ENDIF
ENDIF
7 CONTINUE
J=0
10 IF(J.EQ.(NI-1))THEN
  WRITE(6,*)'ITEGRATION LIMIT EXCEEDED'
  GOTO 999
ENDIF
DIF1=DABS(1-T1(NI-J-1)/T1(NI-J))
DIF2=DABS(1-T2(NI-J-1)/T2(NI-J))
IF(DIF1.LT.XEPS.AND.DIF2.LT.XEPS)THEN
  GOTO 30
ELSE
  J=J+1
  DO 13 I=1,NI-J
    T1(I)=((4**J)*T1(I+1)-T1(I))/(4**J-1)
    T2(I)=((4**J)*T2(I+1)-T2(I))/(4**J-1)
  13 CONTINUE
ENDIF
GOTO 10
30 RES1=T1(NI-J)/(PI*EXP(-AMU*(RX-R)))
RES2=2*T2(NI-J)/(PI*EXP(-AMU*(RX-R)))
RES=RES1*RES2
write(6,*)RES1,RES2
999 RETURN
END
* *****
SUBROUTINE GAX(RX,A,AMU,PI,GX)
IMPLICIT DOUBLE PRECISION (A-H,O-Z)
EBSY=0.0D0
DEBSY=PI/180.0D0
SUM=0.0D0
DO 10 I=1,100
SUM=SUM+(DEXP(-AMU*(RX-A)/(DCOS(EBSY))))*DEBSY
EBSY=EBSY+DEBSY
IF(EBSY.GT.(88.0D0*(PI/180.0D0))) GOTO 20
10 CONTINUE
20 GX=SUM*2.0/(PI*DEXP(-AMU*(RX-A)))
RETURN
END
* *****
SUBROUTINE RAD(RX,A,AMU,PI,GR)
IMPLICIT DOUBLE PRECISION (A-H,O-Z)
EBSY=0.0D0
DEBSY=PI/180.0D0
DD=A/RX
IF(DD.GT.1.0D0) DD=1.0D0
EBSYM=DACOS(DD)
SUM=0.0D0
DO 10 I=1,100
CC=1.0D0-DCOS(EBSY)
BB=DSQRT((RX-A)**2+2*A**2*CC+2*A*(RX-A)*CC)
SUM=SUM+(DEXP(-AMU*BB))*DEBSY

```

```
EBSY=EBSY+DEBSY  
IF(EBSY.GT.EBSYM) GOTO 20  
10 CONTINUE  
20 GR=SUM/(PI*DEXP(-AMU*(RX-A)))  
RETURN  
END
```

## PROGRAM 4

### CALCULATE NEGATIVE ONSET VOLTAGE FOR BARE CONDUCTOR:

```

* *****
* * This computer program calculates the following for a bare conductor:
* * 1.The potential and electric field
* * 2.The negative onset voltage
* *****
PARAMETER (M=150)
IMPLICIT DOUBLE PRECISION (A-H,O-Z)
DIMENSION XB(M),YB(M),XCK(M),YCK(M),TH(M)
COMMON /COM1/ XC(M),YC(M)
COMMON /COM2/ Q(M)
COMMON /COM3/ AV(M,M),BV(M)
COMMON /COM4/ XIZ(180),YIZ(180),CX(180),CY(180),NSX(180)
COMMON /COM5/ AREA(900)
OPEN (UNIT = 5,FILE ='EZA2.DAT',STATUS='OLD')
OPEN (UNIT = 6,FILE ='EZA2.OUT',STATUS='OLD')

READ(5,*)N1,A,V,RF1,H,STEPE
PI=4*DATAN(1.0D0)
EPS=1E-9/(36*PI)
* *****
* * THIS SECTION FINDS CHARGES LOCATION
* *****
* WRITE(6,*)CHARGE 1----- N1'
DTHET=PI/N1
THET=DTHET/2.0
DO 10 I=1,N1
XC(I)=RF1*A*DSIN(THET)
YC(I)=H+RF1*A*DCOS(THET)
THET=THET+DTHET
* WRITE(6,510)XC(I),YC(I)
10 CONTINUE
* *****
* * THIS SECTION FINDS BOUNDARY POINTS LOCATION
* *****
* WRITE(6,*)BOUNDARY 1----- N1'
DTHET=PI/N1
THET=DTHET/2.0
DO 40 I=1,N1
XB(I)=A*DSIN(THET)
YB(I)=H+A*DCOS(THET)
THET=THET+DTHET
TH(I)=THET
* WRITE(6,510)XB(I),YB(I)
40 CONTINUE
* *****
* * THIS SECTION MAKES POTENTIAL COEFFICIENT MATRIX
* *****

DO 75 I=1,N1
BV(I)=V
75 CONTINUE

```

```

DO 80 I=1,N1
DO 80 J=1,N1
DC1=DSQRT((XB(I)-XC(J))**2+(YB(I)-YC(J))**2)
DI1=DSQRT((XB(I)-XC(J))**2+(YB(I)+YC(J))**2)

DC2=DSQRT((XB(I)+XC(J))**2+(YB(I)-YC(J))**2)
DI2=DSQRT((XB(I)+XC(J))**2+(YB(I)+YC(J))**2)
AV(I,J)=DLOG((DI1*DI2)/(DC1*DC2))
80 CONTINUE

* *****
N=N1
CALL NGAUSS(N)
DTHET= PI/N1
THET=0.0
DO 160 I=1,N1
XCK(I)=A*DSIN(THET)
YCK(I)=H+A*DCOS(THET)
THET=THET+DTHET
160 CONTINUE
WRITE(6,*) 'CNDUCTOR POTENTIAL'
DO 170 I=1,N1
X=XCK(I)
Y=YCK(I)
CALL POTE(N1,X,Y,POT)
WRITE(6,510)X,Y,POT
C WRITE(6,*)X,Y,POT
170 CONTINUE

510 FORMAT(08(E12.5,2X))
C STOP
WRITE(6,*)'*****'
DV=V/STEPE
X=0.0
Y=H-A
DO 501 I=1,STEPE
CALL POTE(N1,X,Y,POT)
CALL FELDE(N1,X,Y,EX,EY,E,H)
C WRITE(6,510)Y,E
C WRITE(6,510)X,Y,POT,EX,EY,E
DY=DV/E
Y=Y-DY
501 CONTINUE

* *****
* * THIS PART FINDS THE IONIZATION ZONE
* *****
LL=1
DS=40.0*A
DO 502 I=0,180,10
THET=I*PI/180.0
X=A*DSIN(THET)
Y=H+A*DCOS(THET)
DO 503 L=1,2000
CALL FELDE(N1,X,Y,EX,EY,E,H)
E=E/100.0
ATT=(0.01298-0.541E-3*(E/760.0)+0.87E-5*(E/760.0)**2)*760.0
IF(E/760.0.GE.25.AND.E/760.0.LE.60.0) THEN
C WRITE(6,*)E/760.0,'IONIZATION BET. 25--60'
FION=(4.7786*EXP(-221*760.0/E))*760.0
ELSEIF (E/760.0.GE.60.0.AND.E/760.0.LE.240.0) THEN

```

```

C  WRITE(6,*)E/760.0,'IONIZATION BET.60--240'
  FION=(9.682*EXP(-264.2*760.0/E))*760.0
  ELSE
  WRITE(6,*)E/760.0,'IONIZATION OUT OF THE RANGE',L
  GOTO 561
ENDIF
DIF=FION-ATT
IF(ABS(DIF).LT.0.01*FION) GOTO 560
RZ=.01*FION
DL=DS/E
Y=Y+DL*DCOS(THET)
X=X+DL*DSIN(THET)
C  WRITE(6,*)FION,ATT,DIF,RZ
503 CONTINUE
  WRITE(6,*)'STEPE IS NOT INAF'
  GOTO 561
C560 WRITE(6,*)'THE IONIZATION AND THE ATTACHEMENT WHEN ION=ATT'

560 IF(I.LE.180) THEN
  XIZ(LL)=X
  YIZ(LL)=Y
  WRITE(6,*)XIZ(LL),YIZ(LL),'IONIZATION ',I
  LL=LL+1
ENDIF

C  WRITE(6,*)X,Y
502 CONTINUE
* *****
*  * THIS PART DRAWS THE CONDUCTOR *
* *****

561 KK=1
  DO 504 I=0,180,10
    THET=I*PI/180.0
    X=A*DSIN(THET)
    Y=H+A*DCOS(THET)

    IF(I.LE.180) THEN
      CX(KK)=X
      CY(KK)=Y
      WRITE(6,*)CX(KK),CY(KK),'CONDUCTOR',KK,I
      KK=KK+1
    ENDIF

    *  WRITE(6,*)X,Y
504 CONTINUE
c  STOP
  KK=KK-1
  LL=LL-1
* *****
*  * THIS PART FINDS THE PRIMARY AVALANCHE *
* *****

  sum=0.0
  TNAV=0.0
  GP=3E-3
  NINTG=300
  ISAV=1
  TL=CY(KK)-YIZ(LL)
  STEIN=TL/(NINTG*1.0)
  NINTG=NINTG+1
  DO 303 NN=1,NINTG
    Y=CY(KK)-(NN-1)*STEIN

```

```

X=0.0
CALL FELDE(N1,X,Y,EX,EY,E,H)
IF(NN.EQ.1) THEN
  ET=E/100.0
ELSE
  ESC=1.6E-19*(EXP(SUM)-1.0)/(4.0*PI*EPS*XSC**2)
  ET=(E-ESC)/100.0
ENDIF
CALL ATTION(ET,FION,ATT,DIF)
XSC=1.0/(FION*100.0)
SUM=SUM+STEIN*DIF*100.0
CALL ABSORP(ET,AMU)
RX=H-Y
c  write(6,*)rx,rx,'h','h','y','y'
  RMU=CY(KK)-Y
C  WRITE(6,*)RX,A,AMU,PI

C  WRITE(6,*)res'
C  CALL ROMBERG(RX,A,AMU,RES,PI)
  CALL RAD(RX,A,AMU,PI,GR)
C  WRITE(6,*)res'
  CALL GAX(RX,A,AMU,PI,GX)
  RES=GR*GX

  eion=exp(sum)
  TNAV=TNAV+(RES*GP*(FION*100.0)*EXP(-AMU*RMU)*EXP(SUM))*STEIN
  WRITE(6,*)TNAV,EION
303 CONTINUE
  write(6,*)tl='tl
  STOP
  END
*  ***** END OF NAIM PROGRAM *****

*  *****
*  * THIS SUBROUTINE FINDS POTENTIAL IN THE AIR
*  *****

SUBROUTINE POTE(N1,X,Y,POT)
PARAMETER (M=150)
IMPLICIT DOUBLE PRECISION (A-H,O-Z)
COMMON /COM1/ XC(M),YC(M)
COMMON /COM2/ Q(M)
SUMV=0.0
DO 200 J=1,N1
  DC1=DSQRT((X-XC(J))**2+(Y-YC(J))**2)
  DI1=DSQRT((X-XC(J))**2+(Y+YC(J))**2)

  DC2=DSQRT((X+XC(J))**2+(Y-YC(J))**2)
  DI2=DSQRT((X+XC(J))**2+(Y+YC(J))**2)
  SUMV=SUMV+Q(J)*DLOG((DI1*DI2)/(DC1*DC2))
200 CONTINUE
POT=SUMV
RETURN
END

*  *****
*  * THIS SUBROUTINE FINDS ELECTRIC FIELD IN THE AIR
*  *****

SUBROUTINE FELDE(N1,X,Y,EX,EY,E,H)
PARAMETER (M=150)

```



```

IMPLICIT DOUBLE PRECISION (A-H,O-Z)
COMMON /COM1/ XC(M),YC(M)
COMMON /COM2/ Q(M)
PI=4*DATAN(1.0D0)
SUMX=0.0
SUMY=0.0
DO 200 J=1,N1
RAD1=DSQRT((X-XC(J))**2+(Y-YC(J))**2)
RAD2=DSQRT((X+XC(J))**2+(Y-YC(J))**2)
RAD3=DSQRT((X-XC(J))**2+(Y+YC(J))**2)
RAD4=DSQRT((X+XC(J))**2+(Y+YC(J))**2)

XCOMP1=(X-XC(J))/RAD1**2
XCOMP2=(X+XC(J))/RAD2**2
XCOMP3=(X-XC(J))/RAD3**2
XCOMP4=(X+XC(J))/RAD4**2

XCOMP=XCOMP1+XCOMP2-XCOMP3-XCOMP4

YCOMP1=(Y-YC(J))/RAD1**2
YCOMP2=(Y-YC(J))/RAD2**2
YCOMP3=(Y+YC(J))/RAD3**2
YCOMP4=(Y+YC(J))/RAD4**2

YCOMP=YCOMP1+YCOMP2-YCOMP3-YCOMP4

SUMX=SUMX+Q(J)*XCOMP
SUMY=SUMY+Q(J)*YCOMP
200 CONTINUE
EX=SUMX
EY=SUMY
E=DSQRT(SUMX**2+SUMY**2)
RETURN
END
* *****
* *THIS SUBROUTINE FINDS INVERSE OF MATRIX
* *****
SUBROUTINE NGAUSS(N)
PARAMETER (M=150)
IMPLICIT DOUBLE PRECISION (A-H,O-Z)
COMMON /COM2/ Q(M)
COMMON /COM3/ AV(M,M),BV(M)
DO 4 K=1,N-1
DO 3 I=K+1,N
XMULT=AV(I,K)/AV(K,K)
DO 2 J=K+1,N
AV(I,J)=AV(I,J)-XMULT*AV(K,J)
2 CONTINUE
AV(I,K)=XMULT
BV(I)=BV(I)-XMULT*BV(K)
3 CONTINUE
4 CONTINUE
Q(N)=BV(N)/AV(N,N)
DO 6 I=N-1,1,-1
SUM=BV(I)
DO 5 J=I+1,N
SUM=SUM-AV(I,J)*Q(J)
5 CONTINUE
Q(I)=SUM/AV(I,I)
6 CONTINUE
RETURN

```

```

END
* *****
* *THIS SUBROUTINE FINDS ATT & ION
* *****
SUBROUTINE ATTION(E,FION,ATT,DIF)
IMPLICIT DOUBLE PRECISION (A-H,O-Z)

ATT=(0.01298-0.541E-3*(E/760.0)+0.87E-5*(E/760.0)**2)*760.0
IF(E/760.0.GE.25.AND.E/760.0.LE.60.0) THEN
C  WRITE(6,*)E/760.0,'IONIZATION BET. 25--60'
  FION=(4.7786*EXP(-221*760.0/E))*760.0
  ELSEIF (E/760.0.GE.60.0.AND.E/760.0.LE.240.0) THEN
C  WRITE(6,*)E/760.0,'IONIZATION BET.60--240'
  FION=(9.682*EXP(-264.2*760.0/E))*760.0
  ELSE
  WRITE(6,*)E/760.0,'IONIZATION OUT OF THE RANGE'
  ENDIF
  DIF=FION-ATT
  RETURN
  END
* *****
* *THIS SUBROUTINE FINDS ABSORPTION COEFFICIENT (MU)
* *****
SUBROUTINE ABSORP(E,AMU)
IMPLICIT DOUBLE PRECISION (A-H,O-Z)

E=E/1000.0
IF(E.GE.19.0.AND.E.LE.190.0) THEN
  AMU=100*EXP(-31.568+6.785*LOG(E))
  ELSEIF(E.GT.190.0) THEN
  AMU=100.0*EXP(-11.743+2.78*LOG(E))
  ELSE
  WRITE(6,*)AMU CAN NOT BE CALCULATED E=',E,'KV/CM'
  ENDIF
  RETURN
  END
* *****
* *THIS SUBROUTINE FINDS THE GEOMETRY FACTOR (Grad*Gax)
* *****
SUBROUTINE ROMBERG(RX,R,AMU,RES,PI)
IMPLICIT DOUBLE PRECISION (A-H,O-Z)
DIMENSION T1(15),T2(15)
C  F(X)=EXP(X)
  NI=15
  X01=0.0
  X02=0.0
  XZ=R/RX
  IF(XZ.GT.1.0)THEN
    H01=DACOS(1.0)
C  H01=DASIN(1.0)
  ELSE
    H01=DACOS(XZ)
C  H01=DASIN(XZ)
  ENDIF
  H02=PI/2*(88.0/90.0)
  XEPS=1.0D-6
  DO 7 K=1,NI
    HK1=H01/(2**(K-1))
    Y1=0.0
    HK2=H02/(2**(K-1))
    Y2=0.0

```

```

DO 9 I=1,(2**(K-1))-1
X1=X01+H*HK1
XE1=AMU*DSQRT(RX**2+R**2-2*RX*R*DCOS(X1))
IF(XE1.LT.-100.0)XE1=-100.0
Y1=Y1+EXP(XE1)
X2=X02+H*HK2
XE2=-AMU*(RX-R)/DCOS(X2)
IF(XE2.LT.-100.0)XE2=-100.0
Y2=Y2+EXP(XE2)
9 CONTINUE
X1=X01+H01
Z1=(RX**2+R**2-2.0*RX*R*DCOS(X1))
Z2=(RX**2+R**2-2.0*RX*R*DCOS(X01))
IF(Z1.LT.0.0) THEN
XE1=-AMU*DSQRT(0.0)
ELSE
XE1=-AMU*DSQRT(Z1)
ENDIF
IF(Z2.LT.0.0) THEN
YE1=-AMU*DSQRT(0.0)
ELSE
YE1=-AMU*DSQRT(Z2)
ENDIF
IF(XE1.LT.-100.0)XE1=-100.0
IF(YE1.LT.-100.0)YE1=-100.0
T1(K)=HK1/2.0*(EXP(YE1)+2.0*Y1+EXP(XE1))
X2=X02+H02
XE2=-AMU*(RX-R)/DCOS(X2)
YE2=-AMU*(RX-R)/DCOS(X02)
IF(XE2.LT.-100.0)XE2=-100.0
IF(YE2.LT.-100.0)YE2=-100.0
T2(K)=HK2/2.0*(EXP(YE2)+2.0*Y2+EXP(XE2))
IF(K.GT.1)THEN
DIF1=DABS(1-T1(K-1)/T1(K))
DIF2=DABS(1-T2(K-1)/T2(K))
IF(DIF1.LT.XEPS.AND.DIF2.LT.XEPS)THEN
RES1=T1(K)/(PI*EXP(-AMU*(RX-R)))
RES2=2*T2(K)/(PI*EXP(-AMU*(RX-R)))
RES=RES1*RES2
GOTO 999
ENDIF
ENDIF
7 CONTINUE
J=0
10 IF(J.EQ.(NI-1))THEN
WRITE(6,*)'ITEGRATION LIMIT EXCEEDED'
GOTO 999
ENDIF
DIF1=DABS(1-T1(NI-J-1)/T1(NI-J))
DIF2=DABS(1-T2(NI-J-1)/T2(NI-J))
IF(DIF1.LT.XEPS.AND.DIF2.LT.XEPS)THEN
GOTO 30
ELSE
J=J+1
DO 13 I=1,NI-J
T1(I)=((4**J)*T1(I+1)-T1(I))/(4**J-1)
T2(I)=((4**J)*T2(I+1)-T2(I))/(4**J-1)
13 CONTINUE
ENDIF
GOTO 10
30 RES1=T1(NI-J)/(PI*EXP(-AMU*(RX-R)))

```

```

RES2=2*T2(NI-J)/(PI*EXP(-AMU*(RX-R)))
RES=RES1*RES2
write(6,*)RES1,RES2
999 RETURN
END
* *****

SUBROUTINE GAX(RX,A,AMU,PI,GX)
IMPLICIT DOUBLE PRECISION (A-H,O-Z)
EBSY=0.0D0
DEBSY=PI/180.0D0
SUM=0.0D0
DO 10 I=1,100
SUM=SUM+(DEXP(-AMU*(RX-A)/(DCOS(EBSY))))*DEBSY
EBSY=EBSY+DEBSY
IF(EBSY.GT.(88.0D0*(PI/180.0D0))) GOTO 20
10 CONTINUE
20 GX=SUM*2.0/(PI*DEXP(-AMU*(RX-A)))
RETURN
END
* *****

SUBROUTINE RAD(RX,A,AMU,PI,GR)
IMPLICIT DOUBLE PRECISION (A-H,O-Z)
EBSY=0.0D0
DEBSY=PI/180.0D0
DD=A/RX
IF(DD.GT.1.0D0)DD=1.0D0
EBSYM=DACOS(DD)
SUM=0.0D0
DO 10 I=1,100
CC=1.0D0-DCOS(EBSY)
BB=DSQRT((RX-A)**2+2*A**2*CC+2*A*(RX-A)*CC)
SUM=SUM+(DEXP(-AMU*BB))*DEBSY
EBSY=EBSY+DEBSY
IF(EBSY.GT.EBSYM) GOTO 20
10 CONTINUE
20 GR=SUM/(PI*DEXP(-AMU*(RX-A)))
RETURN
END

```

## **APPENDIX - B**

### **SAMPLES OF THE PROGRAM OUTPUT**

#### **CASE 1**

**OUTPUT REPORT FOR POSITIVE CORONA CRITERIA WHEN THE  
LINEPARAMETERS ARE FIXED AS :**

**Conductor radius = 0.0076125 m**

**Conductor height = 12 .5 m**

**Relative permittivity = 4.2**

**Thickness of coting layer = 0.5 mm**

#### **Potential Values Arround Conductor Surface**

$\theta$ (degree)	calculated potential (V)	error %
0	284000.000	0.3054E-11
60	284000.000	0.2009E-11
120	284000.000	-0.2316E-11
180	284000.000	0.3443E-11

**Potential Values at Interface :**

$\theta$ (degree)	calculated $\Phi_{\text{air}}$ (V)	calculated $\Phi_{\text{dielectric}}$ (V)	error %
0	283465.879	283465.879	.2343E-08
60	283465.709	283465.709	.5853E-09
120	283465.367	283465.367	.5859E-09
180	283465.197	283465.197	.2345E-08

**Field Values at Interface :**

$\theta$ (degree)	calculated $E_{\text{air}}$ (V/m)	calculated $E_{\text{dielec}}$ (V/m)	$E_{\text{air}}/E_{\text{dielec}}$	error %
0	4346883.227	1034972.279	4.1999997	.7906E-05
60	4348272.328	1035302.956	4.1999999	.2036E-05
120	4351053.196	1035965.068	4.1999999	.2035E-05
180	4352444.965	1036296.502	4.1999997	.7908E-05

Primary Avalanche Size : 233741.8

Secondary Avalanche Size : 235465.3

Onset Voltage : 284.0 kV

**CASE 2**

**OUTPUT REPORT FOR POSITIVE CORONA CRITERIA WHEN THE  
LINEPARAMETERS ARE FIXED AS :**

Conductor radius = 0.0151625 m

Conductor height = 17.5 m

Relative permittivity = 4.2

Thickness of coating layer = 3 mm

**Potential Values Around Conductor Surface**

$\theta$ (degree)	calculated potential ( V )	error %
0	537600.000	.8001E-10
60	537600.000	-.8684E-11
120	537600.000	-.4961E-10
180	537600.000	-.2081E-10

**Potential Values at Interface :**

$\theta$ (degree)	calculated $\Phi_{\text{air}}$ (V)	calculated $\Phi_{\text{dielectric}}$ (V)	error %
0	534565.111	534565.111	.2490E-08
60	534563.617	534563.617	.6227E-09
120	534560.626	534560.626	.6229E-09
180	534559.128	534559.128	.2496E-08

**Field Values at Interface :**

$\theta$ (degree)	calculated $E_{\text{air}}$ (V/m)	calculated $E_{\text{dielec.}}$ (V/m)	$E_{\text{air}}/E_{\text{dielec.}}$	error %
0	3887347.624	925559.031	4.1999997	.7917E-05
60	3889281.627	926019.464	4.1999999	.3098E-05
120	3893155.429	926941.798	4.1999999	.3098E-05
180	3895095.235	927403.701	4.1999997	.7919E-05

Primary Avalanche Size : 1658725

Secondary Avalanche Size : 1755689

Onset Voltage : 537.6 kV



**CASE 3**

OUTPUT REPORT FOR POSITIVE CORONA CRITERIA WHEN THE  
LINEPARAMETERS ARE FIXED AS :

Conductor radius = 0.0151625 m

Conductor height = 12.5 m

Relative permittivity = 2.3

Thickness of coting layer = 2 mm

**Potential Values Arround Conductor Surface**

$\theta$ (degree)	calculated potential ( V )	error %
0	493500.000	-.5662E-12
60	493500.000	-.7903E-12
120	493500.000	.9436E-13
180	493500.000	-.1132E-11

**Potential Values at Interface :**

$\theta$ (degree)	calculated $\Phi_{\text{air}}$ (V)	calculated $\Phi_{\text{dielectric}}$ (V)	error %
0	489881.668	489881.668	.1919E-08
60	489879.323	489879.323	.4800E-09
120	489874.626	489874.626	.4804E-09
180	489872.273	489872.273	.1925E-08

**Field Values at Interface :**

$\theta$ (degree)	calculated $E_{\text{air}}$ (V/m)	calculated $E_{\text{dielec.}}$ (V/m)	$E_{\text{air}}/E_{\text{dielec.}}$	error %
0	3913598.920	1701564.803	2.2999999	.3219E-05
60	3916147.261	1702672.749	2.3000000	.1589E-05
120	3921253.939	1704893.044	2.3000000	.1590E-05
180	3923812.288	1706005.398	2.2999999	.3221E-05

Primary Avalanche Size : 1445203

Secondary Avalanche Size : 1523732

Onset Voltage : 493.5 kV

**CASE 4**

**OUTPUT REPORT FOR NEGATIVE CORONA CRITERIA WHEN THE  
LINEPARAMETERS ARE FIXED AS :**

Conductor radius = 0.0076125 m

Conductor height = 12.5 m

Relative permittivity = 4.2

Thickness of coating layer = .5 mm

**Potential Values Around Conductor Surface**

$\theta$ (degree)	calculated potential ( V )	error %
0	255300.000	.2337E-11
60	255300.000	.6612E-12
120	255300.000	-.1231E-11
180	255300.000	.4845E-11

**Potential Values at Interface :**

$\theta$ (degree)	calculated $\Phi_{\text{air}}$ (V)	calculated $\Phi_{\text{dielectric}}$ (V)	error %
0	254819.855	254819.855	.2343E-08
60	254819.702	254819.702	.5854E-09
120	254819.395	254819.395	.5857E-09
180	254819.242	254819.242	.2346E-08

**Field Values at Interface :**

$\theta$ (degree)	calculated $E_{\text{air}}$ (V/m)	calculated $E_{\text{dielec.}}$ (V/m)	$E_{\text{air}}/E_{\text{dielec.}}$	error %
0	3907603.126	930381.770	4.1999997	.7906E-05
60	3908851.850	930679.031	4.1999999	.2036E-05
120	3911351.694	931274.232	4.1999999	.2035E-05
180	3912602.815	931572.173	4.1999997	.7908E-05

Primary Avalanche Size : 768.0

Onset Voltage : 255.3 kV

**CASE 5**

**OUTPUT REPORT FOR NEGATIVE CORONA CRITERIA WHEN THE  
LINEPARAMETERS ARE FIXED AS :**

Conductor radius = 0.0151625 m

Conductor height = 17.5 m

Relative permittivity = 4.2

Thickness of coating layer = 3 mm

**Potential Values Arround Conductor Surface**

$\theta$ (degree)	calculated potential ( V )	error %
0	480200.000	.3081E-10
60	480200.000	.3891E-11
120	480200.000	-.1329E-10
180	480200.000	-.8044E-10

**Potential Values at Interface :**

$\theta$ (degree)	calculated $\Phi_{\text{air}}$ (V)	calculated $\Phi_{\text{dielectric}}$ (V)	error %
0	477489.149	477489.149	.2490E-08
60	477487.815	477487.815	.6225E-09
120	477485.142	477485.142	.6229E-09
180	477483.804	477483.804	.2496E-08

**Field Values at Interface :**

$\theta$ (degree)	calculated $E_{\text{air}}$ (V/m)	calculated $E_{\text{dielec.}}$ (V/m)	$E_{\text{air}}/E_{\text{dielec.}}$	error %
0	3472292.279	826736.322	4.1999997	.7917E-05
60	3474019.786	827147.594	4.1999999	.3098E-05
120	3477479.980	827971.449	4.1999999	.3098E-05
180	3479212.671	828384.035	4.1999997	.7919E-05

Primary Avalanche Size : 704.0

Onset Voltage : 480.2 kV

**CASE 6**

OUTPUT REPORT FOR NEGATIVE CORONA CRITERIA WHEN THE  
LINEPARAMETERS ARE FIXED AS :

Conductor radius = 0.0151625 m

Conductor height = 12.5 m

Relative permittivity = 2.3

Thickness of coating layer = 2 mm

**Potential Values Around Conductor Surface**

$\theta$ (degree)	calculated potential ( V )	error %
0	440870.000	-.1030E-11
60	440870.000	-.8054E-12
120	440870.000	.3301E-12
180	440870.000	-.9242E-12

**Potential Values at Interface:**

$\theta$ (degree)	calculated $\Phi_{\text{air}}$ (V)	calculated $\Phi_{\text{dielectric}}$ (V)	error %
0	437637.550	437637.550	.1919E-08
60	437635.456	437635.456	.4800E-09
120	437631.259	437631.259	.4804E-09
180	437629.157	437629.157	.1925E-08

**Field Values at Interface :**

$\theta$ (degree)	calculated $E_{\text{air}}$ (V/m)	calculated $E_{\text{dielec.}}$ (V/m)	$E_{\text{air}}/E_{\text{dielec.}}$	error %
0	3496227.672	1520099.037	2.2999999	.3219E-05
60	3498504.241	1521088.825	2.3000000	.1589E-05
120	3503066.310	1523072.333	2.3000000	.1590E-05
180	3505351.820	1524066.058	2.2999999	.3221E-05

Primary Avalanche Size : 709.0

Onset Voltage : 440.87 kV



## NOMENCLATURE

$V_{ap}$	:	is the applied voltage
$\Phi$	:	is the electrical potential .
$[G]$	:	is a square $N_f \times N_f$ matrix, $N_f$ is the number of unknown node potential $[\Phi]$
$[B]$	:	is $N_f \times 1$ column matrix of the sum of known potentials of the bounding electrodes
$F$	:	the electrostatic energy functional
$A$	:	represents the area scanned by the triangular element
$[S]$	:	is the stiffness matrix of the element under consideration.
$[\Phi]$	:	is the column vector of vertex potential values.
$[\Phi]_b$	:	are the bound (known) potential of the nodes lying on the electrode surface.
$[\Phi]_f$	:	are the free (unknown) potentials of the other nodes.
$q_j$	:	is the $j$ th simulation charge
$p_{i,j}$	:	is the potential coefficient calculated at the $i$ th point due to the $j$ th simulation charge
$n$	:	is the number of simulation charges
$\epsilon_r$	:	is the permittivity of the medium
$\epsilon_0$	:	Permittivity of air $(= \frac{1}{36\pi} \times 10^{-9} \text{ F / m})$ .
$[P]$	:	is a square $n \times n$ potential coefficient matrix
$[q]$	:	is $(n \times 1)$ column matrix whose elements are the unknown simulation charge

- [v]** : is (n x 1) column matrix whose elements are the potential values of the contour points
- $f_{i,j}$**  : is the field coefficient calculated at the  $i$ th point due to  $j$ th charge
- $U_x$  &  $U_y$** : are unit vectors along the X and Y directions
- $E_x$  &  $E_y$** : are the components of  $\vec{E}$  along the X and Y directions
- $\Phi_I$**  : the potential calculated at any point on the electrode/dielectric-I
- $\Phi_{II}$**  : the potential at any point on the electrode / dielectric-II
- $E_{nI}$**  : is the vector sum of the normal field components due to the simulation charges belonging to the electrode and dielectric-II
- $E_{nII}$**  : is the vector sum of the normal field components due to the simulation charges belonging to the electrode and dielectric-I
- N** : number of unknown simulation charges
- $q_{c_i}$**  : simulated charges inside the conductor
- F1** : is a fraction to make the charges inside the conductor .
- R1** : is the conductor radius
- H** : is the distance from the ground plane up to the center of the conductor
- $\theta$**  : is the angle at which the charges are located
- $q_{D_i}$**  : simulated charges inside the dielectric layer
- F2** : is a fraction to make the charges inside the dielectric .
- R2** : is the coated conductor radius .
- $q_{A_i}$**  : simulated charges in the air
- F3** : is fraction exceed unity to make the charges in the air.
- $CB_i$**  : contour points on the conductor surface
- $IB_i$**  : contour points at the interface between the air and the dielectric layer

- $P_{CB-C}$  : the potential coefficient calculated at the  $i$  th contour point on the surface of the conductor ( $CB_N$ ) due to the  $j$ th simulation charges  $q_{C_j}$
- $P_{CB-A}$  : the potential coefficient calculated at the  $i$  th contour point on the surface of the conductor ( $CB_N$ ) due to the  $j$ th simulation charges  $q_{A_j}$ .
- $DC1_{CB-C}$  : are the distances between the  $i$  th contour point on the  
& conductor surface and the  $j$  th charges which are located to  
 $DC2_{CB-C}$  the right and left sides of the Y-axis inside the conductor.
- $DI1_{CB-C}$  : are the distances between the  $i$  th contour point on the  
& conductor surface and the two images of the  $j$  the charges  
 $DI2_{CB-C}$  (located in the conductor), w.r.t the ground plane.
- $DC1_{CB-A}$  : are the distances between the  $i$  th contour point on the  
& conductor surface and the  $j$  th charges which are located to  
 $DC2_{CB-A}$  the right and left sides of Y-axis in the air as shown in  
section (3.3.1).
- $DI1_{CB-A}$  : are the distances between the  $i$  th contour point on the  
& conductor surface and the two images of the  $j$  th charges  
 $DI2_{CB-A}$  (located in the air), w.r.t the ground plane.
- $P_{IB-D}$  : the potential coefficient calculated at the  $i$  th contour point on the interface between air and dielectric ( $IB_{2N}$ ) due to the  $j$  th simulation charges  $q_{D_j}$

- $P_{IB-A}$  : the potential coefficient calculated at the  $i$  th contour point on the interface between air and dielectric( $IB_{2N}$ .) due to the  $j$  th simulation charges  $q_{A_j}$ .
- $DC1_{IB-D}$  : are the distances between the  $i$  th contour point on interface & between air and dielectric and the  $j$  th charges which are located to the right and left side of Y-axis inside the dielectric.
- $DI1_{IB-D}$  : are the distances between the  $i$  th contour point on interface & between air and dielectric and the two images of the  $j$  th charges (located in the dielectric) , w.r.t. the ground plane.
- $DC1_{IB-A}$  : are the distances between the  $i$  th contour point on interface & between air and dielectric and the  $j$  th charges which are located to the right and left side of Y-axis in the air .
- $DI1_{IB-A}$  : are the distances between the  $i$  th contour point on interface & between air and dielectric and the two images of the  $j$  th charges (located in the air) , w.r.t. the ground plane.
- $f'_{IB-C}$  : is the electric field coefficient calculated at the  $i$  th contour point on the interface between air and dielectric due to the  $j$  th simulation charges in the conductor and their images w.r.t. the ground plane.
- $f'_{IB-D}$  : is the electric field coefficient calculated at the  $i$  th contour point on the interface between air and dielectric due to the  $j$  th simulation charges in the dielectric layer and their images w.r.t. the ground plane.

- $f'_{IB-A}$  : is the electric field coefficient calculated at the  $i$  th contour point on the interface between air and dielectric due to the  $j$  th simulation charges in the air and their images w.r.t. the ground .
- $E_{air}/E_{dielec}$  : the ratio between electric field at air side over the electric field at the dielectric side at the interface between coating layer and surrounding air
- $\alpha$  : Coefficient of ionization by electron collision.
- $\eta$  : Coefficient of electron attachment.
- $N_{pe}$  : the number of electrons at the tip of the primary avalanche during its growth
- $y$  : is the y-coordinate of the tip of the primary avalanche.
- $y_{iz}$  : is the y-coordinate where the primary avalanche starts
- $E_{ap}$  : is the electric field due to the voltage applied to the conductor
- $E_{p.sc}$  : is the electric field due to the positive space charge left in the wake of the primary avalanche
- $\Delta X$  : is a constant increment distance
- $D_{p.sc}$  : is the distance between the positive space charge left in the wake of the primary avalanche and the point at which the field is to be calculated
- $\bar{u}_y$  : is the unit vector in the negative Y-direction
- $N_{ph}$  : number of emitted photons
- $f_2$  : is the ratio between the number of excitation events and the number of ionization events.
- $f_1$  : is the probability of photoionization
- $\mu$  : is the photon absorption coefficient ( $m^{-1}$ )

- $\rho_j$  : is the distance between the tip of the primary avalanche and the sub volume
- $N_{s,e}$  : he number of electrons at the tip of the  $j$ th successor avalanche
- $L_{st_j}$  : defines the starting point of the  $j$ th successor avalanche
- $\bar{E}_{p.sc_j}$  : is the electric field due to the positive space charge left by the primary avalanche .
- $N_{pe}(y_{cs})$  : is the total number of electrons produced by the primary avalanche.
- $D_{s-p.sc_j}$  : is the distance between the location of the positive space charge left by of the primary avalanche and the point at which the field is to be calculated.
- $\bar{E}_{s.sc_j}$  : is the electric field due to the positive space charge at the wake of the successor avalanche starting from the  $j$ th sub-volume .
- $D_{s.sc_j}$  : is the distance between the location of the positive space charges left in the wake of the successor avalanche and the point at which the field is to be calculated .
- $L_{f_j}$  : defines the end points of the successor avalanches starting from the  $j$ th sub-volume.
- $N_{rs.sc}$  : is the total number of positive ions produced by all successor avalanches.
- $M$  : is the total number of sub-volumes in the ionization zone.
- $V_{o+}$  : positive onset voltage
- $NSL$  : number of sub-volume in each level
- $SV$  : sub-volume
- $V_{o-}$  : negative onset voltage
- $N_e(y)$  : the number of electrons at a distance  $y$  from the starting point of the avalanche in negative corona criteria
- $\Delta n(y)$  : number of photons produced over the step  $\Delta y$  of the primary avalanche's in negative corona criteria
- $\vartheta(y)$  : is the rate of production of photons

- $\Delta n_f$  : number of photons produced reach the cathode  
 $g(y)$  : is a geometry factor that accounts for the loss of photons  
 $N_{e\text{ ph}}$  : number of electrons photoemitted from the conductor  
 $\gamma_{\text{ph}}$  : is Townsend's second coefficient due to the action of photons which is equal to  $3 \cdot 10^{-3}$  for both bare and coated surface.  
 $R_{\text{P.sc}}$  : the radius of the primary positive point space charge located on the surface of the conductor in the positive corona criteria  
 $D_e$  : is the electron diffusion coefficient  
 $\tau$  : is the avalanche transit time  
 $k_e$  : is the electron mobility ( $\text{m}^2/\text{sV}$ )  
 $k$  : is Boltzmann's constant ( $=1.37 \times 10^{-23} \text{ W s/K}$ )  
 $T_e$  : is the electron temperature in K  
 $T_g$  : is the gas temperature ( $=298 \text{ K}$  at N.T.P)  
 $e$  : is the electron charge ( $=1.6 \times 10^{-19} \text{ C}$ )  
 $V_e$  : the electron velocity ( $\text{m/s}$ )  
 $V_L$  : Peak of lightning overvoltage wave.  
 $\psi_1, \psi_2$  : Constants related to the lightning overvoltage wave.  
 $N_e$  : Number of electrons produced by the avalanche.  
 $z_1$  : Z-coordinate of the starting point  $p_1$  of the initiatory (primary) avalanche.  
 $z_2$  : Z-coordinate of the end point  $p_2$  of the initiatory (primary) avalanche.  
 $\alpha$  : Coefficient of ionization by electron collision.  
 $\eta$  : Coefficient of electron attachment.  
 $E_{\text{sc}}$  : Space-charge field produced by the positive ions left behind the avalanche.

- e** : Electron charge ( $= 1.6 \times 10^{-19} \text{ C}$ ).
- R<sub>av</sub>** : Radius of the head of the initiatory avalanche.
- D<sub>e</sub>** : Electron diffusion coefficient (m<sup>2</sup>/s).
- τ** : Avalanche transit time (s).
- E<sub>pse</sub>** : Electric field caused by the positive ions left behind the primary avalanche.
- r<sub>s</sub>** : Radial distance from the simulation point charge.



## **REFERENCES**

- [1] E. Kimbark, "Direct Current Transmission", John Wiley & Sons, Inc., 1971.
- [2] M. Khalifa; "The Corona Discharge" in "High-Voltage Engineering Theory and Practice", ed Khalifa, Marcel Dekker, Inc. 1990.
- [3] M. Abdel-Salam and S. Abdel-sattar, "Calculation of Corora V-I Characterstics of Monopolar Bundles Using the Charge Simulation Method", IEEE Trans. Elact. Ensul., Vol. EI-24, No.4, August 1989, pp. 669-679.
- [4] P. Pirotte, "DC Corona Under Rain on Aerial Conductors", Proc. Gas Discharge Conference, London, 1970, pp. 289-292.
- [5] W. Weeks, "Transmission and Distribution of Eectrical Energy", Harper & Raw, Publishers, Inc., 1981.
- [6] K. D. Srivastava, "Insulation Performance of Dielectric-Coated Electrodes in Sulphur Hexafluoride Gas.", IEEE Trans. Elect. Ensul., Vol. EI-10, No.4, December 1975, pp.119-123.

- [7] T. Takashima, R. Ishubashi, "Expression of Electric Field for Systems of Dielectric-coated Cylindrical Conductors.", IEEE Trans, Vol. PSA-97, No.5, Sep./Oct. 1978, pp. 1847-1852.
- [8] J. Clements, C. Paul and A. Adoms, "Computation of the Capacitance Matrix for Systems of Dielectric-Coated Cylindrical Conductors.", IEEE Trans., Vol. EMC-17, No.4, November 1975, pp. 238-248.
- [9] E. Nasser, M. Selim and H. Parekh, "Computation of Electrical field and Potential Around Stranded Conductor by Analytical Method and Comparison with Charge - Simulation Method", Proc. IEEE, Vol. 122, May 1975, pp. 547-550.
- [10] E. Kuffel and Zaengl, "High Voltage Engineering", Pergamon Press, 1984.
- [11] M. Abdel-Salam and T. EL-Mohandes, "Combined Method Based on Finite Differences and Charge Simulation for Calculating Electric Fields", IEEE Trans. Ind. Appl. Vol. IA-25, No. 6, Nov./Dec. 1989, pp. 1060-1066.
- [12] M. Beasley et al, "Comparative Study of Three Method for Computing Electric Fields", Proc. IEEE, Vol.. 126, No. 1, Jan. 1979, pp. 126-134.

- [13] H. Singer, H. Steinbigler. and P. Weiss, "A Charge Simulation Method for the Calculation of High Voltage Fieldes.", IEEE Trans. Power App. Syst., Vol. PAS-93, Sep./Oct. 1974, pp. 1660-1668.
- [14] M. Abdel-Salam and E. Abdel-Aziz, "A New Charge - Simulation - Based Method for Analysis of Monoplar Poissoniam Fields.", J. phys. D: Appl. Phys. 27, 1994, pp. 807-817.
- [15] A. Yializis, E. Kuffel and P. Alexander, "An Optimized Charge Charge Simulation Method for the Calculation of High Voltage fields.", IEEE Trans. Power App. Syst., Vol. PAS-97, 1978, pp. 2434-2440.
- [16] S. Sato and W. Zaengl, "Effective 3-Dimensional Electric Fieled Calculation by Surface Charge Simulation Method.", IEEE Proc., Vol. 133, Pt. A, No. 2, March 1986, pp. 77-83.
- [17] E. Nasser, "Fundamental of Gaseous Ionization and Plasma Electronics", John wiley, 1971.
- [18] M. Abdel-salam, A. Zitoun and M. El-Ragheb, "Analaysis of Discharge Development of a Positive Rod-Plane Gap in Air", IEEE Trans. Power App. syst. Vol. PAS-95, No.4, July/Aug. 1976, pp.1019-1027.

- [19] R. Comsa and Q. Vuhuu, "Influence of Gap Length on Wire-Plane Corona", IEEE Trans. Power App. Syst. , Vol PAS-88, No-10, Oct 1969, pp. 1452-1457.
- [20] W. Masca, P. Ostano and G. Rumi, "HVDC Visual Corona and RIV Testing on Insulators and Conductor Samples", IEEE Trans. Power App. Syst, Vol. PAS-90, No.1, Jan/Feb. 1971, pp. 138-144.
- [21] M. Abdel-salam, M. Khalifa and M. Abu-Seada, " Calculation of Negative Corona Onset Voltages", IEEE Power Eng. Soc., Winter meeting, January 1973, pp 1-7.
- [22] M. Abu-Seada and K. Ali, "Negative Corona Thresholds of Compressed SF<sub>6</sub> in Space Charge Modified Nonuniform Fields", *ibid*, pp. 168-171.
- [23] M. Abdel-salam and D. Witanen, " Calculation of Corona Onset Voltage for Duct-type Precipitators", IEEE Trans. Ind. app. Vol. IA-29, No.2, March/Apr. 1993, pp.274-280.
- [24] M. Abdel-salam, F. Elhazek and M. Goher, " Positive Corona Discharge in a Three-Electrode System.", J. Electrostatics, 1989, pp 33-43.
- [25] A. Ibrahim and Singer, " Calculation of Corona Discharge in Positive Point to Plane Gaps", IEE Conf. Publ.101, 1982, pp.128-131.

- [26] M.Sarma and W. Janischewski, " DC Corona on Smooth Conductors in Air", IEE Proc. Vol.116, No.1, Jan.1969, pp.161-166.
- [27] M. khalifa, R. Radwan, A. Zeitoun and A. Abdel-fattah, " Computation of Corona Current and its Effect on Travelling Surges: Part I", IEEE Trans. Power Syst, Vol. PAS-80.
- [28] E. Nasser and M. Abou-Seada, " Calculation of Streamer Thresholds Using Digital Techniques", IEE Conf. Pub.89, 1970, pp.534-538.
- [29] M. Abdel-salam, "Calculating The Effect of High Temperature on The Onset Voltage of Negative Discharges", J. Phys.D, Appl. Phys, Vol.9, 1976, pp 149-154.
- [30] Y. Gosho and M. Saeki, " Secondary Electron Emission From Dielectric Surface Under Atmospheric Air Condition Due to UV Irradiation", Fifth International Symposium on High Voltage Engineering, Paper# 23-24, Braunschweig, 24-28 Aug 1987, pp.1-4.
- [31] M. Abdel-salam, M. El-Mohandes, " Onset Criterion of Upward Streamers from a Franklin Rod", Journal of Electrostatics, No.24, 1989, pp.45-59.

**Yahya Abdul-Rahman Abu-Shal**

**Date of Birth :** 5 July, 1966

**Place of Birth:** Makkah, Saudi Arabia

**Citizenship:** Saudi

**Education:** B. Sc., Electrical Engineering August, 1990  
King Fahd University of Petroleum and Minerals

**Research  
Interests** High voltage substation design and corona criteria

**Honors,  
Awards** SCECO-East, Engineering and Design Service  
Department, 1990 to present.

**Professional  
Affiliation** Membership in CIGRE